

# Hosts and environments: a (large-scale) radio history of AGN and star-forming galaxies

Manuela Magliocchetti

Received: date / Accepted: date

**Abstract** Despite their relative sparseness, during the recent years it has become more and more clear that extragalactic radio sources (both AGN and star-forming galaxies) constitute an extremely interesting mix of populations, not only because of their intrinsic value, but also for their fundamental role in shaping our Universe the way we see it today. Indeed, radio-active AGN are now thought to be the main players involved in the evolution of massive galaxies and clusters. At the same time, thanks to the possibility of being observed up to very high redshifts, radio galaxies can also provide crucial information on both the star-formation history of our Universe and on its Large-Scale Structure properties and their evolution. In the light of present and forthcoming facilities such as LOFAR, MeerKAT and SKA that will probe the radio sky to unprecedented depths and widths, this review aims at providing the current state of the art on our knowledge of extragalactic radio sources in connection with their hosts, large-scale environments and cosmological context.

**Keywords** Radio continuum: galaxies · Galaxies: general · Galaxies: evolution · Galaxies: clusters: general · Cosmology: large-scale structure of Universe

## Contents

1	Introduction . . . . .	2
2	The difficult art of discerning between radio-active AGN and star-forming galaxies from continuum radio surveys . . . . .	5
3	Hosts of radio-active AGN and star-forming galaxies . . . . .	8
3.1	The role of mass on radio activity . . . . .	9
3.2	What causes the FRI-FRII dichotomy? . . . . .	18
3.2.1	HERGs vs LERGs and the FRI-FRII dichotomy . . . . .	22

M. Magliocchetti  
INAF-IAPS, Via Fosso del Cavaliere 100, 11033, Rome, Italy  
E-mail: manuela.magliocchetti@inaf.it

3.3	Are radio-AGN all hosted in red and dead galaxies? . . . . .	26
3.4	The IR-radio relation in star-forming galaxies and its cosmological evolution . . . . .	32
4	The environments of radio-active AGN and star-forming galaxies . . . . .	40
4.1	Methods for the detection of environment 1: clustering analyses . . . . .	40
4.1.1	Useful definitions . . . . .	40
4.1.2	Early works on radio-galaxy cross-correlations . . . . .	44
4.1.3	The correlation functions of radio sources . . . . .	46
4.2	Methods for the detection of environment 2: direct pinpointing of sources within known structures . . . . .	55
4.2.1	The FRI-FRII and HERG-LERG distinction . . . . .	62
4.3	Methods for the detection of environment 3: search for over-densities around known sources . . . . .	64
4.3.1	Targeted searches around radio-AGN . . . . .	64
4.3.2	Cross-matches of catalogues . . . . .	69
5	Discussion . . . . .	74
5.1	Hosts . . . . .	74
5.2	Environment . . . . .	79
	References . . . . .	82

## 1 Introduction

During the past years, radio galaxies have quickly moved from being an interesting class of extragalactic objects to become one of the fundamental bricks of the wall of our comprehension of the physical processes that shape galaxy formation and evolution. Indeed, radio-emitting AGN have been invoked as the major players in action to halt star-formation in massive galaxies, with an effect that would also prevent their masses to reach unobserved values and produce the local ‘read and dead’ population of ellipticals both in terms of physical properties and number density (the so-called ‘radio-mode’ feedback, e.g., [Croton et al. 2006](#); [Bower et al. 2006](#); [Fanidakis et al. 2012](#); [Weinberger et al. 2018](#)). Furthermore, a very strong connection between radio-AGN and galaxy clusters is now well established, with radio-AGN emission being responsible for a large part of their thermal state (see [McNamara and Nulsen 2012](#); [Brunetti and Jones 2014](#) for reviews on this topic) as well as for enhancing or suppressing star-formation within its member galaxies (e.g. [Gilli et al. 2019](#); [Salomé et al. 2016](#)).

Extragalactic radio sources come in two flavours: AGN and star-forming galaxies. Radio-emitting star-forming galaxies, at least in the local universe, generally coincide with normal spiral and irregular galaxies, typically present low ( $L_{1.4\text{ GHz}} \lesssim 10^{22} \text{ W Hz}^{-1} \text{ sr}^{-1}$ ) luminosities and dominate the radio source counts below the mJy level (see [Padovani 2016](#) for a review). On the other hand, the population of radio-emitting AGN, much brighter and extending to much higher redshifts as observed by current facilities (indeed these were the first galaxies to be found above redshifts one, two, three and four – cf. [Stern and Spinrad 1999](#) and references therein), is way more variegated. Historically, radio-AGN have been sub-divided in two different ways. [Fanaroff and Riley \(1974\)](#) classified sources according to their radio morphologies as type I (FRI), in which the peak of radio emission is located near the core (edge-darkened) and type II (FRII), in which the peak of surface brightness is at the edge of

the radio lobes far from the centre of emission (edge-brightened). A further classification scheme is instead based on the presence and relative intensity of high- and low-excitation lines in their optical spectra (e.g., [Hine and Longair 1979](#)) and divides them into high-excitation radio galaxies (HERGs) and low-excitation radio galaxies (LERGs). HERGs and LERGs are believed to represent intrinsically different types of objects (see [Heckman and Best 2014](#) for a review), with LERGs accreting at low rates (luminosities below 1% of their Eddington limit) and HERGs accreting at high rates (between 1% and 10%).

As a matter of fact, the realm of radio-emitting AGN is even more complex than this. On top of compact/point-like (or FR0 cf. [Baldi and Capetti 2010](#)) galaxies, radio-quiet AGN which are thought to emit at radio wavelengths mainly thanks to star-forming processes taking place within their hosts (cf. [Padovani 2016](#)) and quasars, blazars and BL Lacs believed to be the very same AGN-powered radio galaxies only seen at smaller viewing angles ([Urry and Padovani 1995](#)), in the recent years new populations have been discovered, such as the Compact Symmetric Objects (CSO), the Compact Steep Spectrum (CSS) galaxies and the Gigahertz-Peaked galaxies (GPS). These are all powerful sources ( $L_{1.4\text{ GHz}} > 10^{24} \text{ W Hz}^{-1} \text{ sr}^{-1}$ ), with GPS presenting very compact ( $\lesssim 1 \text{ Kpc}$ ) radio emission with a peak in the GHz range (see [O’Dea and Saikia 2021](#) for a review), and CSS being less compact ( $\lesssim 15 \text{ Kpc}$ ) and with a peak around 100 MHz (see [Miley and De Breuck 2008](#) for a review). CSOs are instead the smallest sources, with sizes of less than a few hundred pc (see [Hardcastle and Croston 2020](#) for a review). We further note that radio-AGN with resolved morphologies can also present themselves as Giant Radio Galaxies (GRG) if their extension goes beyond  $\sim 0.7 \text{ Mpc}$  (e.g., [Willis, Strom, and Wilson 1975](#)) or as Wide Angle/Narrow Angle Tail (WATs or NATs) galaxies when their jets do not lie along a common direction but show various degrees of bending (e.g. [Owen and Rudnick 1976](#)).

Many excellent reviews tackling in a very comprehensive way the AGN phenomenon and more in general radio emission are available in the literature (e.g., [Miley and De Breuck 2008](#); [De Zotti et al. 2010](#); [Heckman and Best 2014](#); [Tadhunter 2016](#); [Padovani 2016](#); [Padovani et al. 2017](#); [Hardcastle and Croston 2020](#)). Our purpose is to extend the content of these reviews by presenting radio galaxies as cosmological objects in connection with the more general context of galaxy and large-scale structure formation and evolution. To this aim, we will present the current state of the art on our knowledge of extragalactic radio sources (both AGN and star-forming galaxies) from the point of view of their galaxy hosts, environments and cosmological behaviour, so to provide a link between radio activity on small (nuclear and sub-galactic) scales and environmental (Kpc to Mpc) properties.

Within this framework, we have decided to concentrate on a number of topics which are mostly still controversial and/or poorly understood. For what concerns the hosts of radio galaxies we will then discuss the role of their mass on radio emission, the FRI/FRII dichotomy, the cosmological evolution of radio-AGN in terms of star-formation activity within their hosts and, in the

case of star-forming galaxies, the properties of the relationship between infrared and radio luminosities (the so-called IR-radio correlation) as obtained at the different radio frequencies and redshifts. Environments will instead be investigated by following three different methods. The choice is dictated by the fact that in general these different methods return different and complementary answers. For example, statistical techniques such as clustering analyses are the only ones capable of providing information on the dark matter content of the structures that host radio-AGN and star-forming galaxies. Furthermore, they can also offer a snapshot of the large-scale structure of our Universe as traced by these sources and on its evolution up to the earliest epochs. The other two methods, which consist in a) searching for structures around pre-selected radio-AGN and b) pinpointing radio-AGN within known structures might seem to be very similar to each other. As a matter of fact though, these two are also complementary since they return results which in some cases differ even by large factors. For instance, the first method finds that most radio-AGN reside within overdense structures, while according to the second method this is true only for a much smaller fraction of sources. This discrepancy reverberates e.g., onto the estimates of the life-time of the radio-active AGN phase and on a number of other issues, so that a direct comparison between the results obtained in these two different ways is not always possible. Furthermore, whenever structures such as groups or clusters of galaxies with available X-ray information are involved, the second method can also return fundamental information on the interaction between radio-AGN activity and the intracluster medium (ICM).

The layout of this review is then the following: Sect. 2 will summarize the main methods adopted in the literature to distinguish between radio-emitting AGN and star-forming galaxies. Section 3 will be devoted to the hosts. In more detail, Sect. 3.1 will investigate the role of galaxy mass on radio (mainly AGN) activity, while Sect. 3.2 will discuss the morphological dichotomy between FRI and FRII galaxies from the point of view of their hosts and nuclear/accretion properties (LERG vs HERG distinction). Section 3.3 will present a detailed analysis of the cosmological evolution of star-forming activity within radio-AGN hosts beyond  $z \gtrsim 1$ , while Sect. 3.4 will review our current knowledge on the controversial issue of the IR-radio relation in star-forming galaxies, its dependencies and eventual redshift evolution. Section 4 will instead be dedicated to the environments of extragalactic radio sources. As previously discussed, these will be presented by following the method adopted to investigate their properties. So, after a brief introduction on the theory behind statistical methods such as the correlation function and cross-correlation function – necessary to understand some of the works reviewed in this sub-section – Sect. 4.1 will present the results obtained so far by making use of the aforementioned techniques. Section 4.2 will instead show our current knowledge on the environmental properties of radio galaxies as obtained by pinpointing them within pre-defined over-densities such as groups and clusters of galaxies, while Sect. 4.3 will do the same but in the case of structures identified around chosen radio sources. Our conclusions will then be summarized in Sect. 5.

Because of its contents, this review is thought to reach an audience which extends beyond radio astronomers. To this aim, it will present the various topics in a somehow didactic way. Each section will first introduce the general problem and then present a historical excursus of the most relevant results obtained throughout the years up to the present days with the aim to understand what has been done so far, what we think is understood, what is still missing and where (if any) contradictions stand. Since sample sizes, completeness issues and depths of the observations are all crucial quantities that can largely affect the outcome of statistical analyses such as those presented in the following sections, we will add these pieces of information when discussing most of the works.

Before moving on though, an important point has to be made. Many names can be found in the literature for the radio-active AGN population. From the historically adopted radio-loud AGN to jetted AGN (Padovani 2016). We personally believe that none of these can correctly describe the considered sources, since the term radio-loud made more sense when radio surveys only sampled bright ‘monsters’, while it is not anymore the case for current facilities that reach the sub-mJy/ $\mu$ Jy regime. On top of that, as it will become more clear in Sect. 2, radio-loudness does not have a univocal definition (e.g., Jarvis et al. 2021) since radio-emitting AGN can be selected in many different ways. At the same time, not all radio-active AGN present jetted structures, so even this terminology only provides a partial description of the radio AGN phenomenon. Our preference goes to the more general terms ‘radio-active AGN’, ‘radio-emitting AGN’ or alternatively ‘radio-AGN’ to indicate all AGN emitting at radio wavelengths because of their nuclear activity. This is the wording that will be used throughout this review. We also stress that throughout the text we will use the word “protocluster” to indicate a non-virialized, overdense structure formed by galaxies and/or AGN, regardless of whether it will subsequently evolve into a cluster. Lastly, whenever mentioned,  $h$  is the reduced Hubble constant. Note that most (if not all) of the works presented in this review and published after 2000 adopt the standard cosmological model  $\Omega_0 \simeq 0.3$ ,  $\Omega_A \simeq 0.7$ ,  $h \simeq 0.7$  (e.g. Aghanim et al. 2018), with  $\Omega_0$  and  $\Omega_A$  respectively present density of (total) matter and dark energy. However, earlier results still consider a universe with  $\Omega_0 = 1$  and  $\Omega_A = 0$ .

## 2 The difficult art of discerning between radio-active AGN and star-forming galaxies from continuum radio surveys

Extragalactic radio sources are a mixed bag of different astrophysical populations. And while until the 1990s the radio sky was dominated by bright enough objects to ensure they were *bona fide* radio-active AGN, indeed with the advent of deep enough radio surveys it became clear that the counts below  $\sim 1$  mJy start to be dominated by different objects such as star-forming galaxies (e.g., Windhorst et al. 1985; Magliocchetti et al. 2000; Prandoni et al. 2001 and references therein) and radio-quiet AGN, whereby – despite the presence

of an AGN – radio emission mainly originates from star-forming processes within their hosts rather than from accretion onto a black-hole (e.g., [Kimball et al. 2011](#); [Condon et al. 2013](#); [Bonzini et al. 2015](#); [Ceraf et al. 2020](#) – see also [Panessa et al. 2019](#) for a review on these objects and [Padovani 2016](#) for a review on the faint radio sky). It follows that, unless the radio-AGN present morphological structures (such as lobes and jets) that uniquely identify them as such, distinguishing between these three different populations in continuum radio surveys is currently an impossible task. Information (both photometric and/or spectroscopic) at wavelengths different than radio is required, but even in this case the answers are not always univocal.

As we will see later in Sect. 3.1, in the local universe radio-AGN are almost ubiquitously associated with massive elliptical galaxies, with little or no ongoing star-forming activity. This prompted early studies to introduce a value for the radio-to-optical (R band) ratio (defined as  $q_R = F_{1.4\text{ GHz}} \cdot 10^{(R-12.5)/2.5}$ , with  $F$  expressed in mJy) larger than  $\sim 30$  (e.g., [Kellermann et al. 1989](#); [Urry and Padovani 1995](#)) as an indicator for a radio-emitting AGN. At the same time, still in the local universe, star-forming galaxies (and radio-quiet AGN) present a very tight correlation between their far-infrared (FIR) and radio fluxes (e.g., [Condon 1992](#), cf. Sect. 3.4). So, distinguishing between radio-AGN and star-forming galaxies at  $z \lesssim 1$  is rather doable.

The situation becomes more complicated once we move to redshifts higher than  $z \sim 1-1.5$ . The explanation is quite straightforward:  $z \sim 1.5$  in fact marks the transition from a relatively quiet universe, to one dominated by AGN and cosmic star-formation activities (e.g., [Merloni, Rudnick, and Di Matteo 2004](#)). In such a universe, many star-forming galaxies are found to host an AGN and the other way round (cf. Sect. 3.3), so a clear distinction between these two classes of sources based on their radio-to-infrared colours is extremely difficult. At the same time, galaxies at  $z \sim 2$  are generally younger than those found in the local universe, therefore also an optical search for radio galaxies as red-and-dead sources is proven to be ineffective. This implies that new techniques have to be applied to try to distinguish between radio-emitting AGN and the other populations. [Padovani \(2016\)](#) (see also [Hardcastle et al. 2019](#) and references therein) provides an excellent summary of the different selection methods. Here we will just briefly list the more commonly used ones in view of their strengths and weaknesses:

a) Optical/NIR spectroscopy: This method (e.g., [Baldwin, Phillips, and Terlevich 1981](#); [Veilleux and Osterbrock 1987](#)) provides the cleanest distinction between AGN and star-forming galaxies and is based on the absence or presence (and relative strength) of emission lines indicating AGN and/or star-forming activity in the optical/NIR spectra of radio galaxies. Despite its success, being spectroscopy a very time-consuming task, a wide application is however currently limited only to relatively local sources, or alternatively to sparse samples of bright objects in the more distant universe. Also, even if line emission in the spectra guarantees the presence of an AGN, it does not provide any information on whether radio emission is due to nuclear activity or to star-forming processes within the host galaxy, as is the case for radio-quiet AGN.

b) SED fitting: This method (e.g., [Smolčić et al. 2008](#)) uses photometry at a number of wavelengths (the more the better) to produce a spectral energy distribution (SED) for the sources in exam. This can be thought as a lower-resolution version of the spectroscopy method, which only considers continuum emission instead of lines. Observations then get fitted with synthetic models for stellar evolution (e.g., [Bruzual and Charlot 2003](#)) to infer a number of galaxy properties, including presence and relevance of an AGN. Less precise but also less expensive than spectroscopy, it can be applied to much higher redshifts. As in the spectroscopy case though, it cannot discern whether in presence of an AGN radio emission originates from the central black hole or from surrounding star-forming regions.

c) Radio/FIR excess: This method (e.g., [Delvecchio et al. 2017](#)) selects as radio-AGN all sources that present a radio excess and lie below the IR-radio relation (cf. Sect. 3.4), and as star-forming galaxies those that either lie on the relation or show a FIR excess. As already discussed, it works very efficiently in the local universe. However, it has to rely on FIR observations which are currently unavailable for many radio sources. Also, it is proven to lose its ability at redshifts  $z \gtrsim 1 - 1.5$  due to the cosmological evolution of the galaxies, most of them co-hosting AGN and star-forming processes at the same time.

d) Radio continuum slope: This method (e.g., [Alberts et al. 2020](#)) relies on radio observations taken at different frequencies. It works well at identifying flat-spectrum or inverted-spectrum AGN, but it is ineffective at distinguishing between steep-spectrum radio-AGN and star-forming galaxies as they generally present very similar values for the radio spectral index,  $\alpha \sim 0.7$  (e.g., [De Zotti et al. 2010](#)).

e) X-ray emission: Most of the AGN emit in the X-ray, therefore another way to distinguish between a radio-AGN and a radio-active star-forming galaxy is by looking at the X-ray emission produced by a radio source. However, this method only (partially) works for very bright objects, since the majority of radio-AGN have X-ray luminosities lower than  $\sim 10^{42}$  erg sec $^{-1}$ , value below which X-ray emission might just as well be due to star-forming processes within the host (e.g., [Fragos et al. 2013](#)). As a matter of fact, the fraction of radio-AGN also detected in the X-ray bands is quite low ( $\sim 5\%$ , e.g., [Hickox et al. 2009](#), value that can however increase according to selection criteria and flux densities, e.g., [Magliocchetti et al. 2020](#)).

f) MIR colours: Another possibility to distinguish between radio-AGN and star-forming galaxies is provided by the investigation of their mid-infrared (MIR) colours (e.g., [Stern et al. 2012](#)). However, this method is also shown to work well only for very luminous and radiatively efficient AGN, while it misses the majority of the radio-active AGN population since it is biased against lower MIR luminosities and higher redshifts (e.g., [Donley et al. 2012](#); [Mingo et al. 2016](#)), both typical of most radio-AGN.

g) Radio Luminosity: The last method presented here ([Magliocchetti et al. 2014b](#)) – which we discuss in greater detail since it is not mentioned in the reviews of [Padovani \(2016\)](#) or [Hardcastle et al. \(2019\)](#) – relies on the radio luminosity of the sources. Indeed, thanks to the steepness of the radio-luminosity



function of star-forming galaxies as opposed to the flatter one exhibited by radio-AGN (e.g., Magliocchetti et al. 2002; Mauch and Sadler 2007), selecting sources brighter than the radio luminosity value at which the two distributions cross, virtually ensures that all *all* of them will be radio-AGN. This holds in the local universe. At higher redshifts, the cosmological evolution of these populations, together with the existence of extreme starburst galaxies, implies that sources with star-forming rates above  $\sim 10^3 M_{\odot} \text{ yr}^{-1}$  will present radio luminosities  $\gtrsim 10^{24} \text{ W Hz}^{-1} \text{ sr}^{-1}$  and therefore be mistakenly identified as radio-AGN (e.g., Hardcastle et al. 2019). However, such sources are relatively rare and furthermore Magliocchetti et al. (2014b) take the evolutionary issue into account by introducing a criterion based on the radio-luminosity function as provided up to redshifts  $\sim 2.5$  by McAlpine, Jarvis, and Bonfield (2013), who indeed find that star-forming galaxies evolve in a much stronger way,  $\propto (1+z)^{2.5}$ , than radio-selected AGN ( $\propto (1+z)^{1.2}$ ). By using this result, Magliocchetti et al. (2014b) adopt an evolving luminosity threshold that scales with redshift as  $\text{Log}_{10}[L_{\text{cross}}(z)] = \text{Log}_{10}[L_{0,\text{cross}}] + z$  (with  $L_{0,\text{cross}} = 10^{21.7} \text{ W Hz}^{-1} \text{ sr}^{-1}$ , roughly corresponding to the break of the local radio luminosity function of star-forming galaxies) up to  $z = 1.8$  and  $L_{\text{cross}}(z) = 10^{23.5} \text{ W Hz}^{-1} \text{ sr}^{-1}$  for  $z > 1.8$ , above which to select radio-AGN. Since the radio-AGN samples selected in this way are contaminated by very few interlopers (Magliocchetti et al. 2014b, 2016, 2018a), the present method has the important advantage of being rather clean while only needing redshift determinations instead of expensive spectroscopy or multi-wavelength information for the sources in exam. On the other hand, it cannot identify star-forming galaxies and misses faint radio-AGN which end up in the mixed bag which also contains radio-quiet AGN.

The main points to be taken from the above discussion are then three:

1. Despite the enormous wealth of multi-wavelength information that is getting more and more accessible to the astronomical community, discerning between radio-active AGN and galaxies dominated by star forming activity is still not a straightforward task.
2. None of the methods highlighted above provides the ‘ultimate’ selection, as they all suffer from various (and generally different) limitations.
3. Different techniques as a matter of fact select slightly different populations, which generally coincide only in the case of sources with very bright (or alternatively very faint) radio luminosities. This is an issue that always needs to be kept in mind when comparing results from different works adopting different selection methods.

### 3 Hosts of radio-active AGN and star-forming galaxies

This section presents results on the connection between radio-activity and host galaxy properties. It is divided into four different parts that will respectively tackle the connection between host (stellar) mass and radio emission (Sect. 3.1), the possible causes for the FRI-FRII dichotomy (Sect. 3.2), the



cosmological evolution of radio-AGN in terms of star-formation activity within their hosts (Sect. 3.3) and – in the case of star-forming galaxies – the IR-radio relation, its eventual dependences and redshift evolution (Sect. 3.4).

### 3.1 The role of mass on radio activity

It has been clear since many years now (Matthews et al. 1964) that the majority of powerful radio-AGN is hosted within the most massive galaxies (stellar masses  $M_* \sim 10^{11} M_\odot$  and above) known in the Universe. This result has been confirmed at least up to  $z \sim 1$  (and in some cases beyond) both by direct estimates (e.g., Heeschen 1970; Ekers and Ekers 1973; Auriemma et al. 1977; Jenkins 1982; Best et al. 2005a; Mauch and Sadler 2007; Smolčić et al. 2009; Magliocchetti et al. 2016; Sabater et al. 2019; Capetti et al. 2022) and also by the extremely tight correlation in the  $M_K - z$  plane exhibited by the hosts of radio-AGN (e.g., Lilly and Longair 1984; Eales et al. 1997; Jarvis et al. 2001; De Breuck et al. 2002; Willott et al. 2003) that can be explained by assuming that the observed  $K$ -band light is dominated by emission from the old stellar population and that radio-AGN have very similar (large) host masses all across half of the age of the Universe. More recent results based on rest-frame  $1.6 \mu\text{m}$  and  $4.5 \mu\text{m}$  photometry also report very high masses for the hosts of radio-AGN, at least up to  $z \sim 3$  if not beyond (Seymour et al. 2007; De Breuck et al. 2010; Gürkan, Hardcastle, and Jarvis 2014; Drouart et al. 2016).

However, these results do not fully answer the question that naturally arises when considering radio-AGN: what causes their radio emission? In a seminal paper by Hickox et al. (2009), it was found that the overlapping between families of AGN selected with different methods (X-ray, *Spitzer*-IRAC bands and radio) was extremely small, especially when it came to radio emission from X-ray- and NIR-selected AGN ( $\sim 5\%$ ). Between a third and a half of X-ray selected AGN were instead observed to have a counterpart in the NIR, and the other way around (cf. top panel of Fig. 1). Although the relative depths of the different samples can provide at least a partial answer to this effect (e.g., Ho 2008), it is also very possible that it might instead be mainly determined by more physical factors.

On the other hand, there are instead cases where radio-AGN emission is almost ubiquitous. Brown et al. (2011) used 1.4 GHz, NRAO VLA Sky Survey (NVSS – Condon et al. 1998) observations of 396 local early-type galaxies selected from the 2MASS Extended Source Catalogue (Jarrett et al. 2000), finding that virtually all 120 galaxies with absolute magnitudes  $M_K < -25$  (corresponding to stellar masses  $\gtrsim 10^{11} M_\odot$ ) were radio emitters with flux densities larger than  $\sim 1 \text{ mJy}$ . This was in line with earlier findings (e.g., Sadler (1999) and references therein). Much more recently, Capetti et al. (2022) have come to the same conclusion for their complete sample of 188 local giant ellipticals with  $M_K < -25$  taken from the 2MASS Redshift Survey (Huchra et al. 2012) and with radio information from the LOFAR Two-Metre Sky Survey Data Release 2 (LoTSS DR2 – Shimwell et al. 2022). Indeed, they show

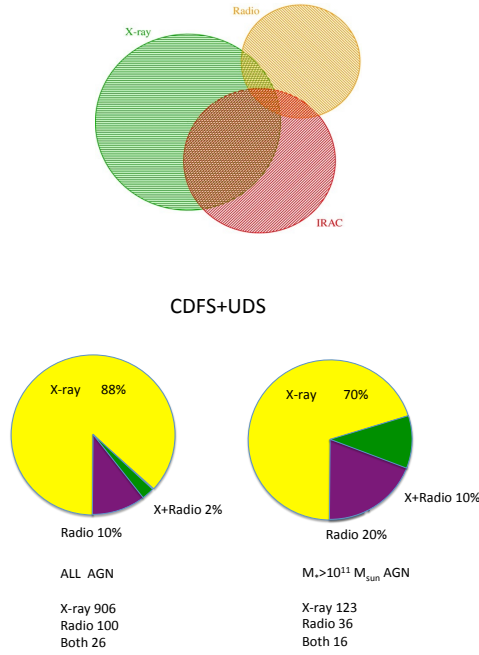


**Fig. 1** Top panel: Venn diagram showing the relative number of AGN with spectroscopic redshifts in the range  $0.25 < z < 0.8$ , selected in the radio, X-ray, and near-infrared (NIR). Out of 122,  $L_{1.4\text{GHz}} > 10^{23.8} \text{ W Hz}^{-1}$ , radio-AGN, only 6 are also detected in the X-ray (down to  $L_X = 10^{42} \text{ ergs s}^{-1}$ ) and IRAC (down to  $L_{4.5\mu\text{m}} = 10^{43} \text{ ergs s}^{-1}$ ) bands. Similarly, out of 296 (199) X-ray-selected (IRAC-selected) AGN, only 6 (6) are also detected at radio wavelengths. Figure from [Hickox et al. \(2009\)](#). Bottom panel: Pie chart illustrating the contribution of the different emitters to the total (radio+X-ray) AGN population obtained by combining together the UDS and CDFS fields. The yellow areas correspond to X-ray emitters, the purple to radio emitters while the green regions indicate the contribution from those AGN which simultaneously emit in the radio and X-ray bands. The left-hand pie shows the case for AGN associated with galaxies of all stellar masses, while that on the right corresponds to AGN residing within hosts with  $M_* \geq 10^{11} M_{\odot}$ . Figure from [Magliocchetti et al. \(2020\)](#).

that about 78% of these sources are detected by LOFAR above  $L_{150\text{MHz}} \gtrsim 10^{21} \text{ W Hz}^{-1}$ , and that *all* the brightest,  $M_K < -25.8$ , giant ellipticals are associated with radio-emission, even if for one case this might be due to star-forming processes. The same result has also been obtained by [Grossova et al. \(2022\)](#) who extend the work of [Dunn et al. \(2010\)](#) by considering 42, very local (distance  $< 100 \text{ Mpc}$ ), optically and X-ray brightest early-type galaxies observed with the highest resolution VLA A configuration in the frequency range 1–2 GHz. Out of these 42 sources, 41 present detectable radio emission.

The discrepancy between the frequency of radio-AGN emission as obtained for local massive galaxies by the aforementioned works and for higher-redshift AGN as obtained by [Hickox et al. \(2009\)](#) is really striking ( $\sim 5\%$  vs  $\sim 100\%$ ). A

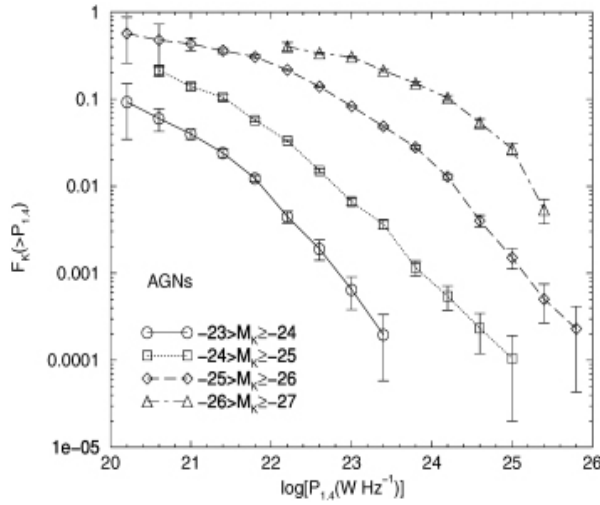


**Fig. 2** Fraction of galaxies  $F_K(> P_{1.4})$  which host a radio-AGN as a function of radio luminosity  $P_{1.4}$  calculated in four bins of absolute  $K$  magnitude ( $M_K$ ) as labelled in the figure. Figure from [Mauch and Sadler \(2007\)](#).

number of factors could contribute to this disagreement, such as galaxy type, nuclear/accretion differences and/or redshift range. However, in the following we will mainly investigate the effects of the host mass. Indeed, already 50 years ago, a number of works had envisaged a strong correlation between the probability for a galaxy to be the host of a radio-active AGN and its optical luminosity  $L_{\text{opt}}$  (e.g., [Colla et al. 1975](#); [Auremma et al. 1977](#); [Hummel et al. 1983](#)). [Best et al. \(2005a\)](#) brought these early works to a much more solid statistical grounding by presenting an analysis performed for 420,  $z < 0.1$  radio-AGN brighter than 5 mJy (corresponding to a radio luminosity limit of  $L_{1.4\text{GHz}} \gtrsim 10^{23} \text{ W Hz}^{-1}$  at  $z = 0.1$ ), selected from the Faint Images of the Radio Sky at Twenty centimeters (FIRST – [Becker et al. 1995](#)) and NVSS surveys, and with spectroscopic information from the second data release of the Sloan Digital Sky Survey (SDSS – [York et al. 2000](#)). Their results clearly showed that there is a steady increase of the fraction of galaxies that host a radio-AGN with increasing stellar mass  $M_*$ . The functional form is of the kind  $F_{\text{radio-AGN}} \propto M_*^{2.5}$  (which holds at all radio luminosities), until a plateau of about 30% is reached for  $M_* \gtrsim 10^{11.7} M_\odot$ . It is interesting to note that [Best et al. \(2005a\)](#) also observe a correlation between  $F_{\text{radio-AGN}}$  and central black hole mass, which is however shallower than what found in the case of the host mass ( $\propto M_{\text{BH}}^{1.6}$ ).

[Mauch and Sadler \(2007\)](#) use a  $z \lesssim 0.15$  sample of 2661 radio-AGN selected from the NVSS survey with radio fluxes above 2.8 mJy, magnitudes  $K > 12.75$  and spectroscopic redshifts from the 6 degree Field Galaxy Redshift Survey

(6dFGRS – Jones et al. 2004). These authors also find that the probability for a galaxy to host a radio-AGN has a strong dependence on the  $K$ -band luminosity (proxy for the stellar mass) of the host galaxy with a functional form  $F_{\text{radio-AGN}} \equiv F_K(> P_{1.4}) \propto L_K^{2.1}$  (cf. Fig. 2). At least  $\sim 60\%$  ( $\sim 100\%$  if one includes upper errors) of their NIR brightest,  $-26 < M_K < -25$ , sources are found to have a radio-AGN counterpart down to  $\sim 10^{20} \text{ W Hz}^{-1}$ . On the other hand, no correlation is observed between radio luminosities and  $K$ -band magnitudes, since radio-AGN span a wide range in  $L_{1.4 \text{ GHz}}$  but are almost all found in the most luminous NIR galaxies.

These results have been recently confirmed by the work of Sabater et al. (2019) who use the LoTTS Data Release 1 (DR1 – Shimwell et al. 2019) cross-matched with the seventh data release of the SDSS (DR7 – Abazajian et al. 2009) to identify with various methods 2021,  $z < 0.3$ , radio-AGN. Their study also shows a strong dependence of the fraction of galaxies hosting a radio-AGN on their stellar mass and radio luminosity. In the most extreme case of  $L_{150 \text{ MHz}} \geq 10^{21} \text{ W Hz}^{-1}$  and stellar masses  $M_* \geq 10^{11} M_\odot$ , the analysis of Sabater et al. (2019) finds that such a fraction reaches the value of 100% i.e., – in agreement with the works of e.g., Brown et al. (2011) and Capetti et al. (2022) – one has that *all* local massive galaxies are switched on to a radio-emitting AGN. As in Best et al. (2005a), Sabater et al. (2019) also conclude that the probability for a galaxy to host a radio-active AGN has a stronger dependence on its host mass rather than on the mass of the powering black hole, suggesting a tighter physical link between radio-activity and gas fuelling with respect to nuclear properties. On a side, we further note that the same dataset used by Sabater et al. (2019) indicates that the morphology of the host galaxy is also related to radio-AGN activity, with sources with  $L_{150 \text{ MHz}} > 10^{23} \text{ W Hz}^{-1}$  more likely to be found within massive, round galaxies, with respect to fainter radio-AGN hosts which instead exhibit more elongated shapes with a distribution which is indistinguishable from that of inactive galaxies with the same stellar mass content (Zheng et al. 2020). This confirms the very early results of e.g., Heeschen (1970) and Hummel, Kotanyi, and Ekers (1983).

Smolčić et al. (2009) repropose the Best et al. (2005a) analysis but at intermediate ( $0.3 < z < 0.7$ ) and high ( $0.7 < z < 1.3$ ) redshifts for a sample of 610,  $L_{1.4 \text{ GHz}} \geq 10^{23.6} \text{ W Hz}^{-1}$  radio-AGN selected from the VLA-COSMOS survey (Schinnerer et al. 2007). No evolution from the local results is found in the intermediate-redshift range, while in the high-redshift range the fraction of galaxies host of a radio-AGN is always higher than that derived up to  $z \sim 0.7$  for all galaxy masses. This increase is however differential in the sense that low-mass galaxies at  $z \sim 1$  present a stronger increment with respect to higher-mass ones. Very similar results are obtained by Williams and Röttgering (2015) who present a study of the evolution of the fraction of radio-active ( $L_{1.4 \text{ GHz}} \geq 10^{24} \text{ W Hz}^{-1}$ ) AGN as a function of their host stellar mass, spanning from  $z \sim 0$  to  $z \sim 2$ . The comparison between local and high-redshift observations is achieved by considering at  $z < 0.3$  the catalogue of Best and Heckman (2012), while in the range  $0.5 < z < 2$  a catalogue of  $\sim 1500$  radio-AGN resulting from combining the VLA-COSMOS survey (Schinnerer et al.

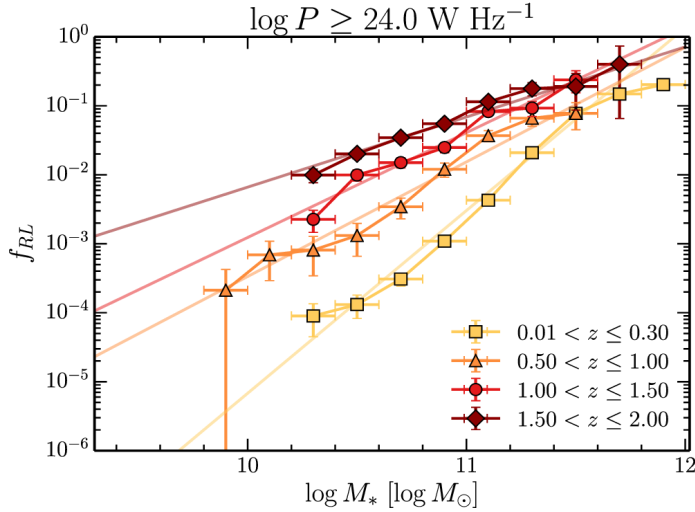


**Fig. 3** Fraction of galaxies hosting a radio-AGN with  $L_{1.4\text{GHz}} > 10^{24} \text{ W Hz}^{-1}$  ( $f_{\text{RL}}$ ) as a function of their stellar mass in the four redshift bins highlighted in the plot. The coloured lines show linear fits over the stellar mass range  $10^{10} < (M_*/M_\odot) < 10^{11.5}$ . Figure from Williams and Röttgering (2015).

2007) with  $Ks < 23.4$  sources selected from the COSMOS/UltraVISTA survey (Muzzin et al. 2013). Also in this case, it is observed that the fraction of galaxies host of a radio-AGN shows a clear increase with host mass and redshift, with a functional form which goes as  $\propto M^{2.7}$  in the local universe and as  $\propto M$  at  $1.5 < z < 2$  (cf. Fig. 3). This implies that radio-AGN activity amongst galaxies of different mass increases differently towards higher redshifts, with a more marked increment (more than an order of magnitude) observed amongst galaxies of lower ( $M_* \lesssim 10^{10.75} M_\odot$ ) mass. The radio-AGN fraction within higher mass galaxies ( $M_* > 10^{11.5} M_\odot$ ) instead stays roughly constant in time. In agreement with the conclusions of Smolčić et al. (2009), these trends are interpreted as being due to a rising contribution of AGN accreting in the radiative mode (see later in this Section) at those earlier epochs thanks to larger reservoirs of gas in lower-mass galaxies.

In terms of redshift evolution, it is also worth noticing that both Lin et al. (2017) and Mo et al. (2020) report a strong increment of the fraction of radio-AGN within galaxies residing in the proximity of cluster centers. In more detail, Lin et al. (2017) analyse the recurrence of  $L_{1.4\text{GHz}} \geq 10^{24.7} \text{ W Hz}^{-1}$  radio-AGN detected with FIRST in galaxies belonging to the 400,  $0.3 < z < 1$ , brightest clusters from the Subaru HyperSuprime-Cam Survey (Aihara et al. 2018), finding that this is a steep function of their stellar mass. Mo et al. (2020) obtain a similar result but based on 194,  $L_{1.4\text{GHz}} \geq 10^{25} \text{ W Hz}^{-1}$ , FIRST-detected radio-AGN found within 500 Kpc from the centres of clusters

selected at  $0.7 < z < 1.5$  by the Massive and Distant Clusters of WISE Survey (MaDCoWS – [Gonzalez et al. 2019](#)). They further report that the fraction of radio-AGN within cluster galaxies is factor  $\sim 3$  higher than within galaxies of the same mass but in the field. [Lin et al. \(2017\)](#) instead observe that the increased fraction of radio-AGN within large stellar mass galaxies at high,  $z \gtrsim 0.8$ , redshifts is due to blue massive galaxies, at variance with the predominance of red galaxies inhabited by a radio-AGN at lower- $z$ . In agreement with e.g., [Smolčić et al. \(2009\)](#) and [Williams and Röttgering \(2015\)](#), the authors conclude that this finding hints to a switch in the dominant accretion mode powering cluster radio galaxies, from cold/efficient at high- $z$  to hot/inefficient at low- $z$  (see below).

Recently, [Magliocchetti et al. \(2020\)](#) presented an analysis of 100 radio-emitting and 907 X-ray emitting AGN from the two cosmological UKIDSS Ultra Deep Field (UDS) and Extended Chandra Deep Field South (CDFS) regions, which showed that the stellar mass of AGN hosts is a fundamental quantity which determines their level of activity. Optical/NIR counterparts, together with precise redshift estimates (both spectroscopic and photometric) for these sources were taken from the VANDELS survey ([McLure et al. 2018](#); [Pentericci et al. 2018](#)). The depths of both radio ([Simpson et al. 2006](#); [Miller et al. 2013](#)) and optical/NIR observations ensure completeness up to at least  $z \sim 3$ . By using this data it was then found not only that all radio-AGN hosts are very massive,  $M_* \gtrsim 10^{10.5} M_\odot$  galaxies, but that the probability for an X-ray-selected AGN to also emit at radio wavelengths is a very strong function of its host mass. Indeed, this increases from  $\sim 1\%$  to  $\sim 13\%$  when the stellar mass goes from  $M_* \sim 10^{10.5} M_\odot$  to  $M_* \sim 10^{11.5} M_\odot$ . Within the same mass range, the chances for a radio-active AGN to also emit in the X-ray go from  $\sim 15\% \sim 45\%$ , value which reaches  $\sim 78\%$  in the deepest CDFS field. These findings, summarized in the bottom panel of Fig. 1 in order to show the variations from the [Hickox et al. \(2009\)](#) diagram for AGN of different masses, led the authors to conclude that the mass of a galaxy host of an AGN plays a crucial role in determining the AGN level of activity, not only in the case of radio emission alone, but even more so for simultaneous emission in the various bands of the electromagnetic spectrum. No dependence was instead found on the cosmological evolution of these sources (i.e., the probability that an AGN will be simultaneously active at both X-ray and radio wavelengths is the same at all epochs) or on their luminosities (radio and/or X-ray), accreting level of the black hole responsible for the AGN signal or even on the star-forming activity of their hosts.

All the results presented so far clearly indicate that radio emission from an AGN is strongly favoured within galaxies of large stellar mass. In the most extreme case of local and very massive ellipticals there is a general consensus on the fact that almost all them present radio emission at some level, mostly of AGN origin. On the other hand, studies performed at high redshifts indicate that galaxies, especially those with a lower stellar mass content, were more prone to host a radio-AGN than those in the local universe. The reason for such a differential trend in host mass is not totally understood, but could be

explained by invoking different accretion properties (and different cosmological evolutions) for radio-AGN within galaxies of different mass. In this light, a possible connection could be envisaged with the two populations of HERGs and LERGs. As already briefly presented in the Introduction, radio-AGN can be divided into high-excitation radio galaxies (HERGs) and low-excitation radio galaxies (LERGs) according to the absence or presence and relative importance of emission lines in their optical spectra (Hine and Longair 1979). HERGs (which also include quasars) are believed to possess high accretion rates onto their super-massive black holes (producing a total luminosity  $> 0.01 L_{\text{Edd}}$ , where  $L_{\text{Edd}}$  is the Eddington luminosity), as opposed to LERGs for which  $\lesssim 0.01 L_{\text{Edd}}$  (see Heckman and Best 2014 for a review). It is further argued (e.g., Hardcastle, Evans, and Croston 2007) that the difference between HERGs and LERGs is dictated by different sources of fuel. In the first case black holes would accrete cold gas via an accretion disc which produces radiation in an efficient manner, while LERGs would be fuelled by the accretion of hot gas from the haloes of their host galaxies and surrounding environments through advection-dominated flows (ADAFs, e.g., Narayan and Yi 1995) and release the accretion energy in the form of jets or winds (e.g., Merloni and Heinz 2007).

Given the differences between the two populations of HERGs and LERGs, it is then worth investigating whether these also reverberate onto their host galaxies. Indeed, in the recent years, more and more works have considered the host properties of these two populations separately. Heckman and Best (2014) (see also Tadhunter 2016) present a detailed review of the LERGs vs HERGs distinction, so we refer the reader to their work. Here we will just briefly summarize the most important findings and concentrate on the more recent results which are mainly obtained at high redshifts. It is observed that in the local universe HERGs appear within systematically smaller, lower-mass and less concentrated galaxies than LERGs and also exhibit higher levels of star-forming activity (e.g., Smolčić 2009; Smolčić and Riechers 2011; Best and Heckman 2012). Furthermore (Jannsen et al. 2012), HERGs are preferentially found within green (i.e., in the process of being quenched) and blue galaxies, and – at all radio luminosities – the probability for a galaxy to host a LERG exhibits a steeper dependence on the mass ( $\propto M_*^{2.5}$ ) with respect to a HERG ( $\propto M_*^{1.5}$ ). These results are also confirmed by IR observations which clearly show that the vast majority of LERGs is associated with galaxies with WISE (Wright et al. 2010) colours that identify them as ‘early-type’, as opposed to HERGs whose hosts are preferentially ‘late-type’ (Sadler et al. 2014), and also by the fact that HERGs are typically about four times more luminous than LERGs in the FIR, 250  $\mu\text{m}$  band (Hardcastle et al. 2013).

On top of these differences, LERGs and HERGs are also found to present different cosmological evolutions at least up to  $z \sim 1$  (e.g., Best et al. 2014; Pracy et al. 2016; Butler et al. 2019), with LERGs substantially not evolving (or even showing negative evolution, at least for low-luminosity sources, Best et al. 2014) and HERGs presenting a strong degree of positive evolution (e.g.,  $\propto (1+z)^7$  for a pure luminosity evolution model in the work of Pracy et al.



2016). It is to be noted though that there is some inconsistency between the different degrees of evolution as found for the two classes of sources by the various works. Also, cf. Williams et al. (2018) who find in the range  $0.5 < z < 2$  no evolution for HERGs and a negative evolution at all radio luminosities for LERGs.

From the above discussion it then appears that in the relatively local,  $z < 1$ , universe the hosts of LERGs and HERGs are quite different. Things however seem to change at higher redshifts. Fernandes et al. (2015) use *Spitzer* information combined with a SED-fitting approach on a sample of 27,  $z \sim 1$  radio-AGN spanning the range in radio luminosity  $10^{25} < L_{151\text{MHz}}/[\text{WHz}^{-1}] < 10^{28}$  to find that HERG and LERG hosts do not differ from each other, since they all present large ( $10^{10.7} \leq M_*/M_\odot \leq 10^{12}$ ) stellar masses. The only dichotomy shown by the Fernandes et al. (2015) sample is in accretion modes, whereby HERGs accrete at a much higher rate ( $\lambda/\lambda_{\text{Edd}} \gtrsim 0.1$ ), while virtually all LERGs cluster around the value  $\lambda/\lambda_{\text{Edd}} \sim 0.01$  (see also Gürkan et al. 2014 for similar results on accretion rates based on WISE observations).

Delvecchio et al. (2017) consider radio sources from the VLA-COSMOS 3 GHz Large Project (Smolčić et al. 2017b) down to a  $1\sigma$  sensitivity of  $2.3 \mu\text{Jy}$ . Available excellent quality multi-wavelength information up to  $z \sim 6$  allows to sub-divide the sample into 1604 high radiative luminosity AGN (HLAGN, close relatives of HERGs) and 1333 low radiative luminosity AGN (MLAGN, close relatives of LERGs) which are then investigated at the different cosmological epochs. Although a number of differences are observed between these two classes of sources also as a function of redshift, when only radio-active HLAGN (i.e., the 30% of the HLAGN population as selected by Delvecchio et al. 2017 which emit at radio wavelengths because of the presence of a radio-active AGN and not ongoing star-formation within the hosts) are considered, the Delvecchio et al. (2017) analysis shows that MLAGN and HLAGN host properties are largely overlapping, with basically no difference in either star-forming activity or (large) mass distributions at all cosmic epochs. Also, no difference between the distributions of mechanical powers (obtained from AGN-related radio emission) for these two classes of sources is observed.

Butler et al. (2018b) apply similar methods to those described in Delvecchio et al. (2017) to select at 2.1 GHz and up to  $z \sim 4$  1729 LERGs, 1455 HERGs (out of which 296 are defined as radio-quiet by the authors, i.e., with radio emission powered by star-formation) and 558 star-forming galaxies (SFGs) from ATCA observations of the XMM extragalactic survey south field (XXL-S – Pierre et al. 2016; Butler et al. 2018a). 76% of the original radio sample is endowed with multi-wavelength information. According to this study, LERGs and radio-active HERGs tend to reside within hosts with substantially the same stellar mass content, gathering around a median value of  $\langle M_* \rangle \sim 10^{11} M_\odot$ , except for a more pronounced tail exhibited by the distribution of HERGs at lower stellar masses. Larger differences are instead observed in the star-forming properties of these sources, whereby LERGs are mainly found amongst lower star-formation (about a factor 5 less) and redder galaxies than HERGs. However, since the Butler et al. (2018b) analysis has been

carried out without a distinction between more local and more distant sources, it is not possible to discern whether their results are due to intrinsic properties of the two HERG and LERG populations or whether these originate from some cosmological evolution. Indeed, LERGs in the [Butler et al. \(2018b\)](#) sample dominate below  $z \sim 1.2$ , while they almost totally disappear at higher redshifts, when only HERGs are found.

[Williams et al. \(2018\)](#) instead consider 624 radio-AGN with  $L_{151\text{MHz}} \geq 10^{25}$  W Hz $^{-1}$  in the redshift range  $0.5 \leq z \leq 2$  as observed with LOFAR on the Boötes field ([Williams et al. 2016](#)). Multi-wavelength information for these sources is used to classify 297 HERGs, 138 LERGs and 199 SFGs. The relative relevance of these populations varies according to the considered redshift range (more HERGs and SFGs beyond  $z = 1$ ). At all redshifts, LERGs appear in massive,  $M_* \gtrsim 10^{11} M_\odot$ , galaxies. Also HERGs are mainly hosted within massive galaxies, but their distribution presents a tail towards lower,  $M_* \lesssim 10^{10.5} M_\odot$  masses, especially beyond  $z \sim 1$ . Furthermore, while below  $z \sim 1$  the  $u - r$  colours of the galaxies host of LERGs and HERGs show marked differences, with LERGs being systematically redder than HERGs, at higher redshifts there is a larger overlap since HERGs are found within galaxies of all SFRs and LERGs shift to more star-forming systems. On the other hand, while the fraction of LERGs within the general galaxy population show no cosmological evolution – result that suggests the same fuelling mechanism for this class of sources at all  $z \lesssim 2$  ([Best et al. 2014](#)) – that of HERGs instead increases with redshift by a factor  $\sim 3$  at all stellar masses. Also the functional form of the dependence of this fraction on the host mass is different, since [Williams et al. \(2018\)](#) find  $F_{\text{radio-AGN}} \propto M_*^{2-2.5}$  for LERGs, while in the case of HERGs the slope is much flatter, going from the  $z \lesssim 1$  value of  $\sim 0.5$  to  $\sim 1.2$  at  $z \sim 2$ . Such a differential evolution implies that beyond  $z \sim 1$  the fraction of HERGs will always be higher than that of LERGs, except for the most massive galaxies which will be as likely to host a LERG as a HERG.

All the works considered so far converge at indicating that locally LERGs and HERGs do not only differ in terms of their accretion properties but also for what concerns their hosts, which are generally less massive, more star-forming and bluer for HERGs with respect to LERGs. The situation is however less clear at redshifts  $z \gtrsim 1$ , since there seems to be no agreement between conclusions originating from different studies. Indeed, in some cases it is found that HERGs are generally associated to more star-forming galaxies than LERGs (result which once again would hint to the need of cold gas in order to trigger efficient accretion), while in others it is instead reported a substantial overlap between the colours (and therefore star-forming properties) of these two populations. Furthermore, there does not seem to be much of a difference for what concerns the masses of their hosts, possibly except for a tail in the distribution of HERGs below  $M_* \sim 10^{10.5} M_\odot$ . These results which generally point to a less marked distinction between LERGs and HERGs with respect to what observed in the more local universe, likely stem from the cosmological evolution of the general galaxy population. Indeed, not only all galaxies become more star-forming as cosmic noon is approached, but also star-formation activity

preferentially shifts to more massive systems (the so-called *cosmic downsizing*, e.g., [Cowie et al. 1996](#)). Another issue that should also be taken into account when comparing local with high-redshift (and also high-redshift with high-redshift) results is that, while in the local universe the LERG-HERG classification is based on the spectral properties of these sources, for  $z \gtrsim 0.5$  it mainly has to rely on less precise multi-wavelength photometric information and on various selection methods. This gives rise to samples of LERGs and HERGs that might not only differ from each other, but that are also more contaminated than local ones.

### 3.2 What causes the FRI-FRII dichotomy?

From the radio morphological point of view, FRI and FRII galaxies look very different, with the first population appearing as ‘edge-darkened’, while the second one – generally more luminous and more extended (up to Mpc scales) than FRIs and presenting small-scale high surface brightness regions (the so-called hot spots) – as ‘edge-brightened’. The remarkable result obtained by [Fanaroff and Riley \(1974\)](#) was that this morphological classification was strongly related to radio luminosity, with sources fainter than  $L_{408\text{MHz}} = 10^{25} \text{ W Hz}^{-1}$  being almost all FRIs, while for  $L_{408\text{MHz}} > 10^{27} \text{ W Hz}^{-1}$  the overwhelming majority of the sources showed FRII morphologies. Whether this dichotomy, and radio morphology in general, are also the result of factors other than radio luminosity has been the subject of debate for many years (e.g., [Fabbiano et al. 1989](#)). In this section we mainly aim at investigating the role of the host galaxies. Eventual differences in their environmental properties will then be discussed in Sect. 4.

Early works found that, while FRI galaxies were associated to giant ellipticals, the hosts of the radio-brighter FRIIs presented lower optical luminosities and smaller sizes (e.g., [Lilly, McLean, and Longair 1984](#); [Lilly and Prestage 1987](#); [Owen and Laing 1989](#); [Owen and White 1991](#); [Baum, Heckman, and van Breugel 1992](#); [Ledlow and Owen 1996](#); [Zirbel 1996](#)). Their main conclusion was that, since FRIs were also mostly associated with the dominant galaxy (roughly coinciding with the BCG) in relaxed groups or clusters of galaxies, while FRIIs mainly appeared in disturbed galaxies, then these two classes of sources could not be different evolutionary stages of a single object. One possible explanation for this different behaviour (e.g., [Heckman et al. 1986](#)) was attributed to different fuelling mechanisms, with FRII galaxies being the product of collision or merger of galaxy pairs, while FRIs would result from accretion of an intracluster medium. On the other hand, other works (e.g., [Zirbel and Baum 1995](#); [Baum, Heckman, and van Breugel 1992](#)) suggested that intrinsic different properties of the central engine should be the main driver of the difference between FRI and FRII galaxies. On top of this, [Ledlow, Owen, and Keel \(1998\)](#) (see also [Ledlow et al. 2001](#)) reported one of the first evidence for the existence of powerful ( $L_{1.4\text{GHz}} > 10^{24} \text{ W Hz}^{-1}$ ) FRIs hosted by spiral galaxies, proving that – although enormously more common – not all FRIs re-

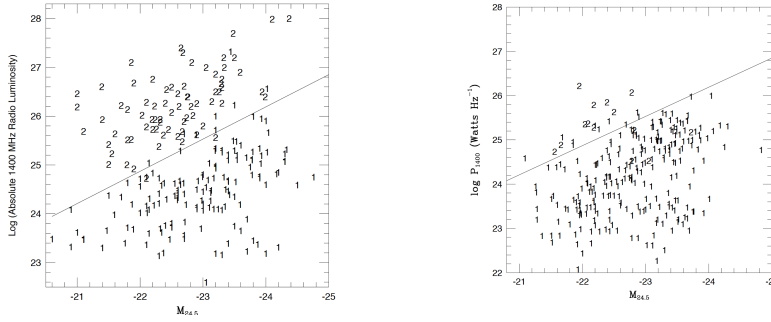


**Fig. 4** Left-hand panel: FRI/II diagram for a sample of objects taken from the literature. Right-hand panel: FRI/II diagram for radio-AGN within the [Ledlow and Owen \(1996\)](#),  $z < 0.25$  cluster sample. Figures from [Ledlow and Owen \(1996\)](#).

side in elliptical galaxies even in the very local universe. It was then clear that the distinction between FRI and FRII sources was everything but a clear-cut case.

In a seminal paper, [Ledlow and Owen \(1996\)](#) consider observations taken from the literature in the redshift range  $z = 0.01 - 0.5$  and for different environments to investigate the dependence of radio morphology on both radio luminosity and optical luminosity of the hosts. It was found that the FRI/II division was a strong function of the optical luminosity of the host galaxy, with radio-AGN above the dividing line  $L_{\text{radio}} \propto L_{\text{optical}}^{1.8}$  being all FRIIs, while those below it being all FRIs. This implied that FRI galaxies could also be found at radio powers equivalent to FRII sources but in galaxies one or two magnitudes brighter (cf. left-hand panel of Fig. 4), and more importantly suggested that “the optical luminosity and the properties of the host galaxy are the most important parameters which affect radio source formation and evolution”, even though no strong dependence of the AGN radio luminosity on the host optical luminosity was reported. On the other hand, in the same work it was also noticed that when considering a more homogeneous and local sample of sources within a cluster environment, some (although very few) FRII galaxies lay below the FRI/FRII dividing line (cf. right-hand panel of Fig. 4). Not much could be however concluded from this finding, given the general paucity of FRII sources. The plot of [Ledlow and Owen \(1996\)](#) quickly gained high visibility and [Ghisellini and Celotti \(2001\)](#) converted it into an AGN-power vs black hole mass relation, with the dividing line between FRI and FRII sources representing a constant ratio between AGN power and Eddington luminosity of the black hole. This suggested the FRII-FRI dichotomy to be determined by a change in the accretion mode, from a radiatively efficient to an inefficient one, possibly in connection with the ageing of the FRII population. We will get back to the ageing issue later in this Section.

As already noted by the authors themselves, the work of [Ledlow and Owen \(1996\)](#) though suffered from a number of biases due to the fact that they used a highly heterogeneous sample of sources taken from the literature. As a result

of that, the population of FRI galaxies lay at redshifts  $z < 0.1$ , while FRIIs were generally found beyond  $z = 0.25$ . Due to a strong redshift-luminosity correlation, this generates a Malmquist bias (only brighter sources are visible at higher redshifts) which is very difficult to disentangle from physically-based effects (e.g., Singal and Rajpurohit 2014). Best (2009) repeated the Ledlow and Owen (1996) analysis for their much more homogeneous sample of  $\sim 1000$  local FIRST and NVSS galaxies endowed with a SDSS counterpart which exhibited extended radio morphologies. Although most of the sources above the Ledlow and Owen (1996) limit were indeed FRII galaxies, while below it they were more likely FRIs, a very large overlap between these two populations in the region below the dividing line was observed. Best (2009) showed that FRIIs in the overlapping region were on average smaller in the radio maps than FRIs. No further difference was instead found in terms of black-hole or host galaxy, apart from a tendency for the hosts of FRIs to be more extended. According to Best (2009), this led to the conclusion that more massive and more extended galaxies are more likely to disrupt the radio jets, therefore leading to an FRI morphology.

Lin et al. (2010) also consider a homogeneous sample of  $\sim 1000$ , FIRST & NVSS  $z < 0.3$  radio-AGN classified according to both their radio morphology and nuclear emission line activity. Similarly to the Best (2009) (but see also Wing and Blanton 2011) results, they find that FRI and FRII sources overlap in their host galaxy properties, except for the sub-class of very extended and high emission-line luminosity FRIIs which are hosted by lower mass galaxies, live in relatively sparse environments, and likely have higher accretion rates onto their central supermassive black hole. Based on these results, Lin et al. (2010) discuss the possibility of radio morphologies being determined by the joint effect of nuclear accretion (playing the primary role) and environment, with bright FRIIs originating from high-accretion rates and FRIs from low-accretion rates within dense galactic structures.

An entirely different point of view was instead provided by Sadler et al. (2014) who analyse 202,  $< z = 0.058 >$  radio-AGN selected at 20 GHz with counterparts from the 6dFGRS. Although with some overlap between the two classes of sources (46 FRIs and 16 FRIIs), Sadler et al. (2014) indeed confirm the Ledlow and Owen (1996) relation to hold even at high frequencies. Furthermore, these authors observe that the FRIIs and FRIs belonging to their sample exhibit marked differences in terms of MIR/WISE (Wright et al. 2010) colours of the host galaxies, as  $\sim 93\%$  of FRIs were found within the population of early-type galaxies, while  $\sim 93\%$  of FRIIs were found to be associated with late-type (i.e., star-forming galaxies and quasars) galaxies. This clearly indicated a near-complete dichotomy between the hosts of FRI and FRII sources.

The reason for such a disagreement between the findings of Sadler et al. (2014) and those of e.g., Best (2009) and Lin et al. (2010) is unclear, as all of them refer to homogeneous samples of local galaxies so that systematic biases should be minimal. Part of the difference could be due to the different flux limits (40 mJy for the AT20G survey used by Sadler et al. (2014) vs 2.5 mJy for

NVSS) and to slightly different classification schemes adopted in the different works. On the other hand, another possibility could be the selection at different frequencies, since it is known that – unlike those carried out at  $\nu \leq 1.4$  GHz – high-frequency surveys preferentially include flat-spectrum sources (e.g., [De Zotti et al. 2010](#); [Massardi et al. 2011](#)). To test for this effect, we can refer to the results of [Vardoulaki et al. \(2021\)](#) who investigate the FRI-FRII dichotomy by considering 59 FRII, 39 FRI and 32 hybrid FRI/FRII galaxies spread between redshift 0 and  $\sim 2.5$  (peak in the distribution at  $z \sim 1$ ), selected at 3 GHz in the COSMOS field ([Smolčić et al. 2017b](#)). However, despite a selection frequency higher than 1.4 GHz (although not by a large amount), at variance with [Sadler et al. \(2014\)](#), no difference either in the hosts or in the environments (cf. Sect. 4.2) of these two populations was reported. It should however be kept in mind that the [Sadler et al. \(2014\)](#) analysis was carried out for very local sources, while that of [Vardoulaki et al. \(2021\)](#) embraces objects up to  $z \sim 2.5$ , therefore including any possible cosmological evolution of the FRI and FRII populations. Interestingly enough though, [Vardoulaki et al. \(2021\)](#) find that as many as  $\sim 50\%$  of the sources in their sample classified as FRIIs at 3 GHz are recognised as FRIs at 1.4 GHz. The authors attribute this effect to the combination of higher sensitivity and resolution of the 3 GHz sample with respect to those of other 1.4 GHz surveys, or alternatively to synchrotron ageing/losses, although the small frequency difference disfavours this second option. Whatever the reason, given the unexplained disagreement between the FRI vs FRII results obtained at 20, 3 and 1.4 GHz, this is an issue that should be carefully better investigated with further data to come.

[Mingo et al. \(2019\)](#) provide the most comprehensive analysis to date of the FRI-FRII dichotomy based on both radio luminosity and host properties. Their sample include 5805 extended radio-AGN from the LoTSS DR1. 1213 FRIs and 345 FRIIs were subsequently identified via automatic tools complemented by visual inspection at  $z < 0.8$ , where this redshift limit was chosen to minimise selection biases, including that of host galaxy coverage. Their analysis clearly shows that there is a huge overlap between the properties of the two FRI and FRII populations. Indeed, while about only 10% of FRIs lie above the radio luminosity break identified by [Fanaroff and Riley \(1974\)](#), as many as 63% of FRIIs are found below that limit. FRII galaxies appear to fill the entire [Ledlow and Owen \(1996\)](#) plane, just as a non-negligible fraction of FRIs is located on its top half (top panel of Fig. 5). The relevant sub-population of low-luminosity FRIIs (i.e., FRII galaxies below the [Ledlow and Owen 1996](#) dividing line) was further compared to its high-luminosity counterpart matched in redshift and distribution of physical sizes, finding that both samples share the same properties, except for host  $K$ -band luminosities (proxy for stellar mass): low-luminosity FRIIs are observed to inhabit fainter (i.e., smaller) galaxies than those hosting higher-luminosity FRIIs. Based on this result, the authors conclude that the majority of radio-faint FRIIs are indeed sources inhabiting relatively sparse environments that prevent their radio jets from being disrupted, at variance with what is expected to happen to FRI sources which are mainly found to reside within overdense structures. [Mingo](#)



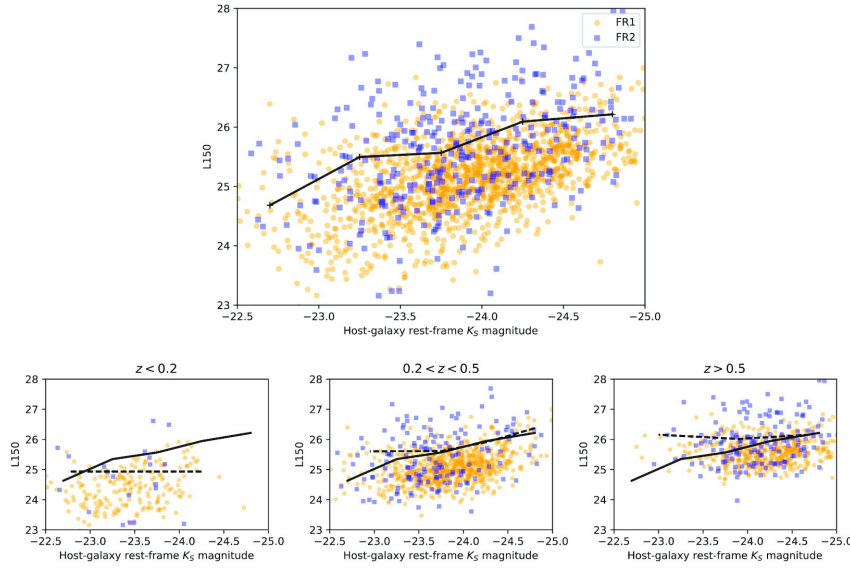


**Fig. 5** Top: the relationship between radio morphology, radio luminosity, and host-galaxy magnitude (a ‘Ledlow & Owen’ plot). The black line indicates the luminosity above which the normalized probability of finding an FRII exceeds that of finding an FRI. Bottom row: the same sample split into three redshift bins, with dashed lines indicating the break luminosity determined for each redshift slice, and the solid lines showing the full-sample relation as in the upper panel. Figures from [Mingo et al. \(2019\)](#).

[et al. \(2019\)](#) explain the general absence of low-luminosity FRIIs from early works as due to the combination of high flux limits of the e.g., 3CR survey ([Bennett 1962](#), see [Laing, Riley, and Longair 1983](#) for an updated version) on which these previous studies were mostly based, together with the rarity of such sources in the local universe (bottom panels of Fig. 5).

### 3.2.1 HERGs vs LERGs and the FRI-FRII dichotomy

So far we have only concentrated on radio morphology, with the distinction into FRI and FRII classes of sources. However, as already seen in Sect. 3.1, radio-AGN can also be sub-divided into HERGs and LERGs. To a zero-th order approximation, FRI galaxies are closely connected to LERGs while FRIIs are strictly related to HERGs. Indeed, in most cases, FRIs and LERGs share the same host properties just as FRIIs and HERGs do, with FRIs and LERGs generally appearing within massive red and passive ellipticals, while FRIIs and HERGs within relatively lower-mass, bluer star-forming galaxies (e.g., [Baldi and Capetti 2008](#); [Smolčić 2009](#); [Buttiglione et al. 2010](#); [Jannsen et al. 2012](#); [Best and Heckman 2012](#); [Hardcastle et al. 2013](#)). However, differences exist, in the sense that it is not unlikely to find mixed populations of sources, especially FRIIs which are also LERGs (e.g., [Laing et al. 1994](#); [Tadhunter et al. 1998](#); [Hardcastle et al. 2006](#); [Sadler et al. 2014](#); [Capetti et al. 2017b](#); [Mingo et al.](#)



2022). It is then worth investigating the properties of FRI and FRII galaxies also in connection with their HERG/LERG distinction.

For instance, it has been known for some years (e.g., Chiaberge, Capetti, and Celotti 1999, 2000; Baldi et al. 2010) that the FRI-FRII distinction is not univocally connected with the optical properties of the nuclei of these sources, since while FRIs of all luminosities are a substantially homogeneous population – with optical/NIR and radio core luminosities being strongly correlated – FRIIs show a much more complex behaviour, with  $\sim 30 - 50\%$  of them exhibiting nuclear properties typical of FRI galaxies. This indicates a common structure of the central engine despite the differences in radio morphology and radio power. More recently, Buttiglione et al. (2010) presented spectroscopy for a  $z < 0.3$  sample of 104 3CR sources. And while they do reproduce the Ledlow and Owen (1996) result (but with the caveat of sampling radio-bright sources), they also find a large fraction ( $\sim 30\%$ ) of FRII galaxies associated with LERG nuclei, with LERGs spanning all the probed radio luminosity range. On the other hand, HERGs were only observed in association with radio-bright FRII sources. About  $\sim 30\%$  of HERGs showed prominent broad lines in their optical spectra, while this does not happen in any of the LERGs. A substantial superposition of the host galaxy luminosities is also reported. Based on these results, Buttiglione et al. (2010) conclude that the LERG vs HERG dichotomy is dictated by different accretion modes set by the initial temperature of the infalling gas (hot vs cold, see also Best and Heckman 2012).

Capetti, Massaro, and Baldi (2017a,b) present two catalogues of 219 FRI and 122 FRII galaxies selected at  $z < 0.15$  from the Best and Heckman (2012) sample. In agreement with some of the previous works, they found that, while the population of FRI hosts is remarkably homogeneous, being composed by all luminous red early-type galaxies, spectroscopically classified as LERGs and containing large mass black holes, FRIIs do behave very differently. First of all, in the Capetti et al. (2017b) sample, only 10% of FRIIs are HERGs, all the remaining sources being classified as LERGs. Furthermore, 75% of them lie below the dividing line identified by Ledlow and Owen (1996). FRII LERG hosts also exhibit properties which are very similar to those of FRIs, being once again all luminous red elliptical galaxies, hosting massive ( $M \gtrsim 10^8 M_\odot$ ) black holes. Even the median radio luminosity of FRII LERGs was observed to be only a factor  $\sim 3$  higher than that measured in FRIs. On the other hand, in agreement with Lin et al. (2010), the few FRII HERGs are found to be very different from the other two sub-populations, since they are associated with lower mass black holes and with hosts which are fainter, optically bluer and MIR redder. At variance with the Ledlow and Owen (1996) but also with the Mingo et al. (2019) results, the main conclusion of Capetti et al. (2017b) is that radio morphology is not related to different properties of the host galaxy, except in the rare cases of FRII HERGs. Similar results on the independence of radio morphology on the host galaxy properties has been recently obtained by Jimenez-Gallardo et al. (2019) by comparing their sample of local, small extension ( $< 60$  Kpc), FRII galaxies to that of FRI galaxies from Capetti

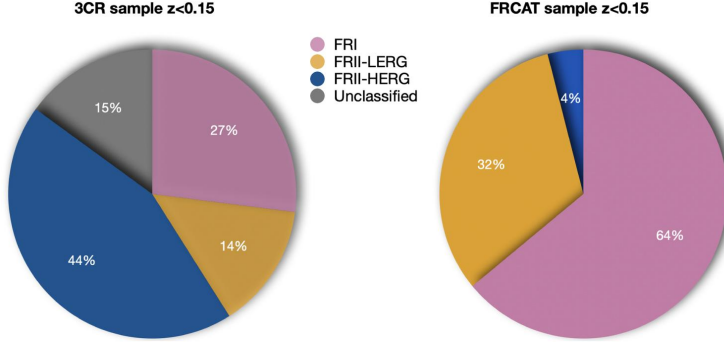


**Fig. 6** Fraction of FRI and FRII radio galaxies with  $z < 0.15$  in the 3CR (left panel) and in the [Capetti et al. \(2017a,b\)](#) (right panel) catalogues. The relevance of LERGs dramatically increases moving down to fainter sources. Figure from [Grandi et al. \(2021\)](#).

[et al. \(2017a\)](#), as both populations are spectroscopically classified as LERGs and found to be hosted in red, early-type galaxies.

[Miraghaei and Best \(2017\)](#) also consider FRI and FRII galaxies and their sub-division into LERGs and HERGs. The FRI/FRII dichotomy was investigated by studying a sample of 108,  $z < 0.1$  FRI LERGs and FRII LERGs with the same stellar mass and total radio luminosity distribution, drawn from the FIRST and NVSS catalogues with a flux cut of  $F_{1.4\text{GHz}} > 40$  mJy. At variance with the results of [Capetti et al. \(2017b\)](#) and [Massaro et al. \(2019, 2020\)](#), it is found that FRIs reside in richer environments (cf. Sect. 4), are hosted by smaller galaxies with higher concentration, higher mass-surface density and higher black hole-to-stellar mass ratio than FRIIs. These findings lead the authors to conclude that their data prefers models employing extrinsic parameters (i.e., jet disruption by the interstellar and intergalactic media) rather than intrinsic ones (e.g., nuclear or jet content) to explain the FRI/FRII dichotomy. At the same time, HERGs are found in more star-forming and disk galaxies, supporting the theory that AGN fuelling source is the main origin of the HERG/LENG dichotomy.

A still different point of view is that provided by [Macconi et al. \(2020\)](#) and [Grandi et al. \(2021\)](#) who investigate the FRI-FRII dichotomy from the jet-accretion system point of view, the former authors concentrating on brighter 3CR sources, [Grandi et al. \(2021\)](#) instead re-considering the [Capetti et al. \(2017a,b\)](#) samples. After restating that in the local,  $z \lesssim 0.15$  universe lowering radio fluxes leads to the appearance of a large number of FRII LERGs

which were basically unobserved in brighter surveys (cf. Fig. 6), Grandi et al. (2021) find that the majority of the analyzed radio sources (excluding the very few FRII HERGs) are at a late stage of their life, both in terms of host properties (which exhibit evolved stellar populations) and accretion capabilities (more massive black holes producing an inefficient engine). This evidence makes the authors envisage an evolutionary scenario whereby FRII-LERGs are aged FRII-HERGs (see also Tadhunter 2016), even if other explanations such as intrinsic differences related to the black hole properties (e.g., spin or magnetic field at its horizon) cannot be excluded. According to this theory, once the nuclear cold fuel has been consumed, the accretion configuration becomes hot and inefficient, even though the extended radio structures still maintain traces of the past activity. Eventually, the ageing process will move along the lobes and these sources will ultimately turn into FRIs.

At the time of writing, the last word on the FRI-FRII vs LERG-HERG dichotomy is that presented by Mingo et al. (2022), who consider a sample of 287 (161 FRIs and 126 FRIIs),  $z \lesssim 2.5$  sources, selected within the LOFAR Two Metre Sky Survey Deep Fields dataset (Tasse et al. 2021; Kondapally et al. 2021; Duncan et al. 2021; Sabater et al. 2021) to have large ( $> 27$  arcsec) separations between their components. Reliable SED information on which to base the LERG/HERG classification is also provided (Best et al. 2022 submitted). 21 sources (out of which 19 FRIIs) are found with sizes greater than 1 Mpc (the so-called giant radio galaxies or GRGs, e.g., Dabhade et al. 2020), showing a non-negligible contribution of this sub-population to the extended source radio counts in deep enough radio surveys. In agreement with previous works, 95% of FRIs are found to be LERGs, while 29% of FRIIs are HERGs, the remaining being associated to the sub-class of LERGs. According to the authors, the fact that LERGs are the dominant sub-population across all morphological types and radio luminosities argues against either accretion mode or jet power as the cause for large-scale radio-morphology. Further, by analysing a sample of FRI and FRII galaxies within the same radio luminosity range, it has been observed that FRIIs inhabit less massive galaxies than FRIs. At the same time, HERGs are strongly favoured within systems with high specific star formation rates (sSFRs). Based on these pieces of evidence, Mingo et al. (2022) conclude that it is the properties of the host galaxy that determine the characteristics of the radio-AGN inhabiting its center, with mass mainly controlling the FRI-FRII dichotomy and gas availability (as inferred from the sSFR) in charge of the LERG vs HERG distinction.

With the data currently at hand, which also includes evidence for a class of hybrid double sources, with a FRI jet on one side and a FRII lobe on the other (e.g., Harwood, Vernstrom, and Stroe 2020 and references therein) and also examples of FRI galaxies with clear quasar nuclei (e.g., Heywood, Blundell, and Rawlings 2007), it is clear that we are far from reaching a consensus on the physical processes that determine the different morphologies in radio-AGN. In particular, two distinct scenarios for the FRI-FRII dichotomy have emerged. The first one attributes differences in radio morphology to the large-scale properties (i.e., host galaxy and environment) of radio-AGN which are expected

to influence the interaction of the radio jet with the external medium (e.g. [Ledlow and Owen 1996](#); [Zirbel 1996](#); [Kaiser and Best 2007](#); [Wing and Blanton 2011](#); [Miraghaei and Best 2017](#); [Mingo et al. 2019, 2022](#)). According to this scenario, differences between HERGs and LERGs would instead be dictated by different fuelling mechanisms, with HERGs powered by accretion of cold gas, provided by e.g., a recent merger with a gas-rich galaxy (e.g., [Jannsen et al. 2012](#)), while LERGs accrete hot intergalactic gas from dense environments at a low rate, with fuelling from major mergers being strongly disfavoured by recent observations (e.g., [Ellison, Patton, and Hickox 2015](#)).

On the other hand, other works do not observe any difference in the host and/or environmental properties of FRI and FRII galaxies except in the rare cases of FRII HERGs (e.g., [Lin et al. 2010](#); [Capetti et al. 2017b](#); [Jimenez-Gallardo et al. 2019](#); [Massaro et al. 2019, 2020](#); [Vardoulaki et al. 2021](#)), so that an alternative mechanism for their large-scale radio behaviour has to be invoked. In this second scenario, ageing processes can be thought as the main driver for the observed morphological differences, with an evolutionary pattern that proceeds from FRII HERGs that switch from efficient to inefficient accretion due to gas starvation and transform themselves into FRII LERGs, sources that still maintain their large radio structures thanks to the past nuclear activity at high efficiency (e.g., [Ghisellini and Celotti 2001](#); [Tadhunter 2016](#); [Macconi et al. 2020](#); [Grandi et al. 2021](#)). The switch off/change in accretion mode will eventually show in the radio morphology with the delay needed to reach Kpc-to-Mpc distances, and the source will ultimately turn into an FRI galaxy.

### 3.3 Are radio-AGN all hosted in red and dead galaxies?

As we already saw in Sect. 3.1, at low  $-z \lesssim 1$  – redshifts, galaxies hosting radio-AGN are dominated by well evolved stellar populations (age  $\sim 8 - 14$  Gyr – e.g., [Nolan et al. 2001](#); [Best et al. 2005a](#)), exhibit a general absence of ongoing star-formation (e.g., [Siebenmorgen et al. 2004](#); [Dicken et al. 2012](#)) or – when present – normally lower than the hosts of their radio-quiet counterparts (e.g., [Hardcastle et al. 2010](#); [Chen et al. 2013](#); [Virdee et al. 2013](#); [Gürkan et al. 2015](#); [Pace and Salim 2016](#)), have rather low dust/gas masses (e.g., [Knapp and Patten 1991](#)), and lie in the same region of the fundamental plane as normal inactive ellipticals (e.g., [McLure et al. 1999](#)). Although differences according to radio-AGN type have been found – with HERGs being on average associated to a factor  $\sim 2-3$  higher star-forming activity than LERGs (e.g., [Hardcastle et al. 2013](#); [Gürkan et al. 2015](#)) – the above pieces of evidence have prompted the introduction of the so-called *radio-mode* feedback in theoretical simulations in order to halt star-formation in massive galaxies and produce the locally observed ‘red and dead’ population of ellipticals (e.g., [Croton et al. 2006](#); [Bower et al. 2006](#); [Best et al. 2006](#); [Fanidakis et al. 2012](#); [Weinberger et al. 2018](#); [Smolčić et al. 2017a](#)), both in terms of physical properties and number density. According to this paradigm, the accretion of matter onto a radio-

active AGN does not lead to a powerful radiative output, but rather to the production of highly energetic jets that can heat (or even expel) the cold gas within galaxies and suppress star-formation.

Cosmological evolution for these sources is however expected from theoretical grounding, and since long-standing evidence suggests that the most of the hosts of radio-AGN have evolved only passively since at least  $z \sim 1$  (e.g., Lilly and Longair 1984; Best et al. 1998; McLure and Dunlop 2000; Jarvis et al. 2001), this means that their epoch of formation must be pushed back to higher redshifts, likely earlier than the so-called ‘cosmic noon’ at  $z \sim 2$  when both galaxies and AGN experienced the peak of their activity (cf. Madau and Dickinson 2014 for a review on this topic). As a consequence of this scenario, both the gas mass and star forming activity within the hosts of radio-active AGN should be strongly increasing functions of redshift as one approaches  $z \gtrsim 2$ .

Indeed, observational evidence for increased star-forming activity with look-back time is presented already between  $z < 0.3$  and  $z \sim 0.6$  by e.g., Chen et al. (2013) for their sample of 1600,  $M_* > 10^{11.4} M_\odot$  radio-active AGN selected from FIRST and NVSS (cf. Fig. 7). Strong evidence for powerful star-formation was also provided by rest-frame UV observations of the hosts of 13 high-redshift ( $2 \lesssim z \lesssim 4$ ) radio galaxies (Pentericci et al. 1998, 1999, see Miley and De Breuck 2008 for a review) which showed morphologies characterised by clumpy structures – likely the sites of ongoing star-formation – or by observations of the  $z = 3.8$ , 4C 41.17 radio galaxy which returned estimates for the rate of ongoing massive star formation activity,  $\sim 10^3 M_\odot \text{ yr}^{-1}$  (Dey et al. 1997). And, as already discussed in Sect. 3.1, also the works of e.g., Smolčić et al. (2009), Williams and Röttgering (2015) and Lin et al. (2017) hint to a switch in the host properties of radio-AGN towards more star-forming systems at  $z \gtrsim 1$ .

However, it has been only with the advent of facilities such as *Spitzer* (Werner et al. 2004), *Herschel* (Pilbratt et al. 2010) and the Sub-millimetre Common User Bolometer Array (*SCUBA*, Holland et al. 1999) which allowed to systematically sample the infrared (both near and far) and sub-millimetre skies to high sensitivity levels, that it has become more and more clear that – especially at high,  $z > 1.5$ , redshifts – radio-active AGN often cohabit with episodes of intense star-formation. Archibald et al. (2001) observed in the sub-millimetre 47 bright ( $L_{151 \text{ MHz}} \gtrsim 10^{25} \text{ W Hz}^{-1} \text{ sr}^{-1}$ ) radio galaxies in the redshift range  $0 < z < 5$ , finding that their typical sub-millimetre luminosities (and hence dust masses) were a strongly increasing function of redshift, with  $L_{850 \mu\text{m}} \propto (1+z)^3$ , in line with the hypothesis of enhanced star-formation within radio-AGN hosts at earlier cosmological epochs. Reuland et al. (2004) expanded on the work of Archibald et al. (2001) by adding 24 radio-AGN, many of which at  $z > 3$ . They confirmed the Archibald et al. (2001) conclusion for a strong redshift evolution of the sub-millimetre luminosity of these sources, found to be associated with intense star-forming activity, with rates of up to a few thousand  $M_\odot \text{ yr}^{-1}$ . Seymour et al. (2007) instead used *Spitzer* observations at all available wavelengths for 69 radio-AGN with  $L_{3 \text{ GHz}} > 10^{26} \text{ W Hz}^{-1}$

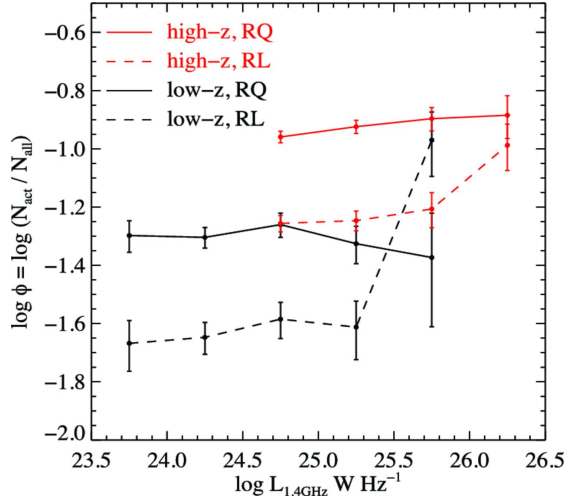


**Fig. 7** Fraction of actively star-forming galaxies as a function radio luminosity. The dashed and solid lines respectively indicate radio-AGN (RL) and the radio-quiet (RQ) control samples, matched in redshift, stellar mass, spatial location and velocity dispersion. High-redshift data (represented in red) refer to  $z \sim 0.6$ , while low-redshift data to  $z < 0.3$ . Figure from [Chen et al. \(2013\)](#).

and  $1 < z < 5.2$ . In agreement with the previous works, it was concluded that these sources not only are associated to very massive,  $M_* \simeq 10^{11}\text{--}10^{12} M_\odot$ , galaxies, but also that most of them can be classified as Luminous Infrared Galaxies (LIRGs) or even as Ultra-Luminous Infrared Galaxies (ULIRGs), given that they exhibit MIR luminosities  $> 10^{11} L_\odot$ . [Magliocchetti, Andreani, and Zwaan \(2008a\)](#) come to the same conclusion for concurrent AGN and star-forming activity in their sample of  $z \sim 1\text{--}3$  radio sources observed with *Spitzer* at  $24\mu\text{m}$  in the First Look Survey field ([Fadda et al. 2004](#)). [Rawlings et al. \(2013\)](#) also derive from MIR, *Spitzer* spectroscopy of seven,  $1.5 < z < 2.6$ , very powerful ( $L_{500\text{MHz}} = 10^{27.8} - 10^{29.1} \text{ W Hz}^{-1}$ ) radio-AGN extremely high star-formation rates, of up to  $\sim 10^3 M_\odot \text{ yr}^{-1}$ , with no significant correlation between radio emission and star formation activity.

A leap forward in the field though is provided by the work of [Seymour et al. \(2011\)](#) who use both *Herschel*-SPIRE ([Griffin et al. 2010](#)) and *Spitzer* data for a sample of 32 powerful radio sources with  $L_{1.4\text{GHz}} = 10^{25} - 10^{26.5} \text{ W Hz}^{-1}$  to derive their total (i.e.,  $[8\text{--}1000] \mu\text{m}$ ) infrared luminosities. Data were subdivided into moderate-redshift ( $0.4 < z < 0.9$ ) and high-redshift ( $1.2 < z < 3$ ) sub-samples and then compared to local ( $z < 0.1$ ) 3CRR sources with available *Spitzer* information ([Dicken et al. 2010](#)). By also taking into account  $250\mu\text{m}$  non-detections, [Seymour et al. \(2011\)](#) estimate the total mean star-formation rates for the three sub-samples to be:  $\sim 3.7$ ,  $29.5 \pm 11.6$  and  $581 \pm 143 M_\odot$ .

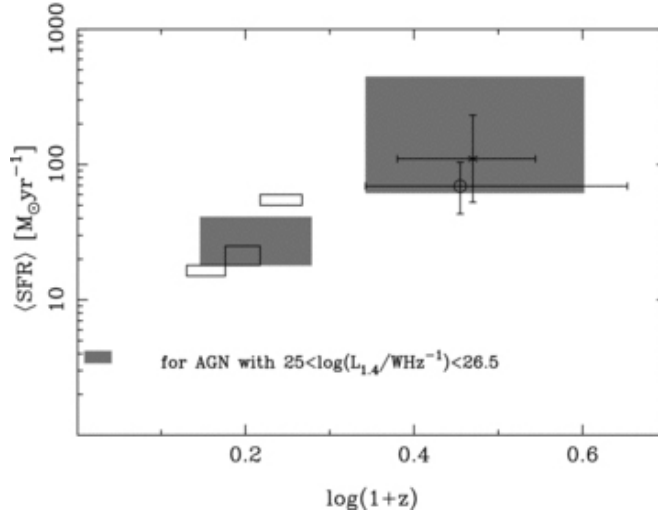


**Fig. 8** Range of mean SFRs plotted as a function of redshift for radio-AGN with  $10^{25} \leq (L_{1.4 \text{ GHz}}/\text{W Hz}^{-1}) \leq 10^{26.5}$  (shaded regions). The open rectangles indicate the results from [Hardcastle et al. \(2010\)](#) using *Herschel* observations of sources with a similar range of radio luminosities. The points with error bars present the approximate mean SFRs of X-ray-selected AGN over the range of redshifts indicated from [Lutz et al. \(2010\)](#) (open circle) and [Shao et al. \(2010\)](#) (asterisk). Figure from [Seymour et al. \(2011\)](#).

$\text{yr}^{-1}$  respectively at low-, moderate- and high-redshift (cf. Fig. 8). This implies an extremely steep increase of the star-formation activity associated with radio-AGN,  $\text{SFR} \propto (1+z)^{4.2 \pm 0.8}$ , with a degree of evolution larger than what observed for the general population of star-forming galaxies. According to the authors, this might indicate that at least some of the inferred star formation may be directly associated with the AGN radio outputs, although no dependence of the star-formation activity on radio luminosity is reported for these sources. [Drouart et al. \(2014\)](#) also considered  $[3.6\text{--}870] \mu\text{m}$  multi-wavelength information for a sample of 70,  $L_{3\text{GHz}} > 10^{26} \text{ W Hz}^{-1}$  radio-AGN spanning the range  $1 < z < 5.2$ , finding that almost all the hosts are ULIRGs with total infrared luminosities  $L_{\text{IR}} > 10^{12} L_{\odot}$ , corresponding to SFRs of up to  $5000 M_{\odot} \text{ yr}^{-1}$ . Again, no connection was found between IR and AGN luminosity. These authors also report higher levels of star-forming activity in radio-AGN at  $z > 2$  with respect to their lower redshift counterparts, as well as a faster growth in terms of stellar assembly when compared to the population of inactive,  $z \gtrsim 2$ , star-forming galaxies (cfr. [Weinmann et al. 2011](#) and references therein). A very similar result is obtained by [Podigachoski et al. \(2015\)](#) who concentrate on a complete sample of 64,  $z > 1$ , 3CR sources. The median infrared luminosity for these radio-AGN is estimated from *Herschel* and *Spitzer* observations to be  $\langle L_{\text{IR}} \rangle \sim 2 \cdot 10^{12} L_{\odot}$ , corresponding to SFRs  $\sim 100 - 1000 M_{\odot} \text{ yr}^{-1}$ . Also, in agreement with [Seymour et al. \(2011\)](#) and [Drouart et al. \(2014\)](#), no



strong correlation between AGN activity and luminosity due to star formation is found.

These results provide clear, breakthrough evidence for intense star forming activity ongoing within galaxies hosting a radio-AGN at high,  $z \gtrsim 1$ , redshifts. However, they are all limited to the bright end of the luminosity distribution at both radio and FIR wavelengths, and therefore by construction miss the bulk of the population of radio-AGN, both in terms of faint radio emission and low,  $\lesssim 100 M_{\odot} \text{ yr}^{-1}$ , star-formation rates. Magliocchetti et al. (2014b, 2016, 2018a) fill this gap by considering radio-AGN selected in the deepest cosmological fields known to date (COSMOS – Magliocchetti et al. 2014b, 2018a and GOODS North, GOODS South and Lockman Hole – Magliocchetti et al. 2016). These fields not only are covered with extremely deep 1.4 GHz and *Herschel* observations (fluxes down to  $\sim 6 \mu\text{Jy}$  and 0.9, 0.6 and 1.3 mJy, respectively at 1.4 GHz and 70, 100 and 160  $\mu\text{m}$ ), but can also rely on a huge amount of multi-wavelength information. Furthermore, since observations on COSMOS are somehow shallower but obtained on a larger area than those on the other three fields, the combination of them allows for the first time to probe, with a good statistical significance, both the mid- and faint-luminosity regimes. The total number of radio-AGN selected on the basis of their radio luminosity (cf. Sect. 2) on the four fields is  $\sim 800$ , 325 of them with a FIR counterpart in the deep PACS Evolutionary Probe (PEP – Lutz et al. 2011) maps. The percentage of FIR identifications greatly varies as a function of FIR depth across the fields, from 39% in the shallower COSMOS, to 72% in GOODS North. No dependence is instead found on either radio flux or redshift, at least for  $z \lesssim 3.5$ . In agreement with all previous studies, the authors find that the hosts of these sources all exhibit very large stellar masses, with 90% of them with  $M_* > 10^{10.5} M_{\odot}$  and 50% with  $M_* > 10^{11} M_{\odot}$ . Also, irrespective of the level of radio-AGN activity, FIR emission was proved to stem from star-forming processes ongoing within the host galaxies and not observed to affect the AGN output, at least at radio wavelengths. More importantly, the Magliocchetti et al. (2014b, 2016, 2018a) analyses clearly indicate that the level of star-forming activity within the hosts of radio-AGN presents a dramatic increase with look-back time, and that relatively powerful radio-AGN much more likely cohabit with a star-forming event at the earliest epochs: indeed, if the probability for FIR emission from the  $z < 1$  host of a  $L_{1.4\text{GHz}} \sim 10^{25.5} \text{ W Hz}^{-1} \text{ sr}^{-1}$  ( $L_{1.4\text{GHz}} \sim 10^{23.5} \text{ W Hz}^{-1} \text{ sr}^{-1}$ ) AGN is  $\sim 0\%$  ( $\sim 20\%$ ), this becomes  $\sim 40\%$  ( $\sim 50\%$ ) at  $z > 2$  (cf. the top panel of Fig. 9). Furthermore, the deep data available for the Lockman Hole and the two GOODS fields shows that virtually *all* radio-AGN beyond  $z \sim 1$  co-exist with a star-formation event of intensity as low as  $\text{SFR} \sim 10 M_{\odot} \text{ yr}^{-1}$ , which proceeds independently of AGN radio luminosity (cf. bottom panels of Fig. 9). These findings put together then imply that negative feedback is present in radio-AGN hosts *only* in the local,  $z < 1$  universe, and with an effectiveness that strongly decreases for decreasing AGN radio power.

As a last step, it is also worth highlighting a number of works that have recently made use of IR information to investigate the star formation histories of

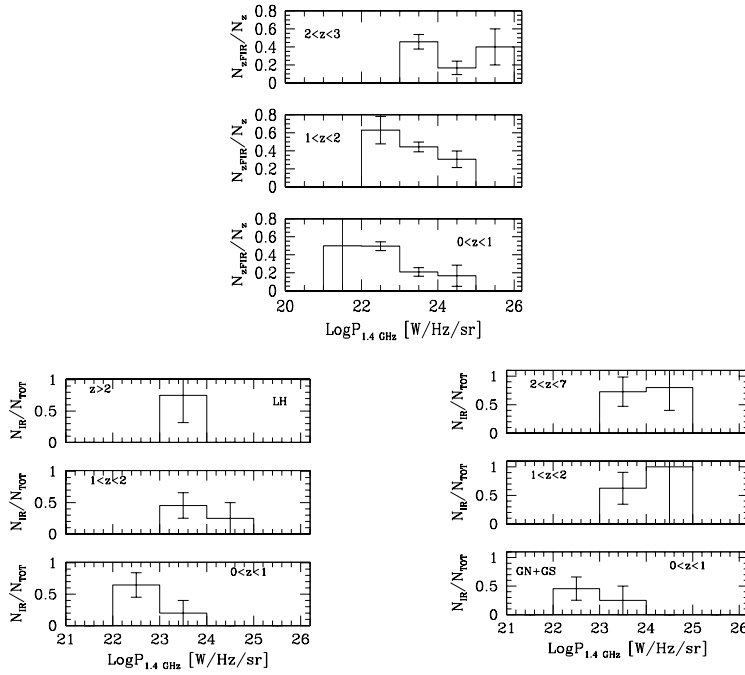


**Fig. 9** Fraction of FIR emitters amongst radio-selected AGN as a function of radio luminosity at different cosmological epochs. The top panel refers to the COSMOS field, while the labels ‘LH’ and ‘GN+GS’ respectively to the Lockman Hole and the combined GOODS North and GOODS South. Figures from [Magliocchetti et al. \(2016\)](#) and [Magliocchetti et al. \(2018a\)](#).

samples of radio-AGN not selected uniquely in radio luminosity as those presented so far, and that further provide comparisons between the star-forming activities of radio-active and radio-quiet populations. [Del Moro et al. \(2013\)](#) find that  $\sim 86\%$  of their 51,  $0 < z < 3$ , AGN presenting a radio excess with respect to the IR-radio relation (cf. Sect. 3.4) have a far-infrared spectrum dominated by star-formation, although their specific star formation rates (sSFRs) are on average lower than those observed for X-ray selected AGN hosts. On the other hand, [Kalfountzou et al. \(2014\)](#) find that in the redshift range  $0 < z < 4$ , radio-active quasars and their radio-quiet counterparts exhibit on average the same star formation activity, except at low optical luminosities, whereby the SFRs of radio-active quasars are about four times as large as those of radio-quiet ones. Also, a strong positive correlation between radio and FIR luminosity is observed for the former population. The authors argue that this is possibly due to powerful radio jets boosting the star formation activity by compressing the intergalactic medium (*positive feedback* – e.g., [Silk and Nusser 2010](#)), especially in radio-active quasars with low nuclear accretion rates. This result was further expanded by [Kalfountzou et al. \(2017\)](#) who analysed a sample of 173,  $z \sim 1$ , AGN sub-divided into radio-active quasars

(74 objects), radio-quiet quasars (72 objects) and radio-active galaxies (27 objects). Clear evidence for enhanced star-forming activity (a factor of  $\sim 2.5$ ) in radio-active quasars with respect to radio-quiet ones matched in black-hole mass and bolometric luminosity and also with respect to radio galaxies is reported, independent of other AGN and host galaxy properties. Given these differences between radio-active quasars and galaxies, the authors argue for a mechanism which works differently according to jet power, with a threshold – also dependent on galaxy mass – that determines when radio-AGN feedback switches from enhancing star formation (by compressing gas) to suppressing it (by heating or ejecting gas).

Based on the above discussion, the picture that emerges from IR observations of radio-active AGN can then be summarized as follows. In the local,  $z \lesssim 1$ , universe star-formation within the hosts of radio-AGN is generally suppressed, and these galaxies appear as passively evolving, massive red ellipticals. However, at higher redshifts and up to the earliest epochs probed by the observations, not only star-formation is enhanced with a growth rate that is a strongly increasing function of  $z$ , but there are indeed cases at  $z \gtrsim 1$  whereby star-formation activity appears to be boosted with respect to galaxies that do not host a radio-AGN (e.g., [Drouart et al. 2014](#); [Kalfountzou et al. 2014, 2017](#)). These findings, which hold irrespective of the depth of both radio and IR observations, point to a scenario whereby at early –  $z \gtrsim 1$  – epochs radio activity of nuclear origin does not quench star formation in the host galaxy, but either favours (*positive feedback*) or proceeds parallel to it, with the two processes evolving independently thanks to the large reservoirs of gas present within massive high-redshift galaxies. According to this second theory, the main responsible for the quenching of the massive galaxy population in the nearby universe would be intense star formation which rapidly consumes the available gas, possibly then followed by the action of the radio jets, that at  $z \lesssim 1 - 1.5$  succeed at removing the residual gas (e.g., [Falkendal et al. 2019](#)). More work and data are needed to assess the validity of either scenarios and also to understand the drastic change in feedback behaviour when moving from  $z \sim 1.5$  down to the local universe.

### 3.4 The IR-radio relation in star-forming galaxies and its cosmological evolution

As already mentioned in the Introduction, radio-emitting star-forming galaxies (SFGs) at low-to-intermediate redshifts do not represent any special category different from star-forming galaxies selected at other wavelengths. Furthermore, from an observational point of view, it has been known since the 1970s that in this population of sources the emission at radio and infrared (IR) wavelengths are strongly correlated. First statistically significant evidence in this direction was provided by [De Jong et al. \(1985\)](#) and [Helou, Soifer, and Rowan-Robinson \(1985\)](#) who both relied on the data acquired by the IRAS satellite ([Neugebauer et al. 1984](#)) to report a remarkably tight, linear correla-

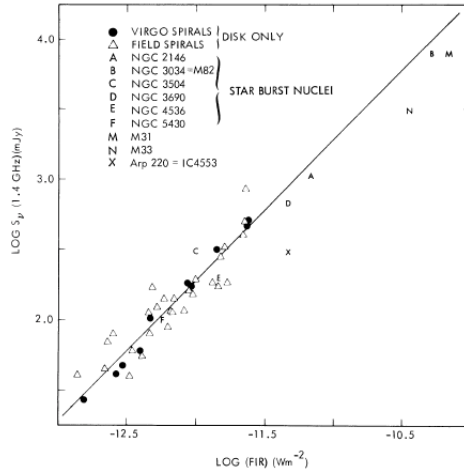


**Fig. 10** Comparison of observed FIR and 1.4 GHz fluxes for galaxies with extended emission and no compact nuclear component detected at 1.4 GHz, both in the Virgo Cluster (*circles*), and in the field (*triangles*). Nine other galaxies with starburst nuclei are also shown for comparison. Figure from [Helou, Soifer, and Rowan-Robinson \(1985\)](#).

tion between far-infrared (FIR) and radio (1.4 GHz) flux densities, extending over three orders of magnitude. This held for a joint sample of blue spirals in the Virgo cluster and in the field, as well as for a subset of galaxies with starburst nuclei ([Helou et al. 1985](#), cf. Fig. 10) and also for a heterogeneous sample of 91 sources which included normal spiral galaxies, irregulars, dwarfs and galaxies containing an AGN ([De Jong et al. 1985](#)).

This incredibly tight relation which – we stress again – was obtained regardless of the galaxy type as long as it hosted ongoing star formation, was parametrized by the FIR-radio luminosity ratio  $q_{\text{FIR}}$ , where

$$q_{\text{FIR}} = \text{Log} \left( \frac{L_{\text{FIR}}[\text{W}]}{3.75 \cdot 10^{12}[\text{Hz}]} \right) - \text{Log}(L_{1.4\text{GHz}}[\text{WHz}^{-1}]) \quad (1)$$

([Helou et al. 1985](#)), with  $L_{\text{FIR}}$  luminosity extending over the far-infrared (rest-frame  $[42.5\text{--}122.5] \mu\text{m}$ ) range and where  $3.75 \cdot 10^{12} \text{ Hz}$  is the frequency at  $80 \mu\text{m}$ , approximately corresponding to the center of the FIR domain. We note that in the literature also the parameters  $q_\lambda$  – with  $\lambda$  within the IR regime – and  $q_{\text{IR}}$  are often used. This latter corresponds to the  $q$  value inferred from the luminosity estimated over the whole,  $[8\text{--}1000] \mu\text{m}$ , infrared range. As [Magnelli et al. \(2015\)](#) note, these different definitions bear no significant impact, since one has  $L_{\text{IR}} = 1.91^{+0.10}_{-0.05} \cdot L_{\text{FIR}}$ , and therefore  $q_{\text{IR}} \simeq q_{\text{FIR}} + 2$ .

As summarized by [Condon \(1992\)](#), nearly all the radio emission from non AGN-powered galaxies is synchrotron radiation from relativistic electrons and

thermal (free-free) emission from HII regions. Only stars more massive than  $\sim 8 M_{\odot}$  can produce the Type II and Type Ib supernovae whose remnants are thought to accelerate most of the relativistic electrons in star-forming galaxies, and can also ionize the HII regions. Since both the life-time of massive stars and that of relativistic electrons are relatively short ( $\lesssim 3 \cdot 10^7$  yr for massive stars and  $\lesssim 10^8$  yr for relativistic electrons), this implies that radio observations are powerful probes of very recent star-formation activity taking place within galaxies. On the other hand, FIR luminosity seems to be a good estimator of the bolometric luminosity produced by relatively massive ( $M \gtrsim 5 M_{\odot}$ ) young stars heating the surrounding dust. To a first order, the very tight FIR-radio correlation is then thought to result from the fact that both emissions are produced by the same sources and within the same regions, as the infrared radiation is the thermal re-radiation from HII regions, while that at 1.4 GHz comes from relativistic electrons accelerated in supernova remnants produced by the same population of massive stars that heat and ionize the HII regions (Harwit and Pacini 1975).

The IR-radio correlation, which is found to extend over five orders of magnitude ( $10^{7.5} \lesssim L_{\text{FIR}}/L_{\odot} \lesssim 10^{13}$ ) with an extremely small dispersion ( $\sigma \lesssim 0.2$ , e.g., Yun, Reddy-Naveen, and Condon 2001), has been used throughout the years in order for instance to: a) distinguish between SFGs and galaxies powered by a radio-active AGN (e.g., Donley et al. 2005; Park et al. 2008; Del Moro et al. 2013; Bonzini et al. 2015; Delvecchio et al. 2017); b) use the radio continuum to estimate the star-formation rate of galaxies in a way which is unaffected by the presence of dust (e.g., Condon 1992; Murphy et al. 2011, 2012; Davies et al. 2017); c) estimate distances and temperatures of high-redshift sub-millimetre galaxies (e.g., Carilli and Yun 1999; Chapman et al. 2005). We also note that, although the correlation was originally found at 1.4 GHz, recent works investigated its validity also at lower (150 MHz; e.g., Gürkan et al. 2018) and higher (3 GHz; e.g., Delhaize et al. 2017) radio frequencies, finding again – at least in the local universe – a tight correlation between radio and FIR luminosities. In particular, by using relatively local ( $z \lesssim 0.35$ ) LOFAR-150 MHz and *Herschel*-250 $\mu\text{m}$  observations, Gürkan et al. (2018) observe a slightly steeper slope than what obtained at 1.4 GHz (cf. Fig. 11). The authors argue that this is due to thermal radiation becoming less important at lower radio frequencies.

However, despite the above explanations and results, many unknowns remain, both from the theoretical point of view and also from observations. Indeed, the “calorimeter theory” (Voelk 1989) which suggests that the IR-radio relation holds because galaxies are both electron calorimeters and UV calorimeters, hence the total radio and IR outputs remain proportional independent of variations within the galaxy, requires galaxies to be optically thick to UV light from the young high-mass stars and thus does not hold for optically thin galaxies. Also, a number of works seem to converge at indicating a change in the slope of the IR-radio relationship at low luminosities (e.g., Yun et al. 2001; Bell 2003; Best et al. 2005b; Gürkan et al. 2018). This effect could be expected if small galaxies were unable to prevent synchrotron electrons

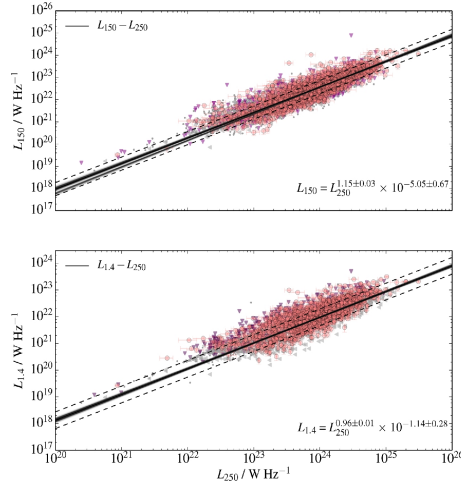


**Fig. 11** Distribution of *Herschel* 250  $\mu\text{m}$  luminosities of SFGs as a function of their LOFAR 150-MHz luminosities. Dashed lines indicate the  $1\sigma$  intrinsic dispersion of the fit. Salmon circles show  $3\sigma$  detections; LOFAR 150 MHz  $3\sigma$  limits are indicated by purple down-pointing triangles and  $3\sigma$  limits on *Herschel* 250  $\mu\text{m}$  luminosities are indicated by grey left-pointing triangles; grey dots indicate  $3\sigma$  upper limits on both quantities. A tight relationship between  $L_{250\mu\text{m}}$  and  $L_{150\text{GHz}}$  is clearly seen. Bottom: Distribution of *Herschel* 250  $\mu\text{m}$  luminosities of SFGs as a function of their FIRST 1.4 GHz luminosities. Symbols and lines as for the top panel. Figure from [Gürkan et al. \(2018\)](#).

to escape, therefore causing a global deficit of radio emission at a fixed star-formation rate (e.g., [Chi and Wolfendale 1990](#)). However, for instance [Gürkan et al. \(2018\)](#) find the opposite effect, with low-SFR objects ( $\lesssim 1 M_{\odot} \text{ yr}^{-1}$ ) exhibiting more radio emission than what would be expected from extrapolations of the trend at higher SFRs.

Possibly the most important open question associated to the IR-radio correlation is its eventual redshift evolution, as erroneous estimates at high redshifts directly translate into erroneous estimates of the star-formation activity of galaxies throughout the cosmic epochs, therefore hampering the huge potential of present and future radio surveys such as SKA to investigate the history of formation and evolution of galaxies since the cosmic dawn. This redshift evolution would indeed be expected, as e.g., electrons might lose energy by inverse Compton interactions with the cosmic microwave background whose energy density scales as  $(1+z)^4$ , resulting in a lower level of radio emission in galaxies at higher redshifts. Also, synchrotron emission is proportional to the square of the magnetic field strength, so any cosmological evolution of this latter quantity should affect the constancy of the  $q_{\text{IR}}$  parameter at earlier epochs (e.g., [Murphy 2009](#)). Furthermore, changes in the galaxy spectral

energy distributions (SEDs) may also be expected due to evolution in dust properties and metallicity (e.g., [Chapman et al. 2005](#); [Amblard et al. 2010](#)).

The possibility for a redshift dependence of  $q_{\text{IR}}$  has started being investigated only in the last 15 years or so, thanks to the advent of IR satellites such as *Spitzer* ([Werner et al. 2004](#)) and *Herschel* ([Pilbratt et al. 2010](#)) which overcame the IRAS limitations of observing just the local universe. [Appleton et al. \(2004\)](#) use *Spitzer* data at  $24\mu\text{m}$  and  $70\mu\text{m}$  from the First Look Survey to analyse the behaviour of the monochromatic quantities  $q_{24\mu\text{m}}$  and  $q_{70\mu\text{m}}$ . By relying on spectroscopic redshifts for  $\sim 500$  objects, these authors find that  $q_{70\mu\text{m}}$  stays invariant up to  $z \sim 1$ . The same conclusion was reached for  $q_{24\mu\text{m}}$  up to  $z \sim 2$ , although with a larger spread that could be attributed to variations in the galaxy SEDs throughout the probed population. Similar results were obtained by [Vlahakis, Eales, and Dunne \(2007\)](#), [Ibar et al. \(2008\)](#), [Garn et al. \(2009\)](#) for sources selected at 610 MHz and [Jarvis et al. \(2010\)](#), although on a more limited,  $0 < z < 0.5$ , redshift range. [Jarvis et al. \(2010\)](#) also report no dependence of the IR-radio relation on the radio luminosity of the sources – as long as they probed the non-AGN regime,  $L_{1.4\text{GHz}} < 10^{23} \text{ W Hz}^{-1}$  – and a factor  $\sim 2$  tighter relationship between radio and  $250\mu\text{m}$  luminosities than what inferred for the whole  $[8 - 1000] \mu\text{m}$  range. In agreement with e.g., [Vlahakis et al. \(2007\)](#), it is argued that this could be obtained if the longer wavelength emission, i.e., in the sub-millimetre regime, were not just produced by massive star formation and thus did not trace the same physical mechanism(s) as the radio or the MIR-to-FIR emission. No evolution was either observed by [Chapman et al. \(2010\)](#) for their sample of  $\sim 70$  sub-millimetre galaxies. On the other hand, [Kovacs et al. \(2006\)](#) – by considering a smaller sample of 15 sub-millimetre galaxies endowed with  $350\mu\text{m}$  fluxes – infer in the redshift range  $1 \lesssim z \lesssim 3$ ,  $q_{\text{IR}} \sim 2.07$ , value which is sensibly lower than that reported for the local universe ( $\sim 2.3$  – e.g., [Condon 1992](#); [Yun et al. 2001](#); [Mauch and Sadler 2007](#)).

[Iverson et al. \(2010a\)](#) find no evolution in the values of  $q_{250\mu\text{m}}$  obtained between  $z \sim 0$  and  $z \sim 2$  for a sample of  $\sim 20$  sources observed with the Balloon-borne Large Aperture Space Telescope (BLAST; [Truch et al. 2009](#)). However, when they instead consider a sample selected at  $24\mu\text{m}$ , with stacked FIR information subdivided into redshift bins, they find that  $q_{\text{IR}}$  is a steadily decreasing function of redshift in the whole range probed by their analysis, with  $q_{\text{IR}} \propto (1+z)^{-0.15 \pm 0.03}$ . The [Iverson et al. \(2010a\)](#) sample suffered the limitations borne by BLAST in terms of low sensitivity and large beam Full Width Half Maximum (FWHM). In order to overcome this problem, [Iverson et al. \(2010b\)](#) consider 65 star-forming galaxies selected in the GOODS North field by *Herschel* at  $250\mu\text{m}$  and with available 1.4 GHz information. By also making use of the enormous wealth of multi-wavelength information available in that field, they find a very mild evolution of  $q_{\text{IR}} \propto (1+z)^{-0.08 \pm 0.07}$  in the redshift range  $0 < z < 2$ , result which is confirmed by a larger sample of  $24\mu\text{m}$ -selected,  $L_{\text{FIR}}$ -matched galaxies. However, when the most local  $q_{\text{IR}}$  value is discarded, the redshift dependence becomes much more appreciable, with a trend similar to that reported by [Iverson et al. \(2010a\)](#),  $q_{\text{IR}} \propto (1+z)^{-0.26 \pm 0.07}$ .



The investigation of the cosmological evolution of  $q_{\text{IR}}$  was subsequently repeated for most of the cosmological deep fields observed by *Spitzer* and *Herschel*, returning somehow discording results. [Sargent et al. \(2010\)](#) considered a homogeneous sample of  $\sim 4000$  sources with comparable IR luminosities over the last 10 Gyr, selected at  $24\mu\text{m}$  in the COSMOS field and, by also taking into account flux limits in their analysis, conclude that there is no evolution in the  $z = 0 - 2$  range. A similar result was obtained by [Mao et al. \(2011\)](#) in the Extended Chandra Deep Field South (ECDFS) for a sample of  $70\mu\text{m}$  *Spitzer*-selected sources, while instead negative evolution was found for  $q_{70\mu\text{m}}$  by [Bourne et al. \(2011\)](#) in the very same ECDFS field by applying stacking analyses to a mass-limited/NIR-selected sample of star-forming galaxies. The main point that emerged from all these studies was that the reported differences were mainly to be attributed to selection effects since, while the radio selection favours higher  $L_{\text{radio}}/\text{SFR}$  ratios, the opposite is true for the FIR and sub-millimetre selections which favour high SFRs. The bias associated with optical and NIR selection is less straightforward; however such a selection is found to under-represent dust-enshrouded, high-SFR galaxies.

[Magnelli et al. \(2015\)](#) bring the IR-radio investigation to much more solid statistical grounding by analysing the variation of the  $q_{\text{IR}}$  parameter for a very large sample of  $\sim 300,000$  galaxies selected on the basis of their stellar masses. All the best known deep extragalactic fields such as GOODS North, GOODS South, ECDFS and COSMOS were considered, and data included both deep *Herschel* FIR (100, 160, 250, 350 and  $500\mu\text{m}$ ) and deep radio 1.4 GHz VLA and 610 MHz GMRT observations. FIR and radio images were then stacked at the positions of this mass-selected sample, complete down to  $M_* = 10^{10} M_{\odot}$  and across  $0 < z < 2.3$ . By doing this, they found  $q_{\text{FIR}} = (2.35 \pm 0.08) \cdot (1+z)^{-0.12 \pm 0.04}$ , where the  $z \sim 0$  value perfectly agrees with local observations (e.g., [Yun et al. 2001](#)) and where the same degree of evolution holds for both normal star-forming galaxies and starbursts, i.e., galaxies with a largely enhanced specific star-formation rate. The authors exclude such an evolution to be due to large variations with redshift of the radio spectral index of the probed population(s) since these are not observed in their data.

The issue of the evolution of the IR-radio correlation has moved in the recent years to radio surveys performed at frequencies different from the "standard" 1.4 GHz, in order to assess its universal validity. [Calistro Rivera et al. \(2017\)](#) use LOFAR-150 MHz data for 810 star-forming galaxies from the Boötes field. At this frequency, they estimate an evolution of the  $q_{\text{IR}}$  parameter which goes as  $\propto (1+z)^{-0.22 \pm 0.05}$ , with an intrinsic scatter of  $\sigma \sim 0.53$ , in the redshift range  $0 < z < 2.5$ . The authors stress that the observed cosmic evolution of the IR-radio relation must be taken into account for the future use of radio luminosity to estimate unbiased SFRs at high  $z$ .

Roughly at the same time, [Delhaize et al. \(2017\)](#) and [Molnar et al. \(2018\)](#) analyze the behaviour of the IR-radio correlation for sources in the VLA-COSMOS 3GHz Large Project. More in detail, [Delhaize et al. \(2017\)](#) – accounting for non-detections in the radio or infrared bands by means of the doubly-censored analysis presented in [Sargent et al. \(2010\)](#) – find that the pa-

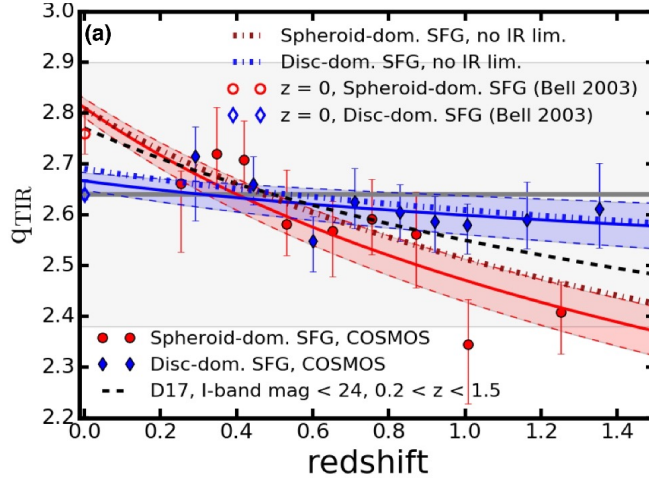


**Fig. 12** Redshift evolution of the IR-radio correlation  $q_{\text{TIR}} \equiv q_{\text{IR}}$ , for disc- and spheroid-dominated star-forming galaxies (blue and red symbols, respectively). The local  $z = 0$  measurements (open symbols) are based on a morphologically-selected subset of the Bell (2003) sample. Shaded regions bordered by dashed lines show the upper and lower limits of the  $1\sigma$  confidence interval of the fit. The black dashed line is the evolutionary trend found for  $0.2 < z < 1.5$  SFGs with I-band magnitude  $< 24$  in the sample of Delhaize et al. (2017). Figure from Molnar et al. (2018).

parameter  $q_{\text{IR}}$  decreases with increasing redshift as  $\propto (1+z)^{-0.19 \pm 0.01}$ . This was in agreement with most of the recent works, even though the authors could not rule out that unidentified AGN contributions only to radio wavelengths may be steepening the observed trend.

We note that, at variance with the local result obtained for low-frequency-LOFAR sources (e.g.,  $q_{\text{IR}} = 1.72 \pm 0.04$ , Calistro Rivera et al. 2017), the  $z \sim 0$  value of  $q_{\text{IR}} = 2.88 \pm 0.03$  at 3 GHz is higher than that obtained at 1.4 GHz (e.g., Yun et al. 2001). This trend can be recovered if one assumes for SFGs a single power-law radio emission with a spectral index  $\alpha \sim 0.73$  in the whole 150 MHz – 3 GHz range (e.g., Calistro Rivera et al. 2017). Delhaize et al. (2017) indeed conclude that the choice for the value of the average radio spectral index directly affects the normalisation of the  $q_{\text{IR}}$  parameter, as well as its estimated trend with redshift. At the same time, an increasing fractional contribution to the observed 3 GHz flux by free-free emission from star-forming galaxies may also affect the derived evolution. Based on their results, the authors conclude that imperfect  $K$ -corrections in the radio regime might be responsible for the decreasing trend of the IR-radio relation with redshift.

Molnar et al. (2018) refine the analysis of Delhaize et al. (2017) and investigate the  $q_{\text{IR}}$  evolution for their sample of 3 GHz-selected SFGs subdivided by morphology into spheroid- and disc-dominated galaxies. These authors find

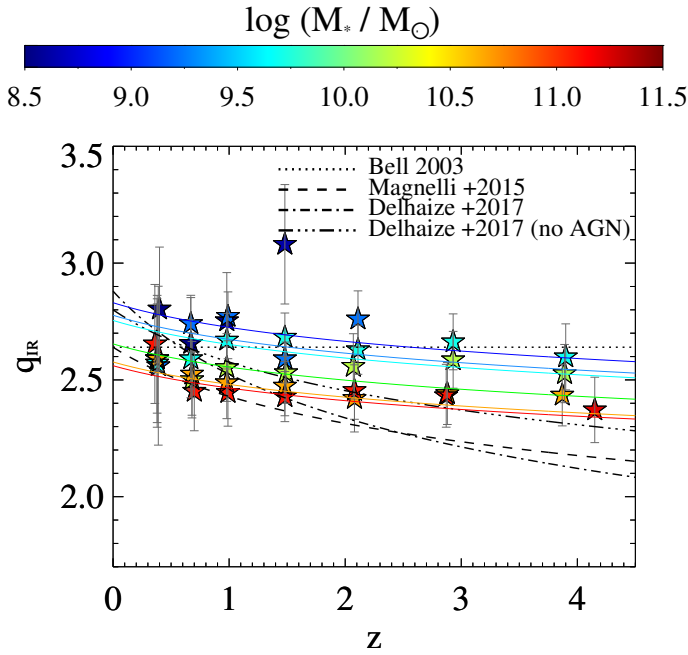


**Fig. 13** Intrinsic  $q_{\text{IR}}$  evolution as a function of redshift (x-axis) and stellar mass  $M_*$  (colour bar). For comparison, other trends with redshift are taken from the literature (black lines): Bell (2003, dotted); Magnelli et al. (2015, dashed); Delhaize et al. (2017, dot-dashed) and their AGN-corrected version after removing  $2\sigma$  outliers (triple dot-dashed lines). Figure from Delvecchio et al. (2021).

that the spheroid-dominated population follows a declining trend for  $q_{\text{IR}}$  versus  $z$ , similar to that measured in the most recent studies. However, for disc-dominated galaxies, where radio and IR emission should be linked to star formation in a more straightforward way, they only measure a very small – if any – change (cf. Fig. 12). This suggests that low-redshift calibrations of radio emission as a star formation rate tracer may remain valid out to at least  $z \simeq 1 - 1.5$  for pure star-forming systems, and that the different redshift evolution of  $q_{\text{IR}}$  for the spheroid- and disc-dominated samples is mainly due to an increasing radio excess in spheroid-dominated galaxies at  $z \gtrsim 0.8$ , fact which hints at some AGN activity in these systems, as already discussed in Sects. 2 and 3.3.

Another step forward in the comprehension of the relation between radio and IR luminosities and of its cosmic evolution is provided by the work of Delvecchio et al. (2021). These authors again use the 3GHz-selected sample of Smolčić et al. (2017b) to calibrate for the first time the  $q_{\text{IR}}$  parameter both as a function of redshift and stellar mass. Starting from a sample of  $\sim 400,000 - M_* > 10.5 M_\odot$ ,  $0.1 < z < 4.5$  – star-forming galaxies selected in the deep COSMOS UltraVISTA catalogue from Muzzin et al. (2013), and relying on radio and IR stacking techniques, these authors conclude that the

main driver of the observed  $q_{\text{IR}} - z$  evolution is the stellar mass, with more massive galaxies systematically displaying lower  $q_{\text{IR}}$  (cf. Fig. 13). A secondary, weaker dependence on redshift is also observed, leading to a total functional form of the kind:  $q_{\text{IR}}(M_*, z) = (2.626 \pm 0.024)(1 + z)^{-0.023 \pm 0.008} - (0.148 \pm 0.013)(\log M_*/M_\odot - 10)$ . No dependence is instead observed on SFRs.

On the other hand, Bonato et al. (2021), when using LOFAR-selected star-forming galaxies from the Lockman Hole field, do find a dependence of the  $\text{SFR}/L_{150\text{MHz}}$  relation on stellar mass, but only for  $z \lesssim 1$  and weaker than what obtained by Delvecchio et al. (2021) (decrement of  $\lesssim 0.1$  as opposed to  $\sim 0.23$  for increasing masses), while Smith et al. (2021) report for LOFAR DR1 observations of the ELIAS-N1 field a linear  $\text{SFR}/L_{150\text{MHz}}$  relation with very little (possibly differential due to mass dependencies) cosmological evolution at least up to  $z \sim 1$ . A linear relation between SFR and 1.4 GHz luminosity is also observed by Tisanic et al. (2022) by using a local,  $z \lesssim 0.1$ ,  $250\mu\text{m}$ -selected sample from the *Herschel* Astrophysical Terahertz Large Area Survey (H-ATLAS; Eales et al. 2010) with both radio detections and stacking information from FIRST and NVSS. This is however at variance with the results of Molnar et al. (2021), who further claim no redshift dependence for the  $q_{\text{IR}}$  parameter, since this would merely arise as the consequence of selection effects, whereby different parts of the non-linear IR-radio correlation are probed for varying redshift ranges and sample depths. From the above discussion it is clear that, despite all the progress made in the recent years, a convergence on  $q_{\text{IR}} -$  especially for what concerns its cosmological evolution – is still far from being reached.

## 4 The environments of radio-active AGN and star-forming galaxies

This Section presents results related to the environmental properties of radio-AGN and – to a lesser extent – of radio-emitting star-forming galaxies. We have chosen to divide them into three categories: those obtained with clustering studies (Sect. 4.1), those derived by pinpointing radio-AGN within known structures (Sect. 4.2) and those stemming from searching for over-densities around known radio-AGN (Sect. 4.3). As already discussed in the Introduction, the choice is dictated by the fact that these different approaches present different points of view that then need to be integrated with each other in order to return a complete and coherent picture of the large-scale behaviour of radio galaxies.

### 4.1 Methods for the detection of environment 1: clustering analyses

#### 4.1.1 Useful definitions

This paragraph is devoted to define a number of quantities which will be used throughout the section.

- a) **The spatial two-point correlation functions** The *spatial two-point auto-correlation* (or more simply, just *correlation*) *function*  $\xi(r, z)$  is one of the most commonly used tools to investigate the large-scale structure traced by a population of sources. It is defined as the excess probability with respect to a Poissonian (random) distribution of finding two galaxies at a distance  $r$  from each other within the volume element  $\delta V$ . By following Peebles (1980), this can be expressed as:

$$\delta P = \bar{N} [1 + \xi(r, z)] \delta V, \quad (2)$$

where  $\delta P$  is the probability and  $\bar{N}$  is the mean number density of galaxies, and where we have made it explicit that the quantity  $\xi$  depends on both scale  $r$  and redshift  $z$ . In most cases of astrophysical (i.e., non-cosmological) interest,  $\xi(r, z)$  can be parametrized as a power-law  $\xi(r, z) = [r/r_0(z)]^{-\gamma}$ , with slope  $\gamma$  and correlation (or clustering) radius (or length)  $r_0$ . Higher values of  $r_0$  imply that the analysed sources are more strongly clustered. Closely related to the two-point correlation function is the *two-point cross-correlation function*  $\xi_{AB}(r, z)$  which compares objects coming from two different datasets A and B and is defined as the joint probability of finding an object from A in the volume element  $\delta V_A$  and object from B in the volume element  $\delta V_B$  at a distance  $r$  (Peebles 1980):

$$\delta P_{AB} = \bar{N}_A \bar{N}_B [1 + \xi_{AB}(r, z)] \delta V_A \delta V_B, \quad (3)$$

where  $\bar{N}_A$  and  $\bar{N}_B$  are the mean number densities of the two sets of objects. The cross-correlation function can also be fitted as a power-law in the same manner as the auto-correlation function discussed above.

From a practical point of view, we note that cross-correlation analyses are necessary whenever the sample of interest is too small to allow for meaningful statistical studies of the auto-correlation function so that a second, much larger, dataset has to be considered in order to beat the uncertainties. This is indeed the reason why this method was so widely used in the early works that tackled the issue of Large-Scale Structure as traced by radio sources.

- b) **The angular two-point correlation function** In the absence of a complete set of redshift information as is the case for many large-area surveys, one can rely on the study of the projected distribution onto the sky of a population of sources via the two-point angular correlation function  $\omega(\theta)$ . This is defined as the excess probability with respect to a Poissonian distribution of finding two galaxies at an angular distance  $\theta$  from each other within the solid angle element  $\delta\Omega$ . In a very similar manner to Eq. (2), the above definition can be expressed as:

$$\delta P_\Omega = \bar{N}_\Omega [1 + \omega(\theta)] \delta\Omega, \quad (4)$$

with  $\bar{N}_\Omega$  mean surface density over the region that subtends the solid angle  $\Omega$ , and  $\delta\Omega$  surface area element. As it was for the spatial correlation function, also  $\omega(\theta)$  can be expressed as a power-law in most of the cases of

astrophysical interest and parametrized as  $\omega(\theta) = A\theta^{1-\gamma}$ , where  $\gamma$  is the same as in the definition of  $\xi$  and  $A$  is the amplitude.

- c) **The Limber equation** The Limber equation (Limber 1953; Peebles 1980) provides the standard way to relate the angular two-point correlation function to the spatial two-point correlation function, once the redshift distribution of the sources under consideration is known. It can be expressed as:

$$\omega(\theta) = 2 \frac{\int_0^\infty \int_0^\infty F^{-2}(x) x^4 \Phi^2(x) \xi(r, z) dx du}{\left[ \int_0^\infty F^{-1}(x) x^2 \Phi(x) dx \right]^2}, \quad (5)$$

where  $x$  is the comoving coordinate,  $F(x)$  gives the correction for cosmic curvature, and the selection function  $\Phi(x)$  satisfies the relation

$$\bar{N}_\Omega = \int_0^\infty \Phi(x) F^{-1}(x) x^2 dx = \frac{1}{\Omega} \int_0^\infty N(z) dz, \quad (6)$$

in which  $\bar{N}_\Omega$  is as in Eq. (4) and  $N(z)$  is the redshift distribution of the sources defined as the number of objects in a given survey within the shell  $(z, z + dz)$ . If  $\xi(r, z)$  can be parametrized as a power-law of the form  $\xi(r, z) = [r/r_0(z)]^{-\gamma}$ , where all the dependency on  $z$  is absorbed by the clustering length  $r_0(z)$ , then Eq. (5) reduces to an integral over  $z$  (cf. Magliocchetti and Maddox 1999)

$$\omega(\theta) = \frac{H_\gamma \int_0^\infty N(z)^2 [x(z)\theta]^{1-\gamma} r_0(z)^\gamma F(z) (dx/dz) dz}{\frac{c}{H_0} \left[ \int_0^\infty N(z) dz \right]^2}, \quad (7)$$

with  $H_\gamma = \Gamma[1/2]\Gamma[(\gamma-1)/2]/\Gamma[\gamma/2]$ ,  $c$  speed of light and  $H_0$  Hubble constant, expressed as  $h \cdot 100 \text{ km s}^{-1} \text{ Mpc}^{-1}$ .

- d) **The bias parameter** The differences in the clustering properties of different classes of extragalactic sources and between these and the background (dark) matter distribution motivate the introduction of the bias parameter  $b$ , defined as (cf. Kaiser 1984):

$$b^2 = \frac{\xi_{\text{gal}}}{\xi_{\text{DM}}}, \quad (8)$$

where  $\xi_{\text{gal}}$  is the spatial correlation function of a population of galaxies/AGN and  $\xi_{\text{DM}}$  that of the dark matter. In the case of cross-correlations between a population A and a population B, the bias  $b_{\text{AB}}$  can be written as:

$$b_{\text{AB}}^2 = \frac{\xi_{\text{AB}}}{\xi_{\text{DM}}} = b_{\text{A}} \cdot b_{\text{B}}, \quad (9)$$

where  $b_{\text{A}}$  and  $b_{\text{B}}$  are expressed as in Eq. (8).

From the theoretical point of view, the paradigm of *biased galaxy formation* states that the efficiency of galaxy formation is higher in dense environments since an object of a given mass will collapse sooner if it lies in a region of large-scale over-density, leading to an enhanced abundance of such objects with respect to the mean (“natural bias” – White et al. 1987). These

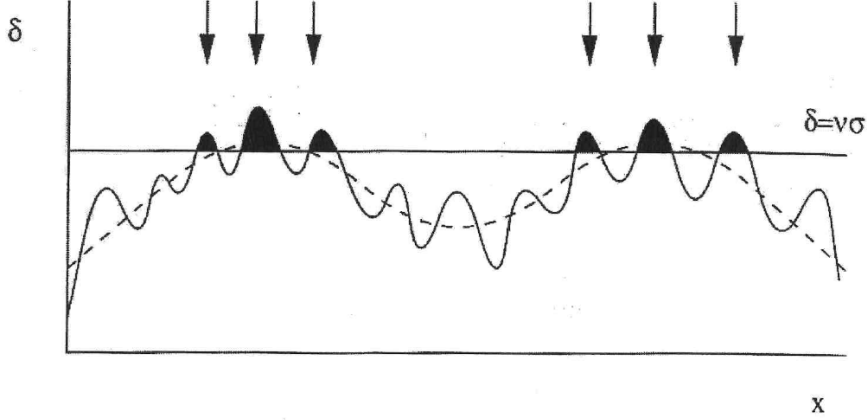


**Fig. 14** The high peak bias model. If we decompose a density field into a fluctuating component on galaxy scales, together with a long-wavelength "swell" (broken curve), then those regions of density that lie above the critical density threshold for collapse of  $\delta = \nu\sigma$ , with  $\sigma$  variance of the density field on a scale  $R$  corresponding to a mass  $M$ , will be strongly clustered. If proto-galaxies are assumed to form at the sites of these high peaks (shaded and indicated by arrows), then this population has a non-uniform (i.e., biased) spatial distribution even before dynamical evolution of the density field. Figure from [Peacock \(1999\)](#).

rare high peaks of a Gaussian random field will then be significantly more clustered than the underlying Gaussian field itself (Fig. 14). [Mo and White \(1996\)](#) provided an expression for the bias  $b$  starting from the extension of the [Press and Schechter \(1974\)](#) formalism which reads:

$$b(M, z|z_F) = \left(1 + \frac{\nu_F^2 - 1}{\delta_F^2}\right), \quad (10)$$

where  $M$  is the mass of the dark matter haloes,  $z_F$  is the redshift of formation of such haloes, and  $\nu_F = \delta_F/\sigma(z)$ , with  $\sigma(z)$  variance of the density field on a mass-scale  $M$  at a redshift  $z < z_F$  and  $\delta_F = \delta_c(1 + z_F)/(1 + z)$  ( $\delta_c$  is the critical linear over-density for spherical collapse). From the above equation it is possible to appreciate that  $b$  depends not only on halo mass



(i.e., more massive haloes cluster more strongly), but also on the epoch when the haloes collapse, being higher for haloes formed at earlier times. Note that there have been suggestions that  $b$  could also be stochastic, non-linear and scale-dependent (e.g., [Dekel and Lahav 1999](#); [Narayanan, Berlind, and Weinberg 2000](#)), but an in-depth analysis of this topic is outside the scopes of the present review.

Following the [Mo and White \(1996\)](#) approach, one then has that the more massive haloes (corresponding to rare peaks in the density field) that collapse earlier in time will be more clustered than haloes of lower mass that collapse in more recent epochs. Assuming that all galaxies are hosted within dark matter haloes, this for instance implies that early-type galaxies – associated with older and more massive haloes – in general cluster more strongly than late-type ones.

The above scenario holds for a one-to-one association between galaxies/AGN and dark matter haloes. As in general dark matter haloes are occupied by more than one galaxy/AGN, in more recent years the Mo & White approach has been implemented with the so-called Halo Occupation framework (e.g., [Scoccimarro et al. 2001](#), see [Magliocchetti and Porciani 2003](#) for an application to 2dFGRS galaxies), which relates the clustering properties of a chosen population of extragalactic objects with the way such objects populate their dark matter haloes. Within this scenario, the two-point correlation function  $\xi$  can be written as the sum of two components,  $\xi_{1h}$  and  $\xi_{2h}$ , where the first quantity accounts for pairs of galaxies residing within the same halo, while the second one takes into account the contribution to the correlation function of galaxies belonging to different haloes. However, since most of the clustering studies presented in this review do not have enough signal-to-noise to investigate the properties of the one-halo term  $\xi_{1h}$  and, from a more physical point of view, since for the overwhelming majority of radio-AGN the approximation one source per halo is a good one (e.g., [Magliocchetti et al. 2004](#)), in the following discussion we will stick to the [Mo and White \(1996\)](#) formalism.

The main point to be taken away from this discussion is that the biased galaxy formation framework has the important advantage of relating the clustering properties of a selected population of sources with the dark matter content of the structures that host them, allowing to provide statistical estimates for their masses. From an operational point of view, the rule of thumb is that, at fixed  $z$ , sources more strongly clustered (i.e., with higher values for  $r_0$  in the parametrization of  $\xi(r)$  as a power-law) will present larger values of the bias parameter  $b$  (cf. equation 8) and therefore (via equation 10) will be hosted by more massive haloes.

#### 4.1.2 Early works on radio-galaxy cross-correlations

For many years after the discovery of radio-emitting sources, their distribution was thought to be isotropic (e.g., [Webster 1976a,b](#)). First attempts to investigate the Large-Scale Structure traced by radio-AGN were presented in the

work of [Seldner and Peebles \(1978\)](#). These authors considered radio sources from the 4C catalogue ([Pilkington and Scott 1965](#)) and correlated them with galaxies from the Lick catalogue ([Seldner et al. 1977](#)), finding that the shape of the cross-correlation function was the same as that of the galaxy-galaxy correlation function, but presented an amplitude which was about 10 times higher. By also interpreting some tentative results on the auto-correlation function of radio sources, [Seldner and Peebles \(1978\)](#) concluded that radio-AGN are not randomly distributed, but rather tend to be found amongst strongly clustered galaxies. This result was confirmed by the work of [Longair and Seldner \(1979\)](#), who further reported a distinct behaviour in faint ( $L_{178\text{ MHz}} \sim 10^{22} - 10^{24} \text{ W Hz}^{-1} \text{ sr}^{-1}$ ) and powerful ( $L_{178\text{ MHz}} \sim 10^{24} - 10^{25} \text{ W Hz}^{-1} \text{ sr}^{-1}$ ) radio galaxies, whereby the latter population (with the noticeable exception of classical double-lobed AGN) prefers to reside in regions of space where the amplitude of the spatial cross-correlation function is about four to five times that of inactive galaxies, while weak radio emitters show no tendency to belong to overdense structures. [Masson \(1979\)](#) also observed the same effect in the 6C catalogue ([Masson 1978](#)), while [Seldner and Peebles \(1981\)](#) speculated on the possibility that this result could be due to faint radio sources residing at higher redshifts than brighter ones.

Some years later, [Prestage and Peacock \(1988\)](#) used cross-correlation techniques to derive the environmental properties of 118 radio-AGN taken from a number of surveys, amongst which the  $S_{2.7\text{ GHz}} \geq 2 \text{ Jy}$  Parkes ([Wall and Peacock 1985](#)) catalogue. For the first time, sources were divided according to their morphology. It was found that, while compact radio sources did not appear in regions of enhanced galaxy density, the same was not true for extended radio-AGN, especially FRI galaxies which were typically found within overdense structures.

The first evolutionary studies were those presented by [Yates, Miller, and Peacock \(1989\)](#), who analysed the environments of 25 radio galaxies drawn from the 3C ([Edge et al. 1959](#)) and Parkes ([Bolton et al. 1979](#)) samples, with flux densities  $> 1 \text{ Jy}$  and redshifts between  $z = 0.15$  and  $z = 0.8$ , although only 11 sources had  $z > 0.35$ . These authors found that the most luminous,  $\langle L_{178\text{ MHz}} \rangle = 10^{27.1} \text{ W Hz}^{-1}$ , sources at  $z \sim 0.5$  lay in rich environments, while the same population at  $z \sim 0.3$  occupied structures which were roughly three times sparser. However, given the limited size of their sample, it was not possible to conclude whether the observed trend was due to cosmological or luminosity evolution. [Ellingson, Yee, and Green \(1991\)](#) instead performed a comparative study between the environments inhabited by radio-active and radio-quiet quasars in the redshift range  $0.3 < z < 0.6$ , finding that the latter population resided in structures which were less rich than those occupied by radio-active quasars. This discovery made the authors conclude that radio-active and radio-quiet quasars did not belong to the same parent population simply observed with a different viewing angle, but were different physical objects. Furthermore, based on the morphology-density relation by [Dressler \(1980\)](#), [Ellingson et al. \(1991\)](#) speculate on the possibility that radio-active quasars could be hosted by elliptical galaxies, while radio-quiet quasars by

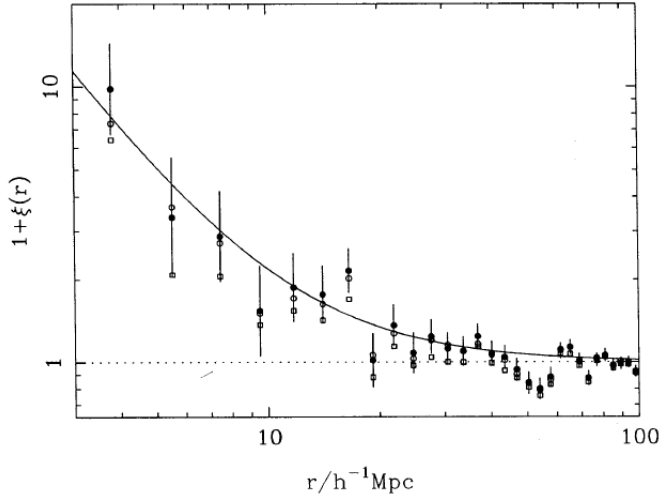


**Fig. 15** The spatial two-point correlation function  $\xi$  for the sample of [Peacock and Nicholson \(1991\)](#). The curve shows the best-fit model  $\xi = (r/r_0)^{-1.8}$ , with  $r_0 = 11$  Mpc/h. Figure from [Peacock and Nicholson \(1991\)](#).

spirals. Finally, in agreement with the results by [Yates et al. \(1989\)](#), they also report an evolution of the environmental properties of radio-active quasars, since a larger number was observed to inhabit regions of enhanced density at the highest redshifts probed by their analysis. No relationship was instead found between environmental properties and radio luminosities.

#### 4.1.3 The correlation functions of radio sources

Although some more studies (mostly of small high-redshift samples) kept relying on the cross-correlation function between radio-AGN and galaxies (e.g., [Best 2000](#); [McLure and Dunlop 2001](#); [Hickox et al. 2009](#); [Ramos Almeida et al. 2013](#); [Lindsay et al. 2014a](#)), the advent in the 1990s of deep ( $\sim$  mJy level), large-area radio surveys such as the Faint Images of the Radio Sky at Twenty centimeters (FIRST – [Becker et al. 1995](#)) and the NRAO VLA Sky Survey (NVSS – [Condon et al. 1998](#)) allowed to probe samples of objects about  $10^3 - 10^4$  times more numerous than what was possible in the past. This in turn allowed for the first time studies of the environmental properties of extragalactic radio sources by means of their auto-correlation function. And, even more importantly, for the first time these studies permitted to derive cosmological information from the distribution of radio galaxies all over the sky.

First works in this direction were presented by [Peacock and Nicholson \(1991\)](#) who analysed the spatial two-point correlation function for a sample of 310 local ( $z < 0.1$ ) and bright ( $F_{1.4\text{GHz}} > 0.5$  Jy) radio galaxies for which

spectroscopic redshifts were available, finding that it showed a power-law shape that could be parametrized as  $\xi(r) = (r/r_0)^{-\gamma}$ , with  $\gamma \sim 1.8$  and  $r_0 \sim 11$  Mpc/h (cf. Fig. 15). Noticeably, while the value of  $\gamma$  resembled that found for correlation function analyses of the more general galaxy population within the same redshift range, that of the correlation length  $r_0$  was about two times higher ( $\sim 5.4$  Mpc/h – e.g., Baugh 1996) and closer to the value found for clusters of galaxies ( $\sim 15$  Mpc/h – e.g., Dalton et al. 1992), in agreement with the early findings of Seldner and Peebles (1978).

But it was really with the work of Cress et al. (1996) that correlation studies of radio sources entered a new era. Indeed, these authors investigated the clustering properties of  $\sim 138,000$  FIRST radio galaxies down to 1.4 GHz fluxes of 1 mJy, finding that the angular (since no 3D information for most of the sources considered in the Cress et al. analysis was available) correlation function could be parametrised as  $\omega(\theta) = A\theta^{1-\gamma}$ , with  $A \sim 3 \cdot 10^{-3}$  and  $\gamma \sim 2.1$ . By also considering only sources fainter than 2 mJy, Cress et al. (1996) found that  $\omega(\theta)$  was shallower than what observed for the whole population, and interpreted this flattening as due to the contribution of star-forming galaxies, expected to dominate the radio counts below the mJy level (e.g., Prandoni et al. 2018).

One problem that affected the Cress et al. (1996) analysis was the presence of extended and multi-component radio-AGN within their sample which, when overlooked or erroneously combined together, produced spurious signal (excess if considering each radio component as a single source or defect in the case all sources within a chosen distance from each other are combined together regardless of their physical association) in the correlation function on scales smaller than  $\sim 0.2^\circ$ . This issue was tackled in better detail by Magliochetti et al. (1998), who provided a simple, but effective recipe for combining multi-component sources together based on the brightness and relative distance of the various members of a single object. The formula read:

$$\theta_{\text{link}} = 100 \left( \frac{F_{\text{TOT}}}{100} \right)^{0.5} \text{ arcsec}, \quad (11)$$

where  $F_{\text{TOT}}$  is the the sum of the fluxes of the components of each apparent multiple source. Equation 11 was then combined with a criterion for the ratio of the fluxes of the components to be around 1, expected for real aggregations since fluxes in this case are correlated. After a careful investigation, Magliochetti et al. (1998) then chose to combine pairs of sources only if their distance  $\theta_{\text{link}}$  was below that identified by equation 11 and if their fluxes differed by a factor less than 4 (i.e.,  $1/4 \leq f_1/f_2 \leq 4$ , with  $f_1$  and  $f_2$  fluxes of two components of a single radio-AGN). Another difference between the work of Magliochetti et al. (1998) and that of Cress et al. (1996) was that the former authors considered a brighter flux limit of 3 mJy for the sources to be considered in their analysis: this was due to the known incompleteness of the FIRST catalogue below those flux levels. Such a sample, corrected for flux incompleteness and the presence of multicomponent sources, comprised 86,074 objects and was then used to investigate the distribution of the second

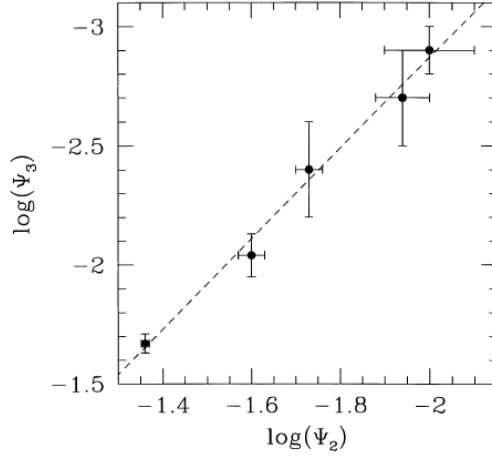


**Fig. 16** Normalized skewness  $\Psi_3$  vs normalized variance  $\Psi_2$ . Errors are estimated from the variance in four random subsets. The dashed line represents the best-fit to the data obtained for a functional form  $\Psi_3 = S_3(\Psi_2)^\alpha$ , with  $\alpha = 1.9 \pm 0.1$  and  $S_3 = 9 \pm 3$ . Figure from Magliocchetti et al. (1998).

(variance) and third (skewness) moments of the radio galaxy distribution. The results from the variance  $\mu_2$  could be then connected to the angular two point correlation function via the relation (Peebles 1980):

$$\mu_2 = \bar{N}_\Omega + (\bar{N}_\Omega)^2 \Psi_2, \quad (12)$$

where  $\bar{N}_\Omega$  is the mean count of radio sources in the solid angle  $\Omega$ , and the reduced variance  $\Psi_2$  is expressed as:

$$\Psi_2 = \frac{1}{\Omega^2} \int w(\theta) d\Omega_1 d\Omega_2. \quad (13)$$

From the above equations, Magliocchetti et al. (1998) obtained for the amplitude of the two-point correlation function  $\omega(\theta) = A\theta^{1-\gamma}$ , the value  $A \sim 10^{-3}$ , in fair agreement with the results of Cress et al. (1996), but derived a steeper slope,  $\gamma \sim 2.5$ . Furthermore, by investigating the third moment of the radio galaxy distribution, Magliocchetti et al. (1998) could measure for the first time in an extragalactic radio sample *positive* skewness  $\Psi_3$  in the distribution of the sources and assess that variance and skewness were related through the functional form  $\Psi_3 = S_3(\Psi_2)^\alpha$ , with  $\alpha \simeq 2$  and  $S_3 = \text{constant}$  (cf. Fig. 16). This result has important cosmological implications, since it meant that the large-scale clustering of radio galaxies was in agreement with the gravitational

instability picture for the non-linear growth of perturbations from a primordial Gaussian field.

These findings were subsequently used by [Magliocchetti et al. \(1999\)](#) to put constraints on the composition and redshift distribution of radio galaxies at the mJy level and also to investigate how their spatial distribution traces that of the underlying dark matter within the biased galaxy formation scenario (e.g., [Mo and White 1996](#), see Sect. 4.1.1). It was found that observations could only be matched if one assumed two populations, a less numerous and more local one made of star-forming galaxies whose spatial distribution follows that of the dark matter, and a more numerous population of radio-AGN, much more strongly clustered and presenting a largely biased distribution with the bias parameter  $b$  (defined in equation 8) increasing with look-back time.

A few years later, [Blake and Wall \(2002a\)](#) and [Blake and Wall \(2002b\)](#) analyzed the clustering properties of 361,644 radio objects brighter than  $F_{1.4\text{GHz}} = 15$  mJy in the NVSS survey. These authors did not correct for the issue of multi-component sources, but rather parametrized the two-point correlation function of radio galaxies as the sum of two power-laws: one at small angular scales that mainly described the spurious clustering signal induced by multiple-component and extended sources, and one on scales larger than  $\sim 0.2^\circ$  that would supposedly only take into account the cosmological signal produced by radio-AGN. By doing this, they found an amplitude on large angular scales  $A \sim 10^{-3}$  and a slope  $\gamma \sim 1.8$ , values that remained unchanged when raising the flux threshold. Conversely, [Overzier et al. \(2003\)](#) – by re-analysing the clustering properties of radio sources in the FIRST and NVSS surveys – found that the amplitude of the projected correlation function increased from  $A \sim 10^{-3}$  for objects fainter than 40 mJy to  $A \sim 7 \cdot 10^{-3}$  at 200 mJy. These authors interpreted their results at high fluxes, mostly dominated by FR II galaxies, as evidence for the fact that these sources preferentially inhabit more massive structures than fainter radio galaxies. By using the redshift distribution models proposed by [Dunlop and Peacock \(1990\)](#), [Overzier et al. \(2003\)](#) estimate a correlation length  $r_0 \sim 14$  Mpc/h (value which depends on the adopted assumption for the cosmological evolution of clustering), in rough agreement with the results of [Peacock and Nicholson \(1991\)](#).

All the aforementioned works contributed in a substantial way at proving that extragalactic radio sources could provide an invaluable contribution to the investigation of the Large-Scale Structure of the Universe. However, better information on their physical and environmental properties as obtained from clustering studies has only been made possible with the combination of radio data with observations at different wavelengths, especially for what concerns the determination of redshifts. To this aim, [Magliocchetti et al. \(2004\)](#) presented the clustering properties of a local,  $z < 0.3$ ,  $F_{1.4\text{GHz}} \geq 1$  mJy sample of 761 FIRST radio galaxies with optical spectra and redshift information from the 2dF Galaxy Redshift Survey (2dFGRS – [Colless et al. 2001](#); [Magliocchetti et al. 2002](#)). On the basis of such spectra, radio sources could be divided into star-forming galaxies (225 objects) and AGN (536 objects). An analysis of the spatial two-point correlation function indicated that these sources presented

clustering properties which were similar to those obtained for a general population of inactive galaxies drawn from the same 2dFGRS parent catalogue (Hawkins et al. 2003; Madgwick et al. 2003):  $r_0 \sim 7$  Mpc ( $h$  is fixed here to the value of 0.7) and  $\gamma \sim 1.6$ . However, when the authors only included *bona-fide* AGN, both the correlation length and the slope increased to  $r_0 \sim 11$  Mpc and  $\gamma \sim 2$ . No difference was found between faint ( $L_{1.4\text{GHz}} \leq 10^{22} \text{ W Hz}^{-1} \text{ sr}^{-1}$ ) and bright AGN-fuelled sources. Comparisons with physical models for the clustering properties of galaxies (i.e., Mo and White 1996) further showed that radio-AGN reside within dark matter haloes more massive than  $\sim 10^{13.4} M_\odot$ , value which is higher than what found for radio-quiet quasars in the same 2dFGRS survey (Porciani, Magliocchetti, and Norberg 2004), and compatible with a scenario that associates radio-AGN with protocluster/cluster-like structures. Taken these results at face value, Magliocchetti et al. (2004) suggest that radio-quiet quasars and radio-AGN are two different populations, with more massive dark matter haloes required for an AGN to trigger radio activity. Similar values for the halo masses of radio-selected AGN have been obtained by Mandelbaum et al. (2009) and Hickox et al. (2009). Mandelbaum et al. (2009) also observe radio-AGN to be associated with more massive dark matter haloes than those hosting both inactive galaxies and optically-selected AGN with the same stellar mass content, finding which implies that radio-activity of AGN origin is enhanced within overdense structures. Hickox et al. (2009) instead report a higher clustering signal (and therefore larger halo masses) for their radio-selected AGN when compared to those derived for the two other populations of AGN respectively selected in the X-ray and *Spitzer*-IRAC bands ( $M_{\text{halo}}^{\text{radio}} \sim 10^{13.5} M_\odot$  vs  $M_{\text{halo}}^{\text{X}} \sim 10^{13} M_\odot$  and  $M_{\text{halo}}^{\text{IR}} \lesssim 10^{12} M_\odot$ ).

Brand et al. (2005) investigated the clustering properties of 206,  $z < 0.5$ ,  $F_{1.4\text{GHz}} \geq 3$  mJy sources drawn from the Texas-Oxford NVSS Structure (TONS) radio galaxy redshift survey, finding a correlation length  $r_0 \sim 9$  Mpc for  $\gamma$  fixed to the standard 1.8 value. Large variation in the amplitude of the two-point correlation function – possibly due to cosmic variance – was observed amongst the various fields of the TONS survey. Wake et al. (2008) instead analysed a sample of 250,  $z \sim 0.55$  radio galaxies drawn from the FIRST and NVSS surveys with spectroscopic redshifts determined from the 2SLAQ Luminous Red Galaxy (LRG) redshift survey (Cannon et al. 2006). They found that the correlation length was  $r_0 \sim 12$  Mpc/h ( $\gamma \sim 1.75$ ), higher than the value obtained for the population of radio-quiet LRGs ( $r_0 \sim 9$  Mpc/h) matched in redshift and optical luminosity. These results implied radio-active LRGs to reside within haloes of typical masses  $\sim 10^{14} M_\odot/h$ , higher than the value of  $\sim 6 \cdot 10^{13} M_\odot/h$  obtained for radio-quiet LRGs, and called for an enhanced probability for LRGs to become radio-emitters if hosted within (more) massive structures. A very similar result was obtained by Fine et al. (2011) who matched NVSS and FIRST radio galaxies with a larger catalogue of LRGs endowed with photometric redshifts. As in Magliocchetti et al. (2004), no difference in the clustering properties was found for sources of different radio luminosity. Donoso et al. (2010) also concentrated on samples of radio-AGN and photometrically-identified LRGs. However, at variance with Fine et al. (2011),



they did find a dependence on radio luminosity on scales below  $\sim 1$  Mpc, and also reported different clustering behaviours for the two sub-classes of radio-galaxies and radio-active quasars, with radio-galaxies clustering more strongly than radio-active quasars matched both in black hole mass and radio luminosity. This result led the authors to conclude that – in disagreement with AGN unification models (e.g., [Antonucci 1993](#)) – radio galaxies and radio-active quasars were powered by different physical mechanisms.

[Lindsay et al. \(2014b\)](#) considered  $F_{1.4\text{GHz}} \geq 1$  mJy FIRST radio sources with spectroscopic and photometric information from the Galaxy and Mass Assembly (GAMA – [Driver et al. 2011](#)) survey, finding for the two-point correlation function at  $z \sim 0.48$  a correlation length  $r_0 \sim 8$  Mpc/h and a slope  $\gamma \sim 2.15$ , with a value for the bias  $b(z = 0.48) \sim 2$ . [Lindsay, Jarvis, and McAlpine \(2014a\)](#) instead concentrated on 766 radio sources brighter than  $F_{1.4\text{GHz}} = 90\mu\text{Jy}$  drawn from the VIDEO survey ([Jarvis et al. 2013](#)) and, by cross-correlating this population with  $K_s \leq 23.5$  galaxies observed within the same field, found that their clustering signal sensibly increased with look-back time. This in turn implied an increment of the bias function  $b(z)$  from the value of  $\sim 0.6$  at  $z \sim 0.3$  to  $\sim 8$  at a redshift  $z \sim 2.2$ . [Lindsay et al. \(2014a\)](#) also report a noticeable dependence of the clustering strength on the radio luminosity of the sources even though, with the luminosity range probed by their work, their finding simply restated the well-known effect of (radio brighter) radio-AGN preferentially residing in denser environments than (radio fainter) star-forming galaxies.

[Magliocchetti et al. \(2017\)](#) considered  $\sim 1000$  radio sources from the VLA-COSMOS survey ([Bondi et al. 2008](#)) endowed with photometric redshifts. By relying on their radio-luminosity as it was done in [Magliocchetti et al. \(2014b, 2016, 2018a\)](#) (cf. Sect. 2), these objects were classified as AGN (644 sources) and star-forming galaxies (247). Their clustering properties returned values for the correlation length of  $\sim 7.8$  Mpc for star-forming galaxies and  $\sim 11$  Mpc for radio-AGN ( $h = 0.7$ ). This implied radio-AGN to be hosted within dark matter haloes more massive than  $\sim 10^{13.6} M_\odot$ , in full agreement with the results obtained both locally by [Magliocchetti et al. \(2004\)](#) and [Mandelbaum et al. \(2009\)](#) and in the more distant universe by [Hickox et al. \(2009\)](#), [Hatch et al. \(2014\)](#) and [Allison et al. \(2015\)](#) (cf. Sect. 4.3), and in line with the idea that radio-active AGN preferentially reside in group/cluster-like structures.  $M_{\text{halo}} > 10^{12.7} M_\odot$  was instead found for star-forming galaxies (group which – we remind – given the adopted selection method also includes radio-quiet AGN) at  $z < 0.9$ . These authors took a step further and compared the above results with information on the stellar mass content of the galaxies harbouring a radio-active source as derived for the COSMOS population by [Laigle et al. \(2016\)](#). This allowed to estimate the relationship between dark and luminous matter in both populations: for radio-AGN it was found  $\langle M_* \rangle / M_{\text{halo}} < 10^{-2.7}$  (here  $\langle M_* \rangle$  is the average stellar mass), while for star-forming galaxies they obtained  $\langle M_* \rangle / M_{\text{halo}} < 10^{-2.4}$  at all redshifts and  $\langle M_* \rangle / M_{\text{halo}} < 10^{-2.1}$  at  $z < 0.9$ , result that clearly showed the cosmic process of stellar build-up as one moves towards the more local universe. Lastly, comparisons of the observed

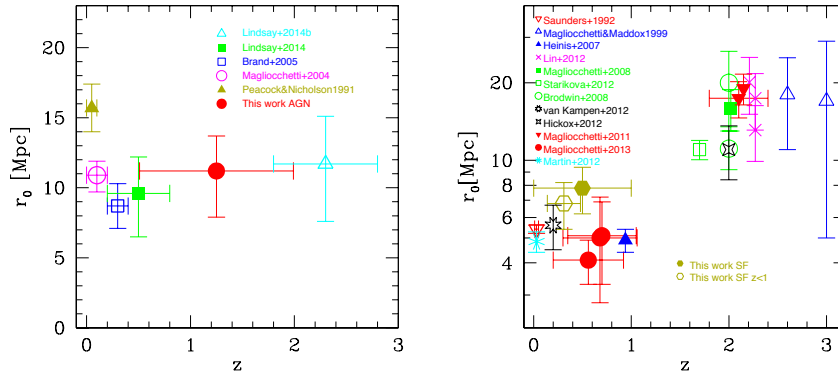


**Fig. 17** Redshift evolution of the clustering length  $r_0$  in the case of radio-selected AGN (left-hand panel) and star-forming galaxies (right-hand panel). The left-hand panel compares the results from the work of Magliocchetti et al. (2017) with those of Peacock and Nicholson (1991), Magliocchetti et al. (2004), Brand et al. (2005), Lindsay et al. (2014b) and Lindsay et al. (2014a). The right-hand panel instead includes star-forming galaxies selected in different ways: Far-Infrared (Saunders et al. 1992; Magliocchetti et al. 2011, 2013; Hickox et al. 2012; Van Kampen et al. 2012), UV (Magliocchetti and Maddox 1999; Heinis et al. 2007), Mid-Infrared (Brodwin et al. 2008; Magliocchetti et al. 2008b; Starikova et al. 2012), BzK method (Lin et al. 2012), HI emission (Martin et al. 2012) and radio at 1.4 GHz (Magliocchetti et al. 2017, where the entire population of star formers is represented by the full hexagon, while the empty one is for more local,  $z < 1$ , sources). Figure from Magliocchetti et al. (2017).

abundance of radio-AGN with that predicted by cosmological models for dark matter haloes more massive than the value of  $10^{13.6} M_\odot$  obtained from the above clustering measurements, indicated that about one in two  $z < 2.3$  haloes is associated with a radio-emitting black hole. This led to estimates for the lifetime of the AGN radio-active phase of  $\sim 1$  Gyr, possibly suggesting evidence for a recurrent phenomenon, whereby each halo undergoes multiple episodes of radio-AGN activity between  $z = 2.3$  and  $z = 0$ .

Magliocchetti et al. (2017) further provide a compilation of the results obtained to date for what concerns the large-scale properties of AGN active in the radio band (mainly at 1.4 GHz) and star-forming galaxies. Figure 17 reports the various values taken from the literature for the correlation length  $r_0$  of radio-AGN of different luminosity (left-hand panel) and star-forming galaxies selected at all wavelengths (right-hand panel). Once again, radio-AGN were classified as such on the basis of their luminosity as in Magliocchetti et al. (2014b, 2016, 2018a). Note that the results from Wake et al. (2008), Donoso et al. (2010) and Fine et al. (2011) were not included in the AGN compilation as they refer to sub-populations of radio-active LRGs which are known to present enhanced clustering strengths due to the properties of their parent population made of very massive galaxies.

Comparisons of the various works clearly show that:

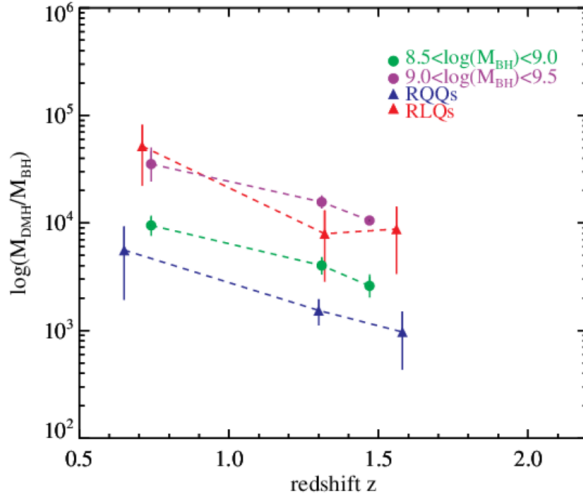


**Fig. 18** Ratio between dark matter halo (DMH) masses and average virial black hole masses for the quasar samples in [Retana-Montenegro and Röttgering \(2017\)](#) as a function of redshift. The labels RLQs and RQQs respectively correspond to radio-active and radio-quiet quasars. Figure from [Retana-Montenegro and Röttgering \(2017\)](#).

1. In the case of radio-AGN there is no dependence of their clustering signal on either radio luminosity or redshift. This implies similar environmental properties (and therefore similar hosts) at all different radio luminosities and – possibly more importantly – no evolution of such properties throughout cosmic epochs, from  $z \simeq 2.5 - 3$  down to the very local universe.
2. In the case of galaxies which form stars at relatively high rates,  $\text{SFR} \gtrsim 30 M_{\odot} \text{ yr}^{-1}$ , there is no difference between the environmental properties of objects selected at different wavelengths, including the radio band. This also holds irrespective of the star-forming rate, as long as it is above the aforementioned value. The striking feature highlighted by clustering studies of star-forming galaxies is that in the relatively local universe these sources are all hosted by relatively small dark-matter haloes, of the order of  $\sim 10^{12} M_{\odot}$  or less, while beyond  $z \sim 1.5$  vigorous star-formation is only found within very massive,  $M_{\text{halo}} > 10^{13.5} M_{\odot}$  structures. Taking these results at face value implies that star-forming galaxies at high and low redshifts belong to two different populations, with intense star-forming activity at  $z \gtrsim 1.5$  preferentially happening in protocluster- or cluster-like structures ([Magliocchetti et al. 2014a](#)).

[Retana-Montenegro and Röttgering \(2017\)](#) also used the large-scale structure results obtained from large samples of radio-active and radio-quiet quasars selected in the  $0.3 < z < 2.3$  range to infer information on the physics of these

two populations. They find that radio-active quasars are more strongly correlated at all redshifts, with mean dark matter host masses of  $\sim 5 \cdot 10^{13} M_{\odot}/h$ , to be compared with those of radio-quiet quasars for which they find  $\sim 2 \cdot 10^{12} M_{\odot}/h$ . Intriguingly, the large-scale properties of quasars are also found to depend on their black hole mass, with quasars powered by more massive black holes clustering more strongly than quasars harbouring less massive nuclei (cf. Fig. 18). For black hole masses above  $10^9 M_{\odot}$ , radio-quiet quasars are found to have the same clustering properties and therefore the same environmental properties of radio-active quasars. This suggests that for the onset of the radio-active phase, black holes need to be at least more massive than the aforementioned value (also see e.g., Laor 2000; McLure and Jarvis 2004; Metcalf and Magliocchetti 2006).

Hale et al. (2018) were the first to present statistically significant clustering estimates for a population of radio sources selected at frequencies different from 1.4 GHz. These authors consider 2937 objects observed at 3GHz in the COSMOS field (Smolčić et al. 2017b) and divide them into star-forming galaxies and radiatively efficient (roughly corresponding to HERGs) and inefficient (roughly corresponding to LERGs) AGN on the basis of a number of criteria, such as AGN emission in other bands. By restricting their analysis to  $z < 1$ , these authors find for star-forming galaxies values for the halo mass  $\sim 3 - 5 \cdot 10^{12} M_{\odot}/h$ , while for AGN  $M_{\text{halo}} \sim 1 - 2 \cdot 10^{13} M_{\odot}/h$ , in line with previous studies. By further analyzing the two populations of high-efficiency and low-efficiency radio-AGN separately, it was found that low-efficiency AGN cluster slightly more strongly, and therefore inhabit slightly more massive haloes than high-efficiency AGN ( $M_{\text{halo}} \sim 3 - 4 \cdot 10^{13} M_{\odot}/h$  vs  $M_{\text{halo}} \sim 1 - 2 \cdot 10^{13} M_{\odot}/h$ ). A dependence of the clustering strength on the radio luminosity of the AGN was also reported, whereby higher-luminosity sources seem to be hosted by more massive haloes than lower-luminosity ones.

Other recent works which use observations at frequencies different from 1.4 GHz are those of Rana and Bagla (2019) and Chakraborty et al. (2020). The first paper uses GMRT observations at 150 MHz of about 90% of the whole sky (TGSS survey) and therefore can only provide information on projected quantities, which nevertheless show that the 2D clustering amplitude increases with radio flux threshold, hinting to the conclusion that brighter objects are hosted by more massive haloes. It should however be noted that the clustering signal as measured from TGSS exhibits an unexplained excess mostly on large ( $\theta \gtrsim 0.3^\circ$ ) scales with respect to that derived from NVSS (Dolfi et al. 2019). The second paper instead concentrates on the much smaller region of ELIAS-N1 and can therefore rely on the availability of multi-wavelength observations. Chakraborty et al. (2020) then consider  $\sim 2500$  radio sources observed with uGMRT in the 300-500 MHz band. About 60% of them are endowed with photometric redshifts and objects were subdivided into AGN and star-forming galaxies on the basis of their radio luminosity as in Magliocchetti et al. (2014b, 2016, 2018a). Their analysis of the clustering properties of these sources returns values for the correlation length of  $r_0 \sim 4.6$  Mpc/h and  $r_0 \sim 7.3$  Mpc/h, respectively for star-forming galaxies and AGN. We note that these values are

in excellent agreement with those of [Magliocchetti et al. \(2017\)](#) and [Hale et al. \(2018\)](#) obtained for sources selected at higher radio frequencies.

At the time of writing, observations stemming from LOFAR ([van Haarlem et al. 2013](#)) have started providing breakthrough insights on the radio phenomena as seen at low frequencies. The first results on the large-scale properties of LOFAR galaxies are provided in [Siewert et al. \(2020\)](#), where the authors investigate the first and second moments of the radio galaxy distribution, finding for sources from the DR1 brighter than  $F_{144\text{ MHz}} = 2\text{ mJy}$  an angular correlation function described by a power-law with amplitude  $A \sim 5 \cdot 10^{-3}$  and slope  $\gamma \sim 1.7$ . More works in this direction are those of [Alonso et al. \(2021\)](#), who cross-correlate LOFAR data with CMB lensing in order to calibrate the (unknown) redshift distribution of LOFAR sources and of [Tiwari et al. \(2021\)](#) who provide the first results for the angular power spectrum. As it was in the 1990s for FIRST and NVSS, the main limitation of these studies performed with LOFAR observations is the lack of reliable redshift information for the majority of the sources. This issue is going to be overcome soon with DR2, especially since multi-wavelength data for the deep fields will also be released ([Best et al. 2022 submitted](#)).

#### 4.2 Methods for the detection of environment 2: direct pinpointing of sources within known structures

A second method used to investigate the environmental properties of radio galaxies is based on direct searches for these sources within known structures. In the case of virialized groups and clusters with available X-ray information, this approach also has the advantage of investigating their thermal properties in the presence or absence of a radio-AGN and therefore to study the interaction between radio emission and intracluster medium (ICM).

After some early works aimed at assessing the effects of dense/cluster-like environments on radio-AGN activity that involved a relatively limited number of sources (e.g., [Jaffe and Perola 1976](#); [Auremma et al. 1977](#); [Lari and Perola 1978](#); [Fanti et al. 1982](#)) to our knowledge [Ledlow and Owen \(1996\)](#) were the first ones to provide statistical robust results on the recurrence of radio-AGN within known structures. This was obtained by performing a 1.4 GHz survey of 188,  $z \leq 0.09$ , radio-AGN within Abell clusters and by computing their radio and bivariate radio/optical luminosity functions. Such functions were then compared to those of other samples of radio sources not residing in rich clusters in order to determine the effects of the environment on radio-AGN evolution. By doing so, [Ledlow and Owen \(1996\)](#) found no significant dependence on the local galaxy density, evidence that made the authors conclude that the radio luminosity function is representative of the intrinsic properties and evolution of radio galaxies as one class, independent of the the large-scale structure within which these sources reside.

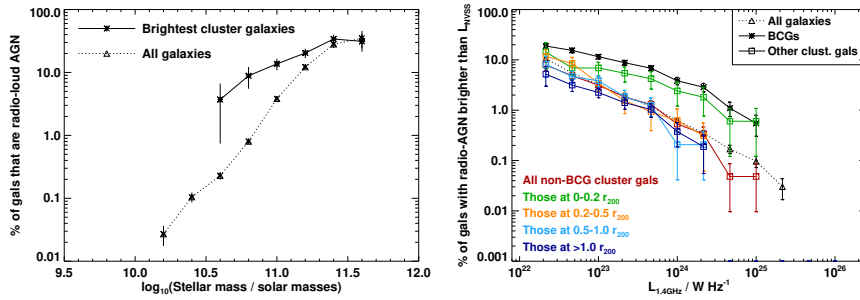


**Fig. 19** Left-hand panel: the percentage of galaxies that host a radio-AGN, as a function of stellar mass, for all galaxies and for BCGs. BCGs are more likely to be radio-active than other galaxies of the same stellar mass, and the two relations have different slopes. Right-hand panel: the percentage of galaxies which host a radio-AGN brighter than a given radio luminosity for non-BCG cluster galaxies (red line) as compared to the all galaxy (dotted black line) and BCG (solid black line) samples. The other coloured lines indicate the equivalent relations for different subsets of the non-BCG cluster galaxies with different distances from the center. The radio-AGN fraction is boosted for galaxies within  $0.2 r_{200}$  of the cluster center, but retains the same overall shape. Figures from Best et al. (2007).

A decade later, Best et al. (2007) used a sample of 625,  $z < 0.1$  groups and clusters of galaxies selected from the Sloan Digital Sky Survey (Miller et al. 2005; von der Linden et al. 2007) and cross-correlated them with the NVSS and FIRST radio samples in order to study the properties of radio-AGN hosted by the Brightest Cluster Galaxies (BCGs). In their work they show that the fraction of BCGs that are radio-active AGN increases linearly with (stellar) mass up to a plateau level of about  $\sim 20 - 30$  per cent reached for their highest mass range which is about  $M_* \sim 10^{11.5} M_\odot$  (cf. left-hand panel of Fig. 19), and that BCGs are more likely to host a radio-AGN than other galaxies of the same stellar mass. This trend is independent of the velocity dispersion (i.e., the mass) of the clusters, as is the radio luminosity distribution, which is observed to be the same for clusters of different masses. Interestingly enough, the same behaviour is also observed for non-BCG cluster galaxies but only as long as they reside in the proximity of the cluster center ( $r < 0.2 r_{200}$ , cf. right-hand panel of Fig. 19, where  $r_{200}$  is the radius within which the average density equals 200 times the critical density  $\delta_c$  for spherical collapse, see Sect. 4.1.1). The above findings led the authors to conclude that radio activity of AGN origin is associated with the cooling of gas from the hot envelopes of elliptical galaxies and, in the case of central cluster galaxies, also from the intracluster medium. This is because accretion of hot gas from a strong cooling flow is able to explain both the boosted likelihood of BCGs hosting radio-active AGN, and the different slopes of the mass dependencies of the radio-AGN fractions for BCGs and other galaxies.

Indeed, by then, evidence for a connection between radio-AGN activity and thermal state of groups and clusters of galaxies had already started to accumulate, although it was only based on a handful of observations (e.g.,

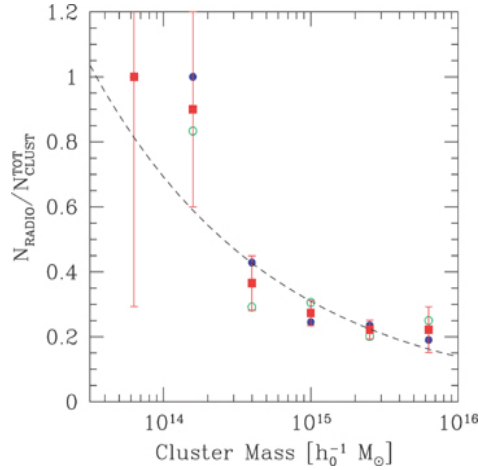


**Fig. 20** Ratio between number of clusters with a central radio counterpart brighter than 3 mJy in the NVSS maps and the whole  $F_X \geq 3 \cdot 10^{-12} \text{ erg s}^{-1} \text{ cm}^{-2}$  cluster population as a function of cluster mass. Open (green) circles are for NORAS objects, filled (blue) dots for REFLEX, while (red) squares and associated error bars represent the combined REFLEX + NORAS dataset. The dashed line indicates the best fit to the data. Figure from Magliocchetti and Brüggén (2007).

Smith et al. 2002; Kraft et al. 2002; Croston et al. 2003). Croston, Hardcastle, and Birkinshaw (2005) were the first ones to systematically investigate a well-defined and homogeneous sample of 30 local groups with available X-ray information (Osmond and Ponman 2004), reporting evidence for the gas properties of groups containing radio-active galaxies (about 60% of them) to differ from those not hosting them, in the sense that radio-active groups were likely to be hotter at a given X-ray luminosity. They attributed this effect to the heating induced by radio galaxies.

Magliocchetti and Brüggén (2007) extended the analysis of Croston et al. (2005) and Best et al. (2007) to clusters of higher mass and with known X-ray information, again in order to assess the importance of (central) AGN radio emission on the thermal properties of the ICM. This was done by considering combined observations from the REFLEX (Bohringer et al. 2004) and NORAS (Bohringer et al. 2000) cluster surveys with NVSS for 145,  $z < 0.3$ , X-ray selected clusters brighter than  $3 \cdot 10^{-12} \text{ erg s}^{-1} \text{ cm}^{-2}$  that showed central radio emission above 3 mJy. For cluster masses  $M_{\text{CL}} \leq 10^{14.5} M_{\odot}$ , 11 clusters out of 12 (corresponding to 92 per cent of the systems) were found to be inhabited by a central radio source. This fraction decreases for higher masses as  $\propto M_{\text{CL}}^{-0.4}$  (cf. Fig. 20). By further dividing the sample into clusters harbouring either a point-like or an extended radio-AGN (about 41% of the analyzed cases, a percentage which is much higher than what is generally found for radio galaxies within the same redshift range and at similar radio flux levels,  $\sim 5\%$  – e.g., Magliocchetti et al. 2002), these authors observed that the steepening of the X-



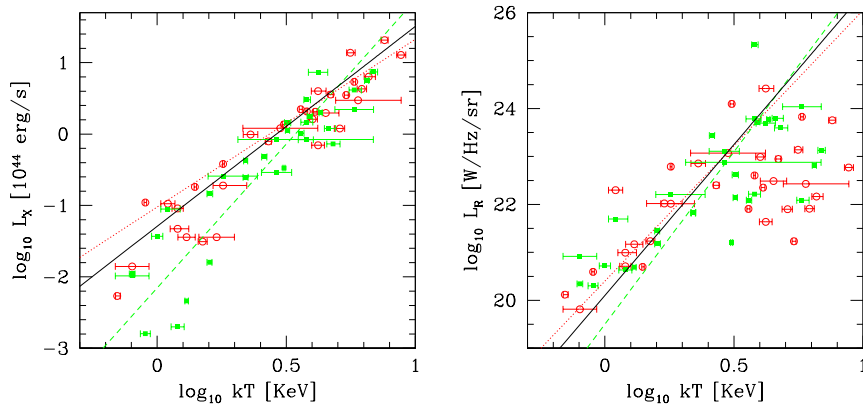


**Fig. 21** Left-hand panel: X-ray luminosity versus cluster temperature for those X-ray-selected clusters brighter than  $3 \cdot 10^{-12} \text{ erg s}^{-1} \text{ cm}^{-2}$  which exhibit central radio emission above 3 mJy. Open (red) circles represent clusters associated with point-like radio sources, while solid (green) squares indicate clusters inhabited by radio-AGN presenting extended structures. The dashed (green) line indicates the  $L_X$ – $kT$  best fit for the sub-population of extended radio sources, while the dotted (red) one is for point-like radio objects. The solid line is the best fit to the whole radio cluster sample. Right-hand panel: radio luminosity of the sources associated with cluster centres versus cluster temperature. Symbols are as before. Figure from Magliocchetti and Brüggen (2007).

ray Luminosity-Temperature ( $L_X - T$ ) relation observed in low-temperature clusters (e.g., Helsdon and Ponman 2000) was strongly associated with the presence of central radio-AGN with extended jets and/or lobed structures. In this latter case,  $L_X \propto T^4$ , while for point-like sources one recovers the approximately self-similar relation  $L_X \propto T^2$  (cf. left-hand panel of Fig. 21), expected when gravity is the only source of heating. This bimodal behavior suggests a more efficient mode with which extended sources can permeate the surrounding ICM and transfer heat within the cluster. Interestingly, the net effect of extended radio-AGN on the ICM is observed to decrease with increasing cluster mass (i.e., increasing  $kT$ ), and at larger masses also any relationship between AGN radio luminosity and cluster temperature is lost (cf. right-hand panel of Fig. 21). Based on their data combined with Montecarlo simulations, Magliocchetti and Brüggen (2007) conclude that the presence of radio-AGN with an extended structure is responsible for the overheating of the intracluster gas, with an importance which dramatically increases in low-mass systems. At the same time, Lin and Mohr (2007) considered a sample very similar to that of Magliocchetti and Brüggen (2007) and estimated the radio-luminosity function of radio-AGN within  $r_{200}$ . At variance with Ledlow and Owen (1996), their results showed that it was about seven times more likely for a galaxy to be radio-active if it resided within a cluster environment rather than in the field, 10 ( $\sim 30$ ) times more likely in the case of associations between BCGs and  $L_{1.4 \text{ GHz}} > 10^{23} \text{ W Hz}^{-1}$  ( $L_{1.4 \text{ GHz}} > 10^{25} \text{ W Hz}^{-1}$ ) AGN. The authors also found that the surface density profiles of the hosts of radio-

AGN were much more concentrated than those of inactive galaxies, and that more powerful radio sources were more concentrated than weaker ones. All these pieces of evidence made the authors invoke radio-AGN activity as an important heating source for the intracluster medium, especially within 10% of the clusters virial radii. Lastly, by converting the estimated radio-luminosity function into a life-time for the radio-active AGN phase, [Lin and Mohr \(2007\)](#) derived values of about 0.6 Gyr, in rough agreement, even though on the lower side, with [Magliocchetti et al. \(2017\)](#).

[Smolčić et al. \(2011\)](#) moved the analysis to higher redshift sources and investigated the recurrence of 217 low-power ( $10^{23.6} < L_{1.4\text{GHz}}/[\text{W Hz}^{-1}] < 10^{25}$ ) radio-AGN selected in the COSMOS field out of  $z = 1.3$  within X-ray selected groups of masses  $10^{13.2} < M_{200}/M_{\odot} < 10^{14.4}$  ( $M_{200}$  is total mass of the group enclosed within  $r_{200}$ ). In agreement with [Best et al. \(2007\)](#), they found a strong enhancement of radio-AGN in group centers ( $< 0.2 r_{200}$ ). Furthermore, by comparing their radio-AGN to a control sample of inactive galaxies with the same stellar mass and colour distributions, they observed that the fraction of radio-AGN was enhanced by a factor  $\sim 2$  in galaxy groups. By using these results combined with Halo Occupation methods (cf. Sect. 4.1.1), [Smolčić et al. \(2011\)](#) also estimate the average time a massive red galaxy in a galaxy group is switched on to a radio-active AGN phase to range between 0.6 and 3.5 Gyr, value which depends on the mass of the group (the more massive the group, the longer the active phase), in good agreement with the findings of [Lin and Mohr \(2007\)](#) and [Magliocchetti et al. \(2017\)](#) obtained from clustering methods. It is also worth mentioning that *all* galaxies with stellar masses  $M_* > 10^{12} M_{\odot}$  in the [Smolčić et al. \(2011\)](#) sample are radio-active AGN found to reside within groups.

[Mo et al. \(2018\)](#) instead investigate the interaction between radio-AGN activity and cluster environment for 2300 galaxy clusters (212 with an embedded radio-AGN from the FIRST survey) from the MaDCoWS survey ([Brodwin et al. 2015](#)), which selected galaxy over-densities in the WISE bands up to  $z \sim 1$ . Radio-AGN are observed to be more concentrated towards the cluster centers, in line with the behaviour of MIR-selected AGN but at variance with optically-selected AGN (cf. Fig. 22). Also, the radio-AGN fraction was reported to be more than 2.5 times that of the field, implying – in agreement with e.g., [Best et al. \(2007\)](#) and [Smolčić et al. \(2011\)](#) – that the centers of clusters favour the triggering of radio emission in AGNs. No statistically significant change in the AGN fraction as a function of cluster richness was instead found. [Mo et al. \(2020\)](#) further find that the probability for a cluster to host a radio-active AGN with  $L_{1.4\text{GHz}} > 10^{25} \text{ W Hz}^{-1}$  is a steep function of redshift, showing a factor  $\sim 10$  increase in the range  $0 \lesssim z \lesssim 1.2$  (see also e.g., [Donoso, Kauffmann, and Best 2009](#); [Birzan et al. 2017](#)), and that such a probability is also strongly dependent on radio luminosity.

[Magliocchetti et al. \(2018b\)](#) analyse the recurrence of 218,  $z \leq 1.2$  radio galaxies from the same COSMOS-VLA survey ([Schinnerer et al. 2007](#); [Bondi et al. 2008](#)) considered by [Smolčić et al. \(2011\)](#), but within the different components of the cosmic web such as clusters, filaments and the field as

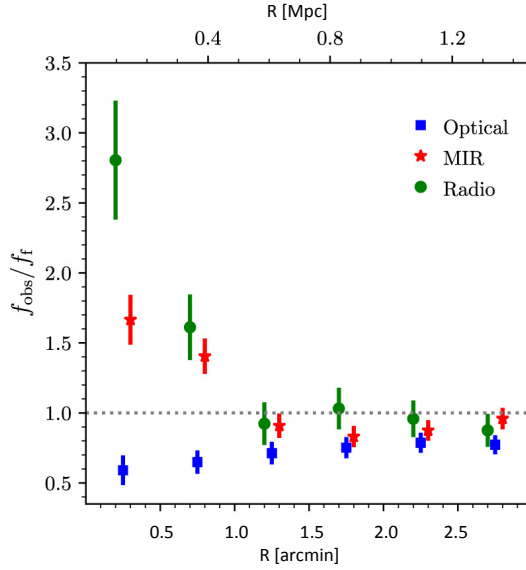


**Fig. 22** Observed AGN fraction in MaDCoWS clusters divided by the field fraction as a function of cluster-centric distance. Deviations from the field level are in the central  $1'$  region and are dependent on the selection method of the AGN catalogue. The bottom x-axis represents the distance from the cluster center expressed in arcmin, while the top x-axis that in Mpc. Figure from [Mo et al. \(2018\)](#).

reconstructed by the work of [Darvish et al. \(2017\)](#). It was found that while radio-emitting star-forming galaxies are distributed in a fashion which is similar to the more general population of COSMOS galaxies, radio-AGN tend to be more preferentially hosted by dense environments (20% vs  $\sim 10\%$  of the general population). Furthermore, radio-AGN with  $L_{1.4\text{GHz}} > 10^{23.5} \text{ W Hz}^{-1} \text{ sr}^{-1}$  are twice more likely to be found in clusters with respect to fainter sources ( $\sim 38\%$  vs  $\sim 15\%$ , cf. left-hand panel of Fig. 23), just as radio-selected AGN hosted by galaxies with stellar masses  $M_* > 10^{11} M_\odot$  are twice more likely to be found in overdense environments with respect to objects of lower mass ( $\sim 24\%$  vs  $\sim 11\%$ , cf. right-hand panel of Fig. 23), and to avoid underdense structures more than inactive galaxies with the same stellar mass content. Stellar masses also seem to determine the location of radio-active AGN within clusters as  $\sim 100\%$  of the AGN coinciding with a BCG have  $M_* > 10^{11} M_\odot$ . No different location within the cluster was instead observed for AGN of different radio luminosities. Furthermore, in agreement with the early work of [Tasse et al. \(2008\)](#), radio-AGN which also emit in the MIR are observed to present a marked preference to be found as isolated galaxies ( $\sim 70\%$  of the subsample) at variance with those also active in the X-ray that all seem to reside within overdensities. Based on the above results, [Magliocchetti et al. \(2018b\)](#) advocate for a strong link between processes taking place on sub-pc/pc/Kpc scales and the large-scale – Mpc – environment of radio-emitters, irrespective

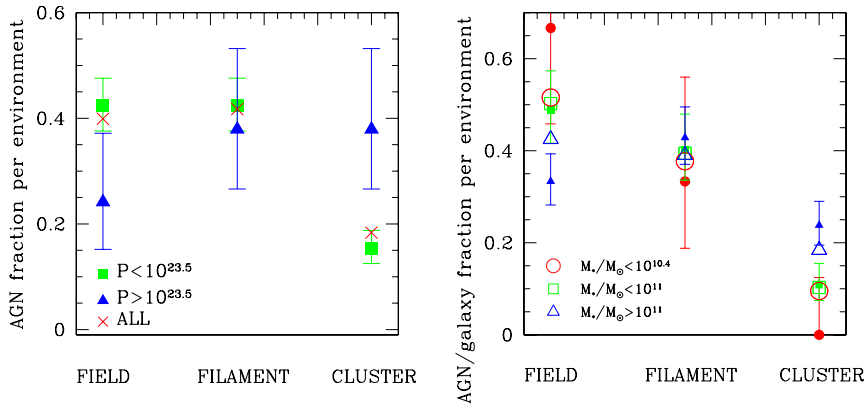


**Fig. 23** Left-hand panel: Distribution of radio-selected AGN within different environments for different values of the AGN radio luminosity (expressed in  $\text{W Hz}^{-1} \text{sr}^{-1}$ ). Right-hand panel: Fraction of radio-selected AGN (small filled symbols) and galaxies from Darvish et al. (2017) (large open symbols without error bars) within different environments for various values of the stellar mass of the hosts. The circles indicate the results obtained for sources with stellar masses  $M_*/M_\odot \leq 10^{10.4}$ , squares for sources with  $M_*/M_\odot \leq 10^{11}$ , and triangles for  $M_*/M_\odot > 10^{11}$ . In all cases error-bars show  $1\sigma$  Poisson uncertainties. Those corresponding to the galaxies from Darvish et al. (2017) are smaller than the symbol sizes. Figures from Magliocchetti et al. (2018b).

of whether star-forming galaxies or AGN. A strong dependence of the probability for a radio-active AGN to belong to an overdense structure on its radio luminosity ( $\sim 10\%$  at  $L_{150\text{MHz}} = 10^{22.5} \text{ W Hz}^{-1}$  vs  $\sim 30\%$  at  $L_{150\text{MHz}} = 10^{26} \text{ W Hz}^{-1}$ ) is also found by Croston et al. (2019), who use a sample of 8745,  $z < 0.4$  radio-active AGN taken from the LoTSS DR1 catalogue (Shimwell et al. 2019; Hardcastle et al. 2019) matched with two cluster catalogues from the SDSS DR8 (Wen et al. 2012 and Rykoff et al. 2014). These authors further observe that cluster richness and AGN radio luminosity are related, since AGN with  $L_{150\text{MHz}} > 10^{25} \text{ W Hz}^{-1}$  are likely to be found in rich cluster environments, and that the location of a radio-AGN within its overdense region is also dictated by its radio luminosity, as the most radio-luminous AGN are typically found close to the centre. In agreement with Magliocchetti et al. (2018b) though, it is concluded that stellar mass is likely to be the dominant cause for the different location preferences of low- and high-luminosity AGN.

Miraghaei (2020) also investigates radio and optical AGN activity as a function of environment spanning from voids to clusters of galaxies. Data were taken from the value added spectroscopic catalogue of Best and Heckman (2012). No dependence of radio-AGN recurrence on environment is found in either blue (i.e., with ongoing star-formation) or green (i.e., in the process of being quenched) galaxies, while it is reported as significant in the case of radio-AGN hosted by red galaxies, whereby radio activity is observed to increase in dense environments. These findings lead the author to conclude that the efficiency of gas accretion from small- or large-scale environments

onto super massive black holes is low in the presence of cold gas within the galaxies while, in its absence, the hot gas from the intergalactic medium filling a dense environment efficiently triggers radio-AGN activity.

Lastly, it is worth mentioning the first attempts to investigate the environments of radio-AGN by pinpointing these sources within known structures at redshifts as high as  $z \sim 4$  (Uchiyama et al. 2022). In this case, no preference for high-redshift radio galaxies to reside within overdense structures is observed. However, Uchiyama et al. (2022) report an excess of  $g$ -dropout galaxies around faint ( $L_{1.4\text{GHz}} \sim 10^{26.0-26.5} \text{ W Hz}^{-1}$ ) radio-AGN, while no difference is found between the densities of galaxies surrounding brighter radio-AGN and of those belonging to the field. Perhaps most interestingly, these authors observe that the galaxies surrounding their sources tend to distribute along the major axes of the radio jets. If confirmed, this would imply the onset of filamentary structures around radio-AGN at an epoch as early as  $z \sim 4$ . Masses for the haloes hosting these sources are estimated to be  $\sim 10^{13.1} M_{\odot}$ , result which extends the observed independence of radio-AGN environmental properties from look-back time (cf. Sect. 4.1) up to  $z \sim 4$ .

#### 4.2.1 The FRI-FRII and HERG-LENG distinction

So far we have mainly considered radio-AGN as a single population of sources. However (cf. Sects. 3.1 and 3.2), they indeed come in a number of flavours, mostly as FRI vs FRII galaxies and/or as LERGs vs HERGs. It is therefore of interest investigating the environmental properties of these sub-classes of sources separately. A small number of early works (e.g., Prestage and Peacock 1988; Allington-Smith et al. 1993; Zirbel 1997; Best 2004, see also later in this Section) already tackled this issue, coming to the general conclusion that in the local universe FRIs and LERGs occupy denser structures than FRIIs and HERGs, even if there were hints for a positive cosmological evolution of FRII environments, at least up to  $z \sim 0.5$ . Wing and Blanton (2011) extended these studies by considering  $\sim 700$  FRI and  $\sim 200$  FRII galaxies from the FIRST survey with a counterpart in the SDSS DR7. They observed a preference for extended radio-AGN of any kind (i.e., with straight or bent morphologies) to reside within overdense environments as opposed to point-like sources (up to  $\sim 80\%$  in the case of bent-lobed AGN vs  $\sim 10 - 30\%$  for single objects), and also found more FRI galaxies within  $z \lesssim 0.5$  to inhabit rich structures (such as groups or clusters or galaxies) than FRIIs (e.g., in the case of straight extended radio emission,  $\sim 60\%$  vs  $\sim 40\%$  in group-like structures and  $\sim 37\%$  vs  $\sim 21\%$  in cluster-like structures). Gendre et al. (2013) applied the same method of Wing and Blanton (2011) to investigate the richness of the structures surrounding 88 LERGs and 70 HERGs set at  $z < 0.3$ , further divided into FRIs and FRIIs. These authors found that HERGs were more likely associated with poor over-densities regardless of their further division into FRI and FRII morphologies, while LERGs of any type could be found within both relatively poor and rich environments.

Ineson et al. (2013) and Ineson et al. (2015) present the results of the Environment of Radio-loud AGN (ERA) program characterizing the cluster environment of radio-AGN. In their first work they concentrate on 26 radio-AGN at  $z \sim 0.5$  drawn from the McLure et al. (2004) sample in order to beat effects due to cosmological evolution and conclude that there is some weak correlation between radio luminosity and host cluster X-ray luminosity, correlation driven by the sub-population of LERGs, with HERGs showing no significant correlation. Ineson et al. (2015) confirmed the above results on 55 lower-redshift ( $z < 0.2$ ) AGN, finding strong correlations between radio luminosity, cluster richness and central density in the case of LERGs and no correlation between radio luminosity and cluster richness, or between radio luminosity and central density for HERGs. HERG environments appear to be poorer at lower redshifts with respect to  $z \sim 0.5$ . No cosmological evolution of structure density is instead observed for LERGs.

Miraghaei and Best (2017) also investigate the environmental properties of radio galaxies selected according to their radio morphology (i.e., FR II, FR I, compact and with unusual morphologies) as well as their accretion properties (LERGs vs HERGs). The AGN sample adopted for their analysis is the one presented in Best and Heckman (2012) which includes low-redshift ( $z < 0.4$ ) radio sources from the NVSS and the FIRST surveys cross-matched with SDSS DR7, while that for the environments was taken from Sabater, Best, and Argudo-Fernández (2013). These authors conclude that the environments of LERGs display higher densities compared to those of HERGs, supporting the hypothesis that the source of AGN fuelling is the main origin of the HERG/LE RG dichotomy. Furthermore, by comparing FR I LERGs with FR II LERGs at fixed stellar mass and radio luminosity, they show that FR I galaxies typically reside in richer environments and are hosted by smaller galaxies with higher mass-surface density (cf. Sect. 3.2), in agreement with a scenario invoking extrinsic effects of jet disruption driving the FR dichotomy. No environmental difference is instead found between extended and compact LERGs. Croston et al. (2019) also observe that FR I radio galaxies inhabit systematically richer environments than FR IIs, and that the probability for an FR I to be found within an over-density strongly increases with its radio luminosity, at variance with bright FR IIs that tend to avoid rich structures.

Massaro et al. (2019, 2020) however argue that the above results on the environmental differences between FR I and FR II galaxies as well as between LERGs and HERGs mostly originate from selection biases and present a new analysis which could minimize them. The adopted catalogues are those of visually-inspected FR Is and FR IIs from Capetti et al. (2017a) and Capetti et al. (2017b) (cf. Sect. 3.2), with a redshift range limited to  $z < 0.15$ . The environments of the 195 FR I + 115 (14 of which classified as HERGs, all the others being LERGs) FR II galaxies are then investigated by making use of various techniques which include both cross-matching the radio sources with known catalogues of clusters and groups of galaxies as well as direct search for over-densities around the selected radio-AGN using them as beacons. By combining these methods together, they find that in the local universe FR Is

and FRIIs as well as HERGs (all FRIIs in their catalogue) and LERGs all live in overdense environments having the same richness, independent of the redshift range considered, their radio luminosity or the absolute magnitude of their hosts, even though the probability of finding an FRI in such structures seems to be enhanced with respect to the population of FRIIs.

More recently, [Vardoulaki et al. \(2021\)](#) brought this analysis to higher redshifts and considered the recurrence of 3GHz-selected radio-AGN down to  $\mu\text{Jy}$  level subdivided into FRI (39 sources), FRII (59 sources) and compact/jetless radio emitters (1818 sources) within 247,  $0.08 \leq z \leq 1.53$ , X-ray detected groups of galaxies in the COSMOS field ([Gozaliasl et al. 2019](#)). At variance with most of the results presented so far in the literature, they find no preference for radio-AGN of any morphology to reside within over-densities. They ascribe their results as possibly due to the lack of high sensitivity and resolution in previous radio observations that could in principle have prevented the detection of fainter and/or smaller radio sources. These conclusions are however in disagreement with the findings obtained by the same authors when they compare their radio samples with the density field reconstructed in COSMOS by [Darvish et al. \(2017\)](#). Indeed, in this latter case they observe that point-like radio sources preferentially reside within the field (40% of the sub-sample), while FRII galaxies are more often hosted by cluster-like environments (46%), although the small number of objects involved in the analysis does not allow to draw strong conclusions.

#### 4.3 Methods for the detection of environment 3: search for over-densities around known sources

A third method to investigate the environmental properties of radio galaxies consists in adopting an opposite approach to that discussed in Sect. 4.2 and observe the structures that surround pre-selected radio sources. In this case the analysis can be divided into i) targeted searches around radio-AGN and ii) cross-matches of radio and optical (or IR) catalogues

##### 4.3.1 Targeted searches around radio-AGN

Targeted searches for clusters and protoclusters of galaxies embedding radio-active AGN have been proven throughout the years to be very successful. [Hill and Lilly \(1991\)](#) were amongst the first ones to investigate the environment around powerful radio-AGN by estimating the net excess number of galaxies within 0.5 Mpc from the radio galaxy and within a magnitude range  $m_1$  and  $m_1 + 3$ , where  $m_1$  was the magnitude of the radio galaxy itself. They observed 45 radio galaxies and 6 radio-active quasars of radio luminosities spanning 4 dex within the narrow redshift range  $0.35 < z < 0.55$ . By doing so, they found that radio-AGN on average resided in rich environments. This held for both powerful (i.e., above the break of the radio-luminosity function) and less powerful sources, at variance with results from the more local universe



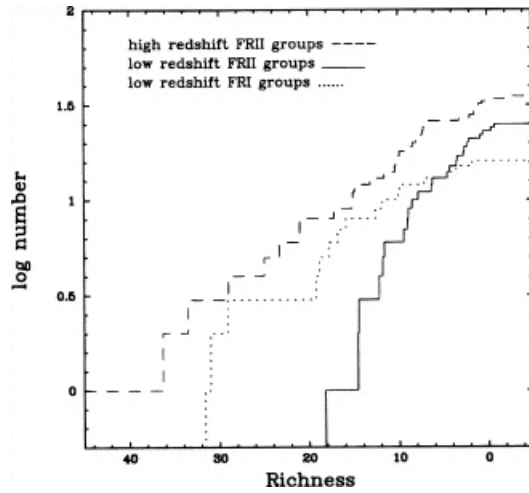


**Fig. 24** Cumulative richness distributions of low-redshift groups surrounding FRI galaxies (dotted line), low-redshift groups surrounding FRII galaxies (solid line), and  $z \sim 0.5$  groups surrounding FRII galaxies (dashed line). Figure from [Zirbel \(1997\)](#).

obtained by previous studies (i.e., [Prestage and Peacock 1988](#), cf. Sect. 4.1) which showed that only FRI galaxies resided in overdense structures.

Another seminal work was that of [Allington-Smith et al. \(1993\)](#) who applied the same method of [Hill and Lilly \(1991\)](#) to a catalogue of 98,  $z < 0.5$ , radio galaxies selected within a narrow interval in radio luminosity ( $L_{408\text{MHz}}$  between  $10^{26}$  and  $10^{28}$  W Hz $^{-1}$ ) and subdivided into two redshift ranges,  $z < 0.25$  and  $0.25 < z < 0.5$ . They found that these sources mostly resided in rather poor clusters (or groups of galaxies), with three to ten members and a richness that roughly doubled from the low- $z$  to the higher- $z$  sample. Furthermore, as also re-stated by [Zirbel \(1997\)](#), they managed to reconcile the disagreement between the results of [Hill and Lilly \(1991\)](#) and those of [Prestage and Peacock \(1988\)](#) as it was observed that, while at low redshifts FRII galaxies avoided overdense regions, they indeed existed in rich groups at redshifts  $z \sim 0.5$  (cf. Fig. 24). From the same [Allington-Smith et al. \(1993\)](#) sample, [Zirbel \(1997\)](#) also showed that the high- and low-redshift groups surrounding FRI and FRII galaxies belonged to separate subsets, and that FRI groups were dynamically more evolved than FRII groups.

Thanks to all the work and efforts put into analysing the environmental properties of radio-AGN in the previous years (cf. also Sects. 4.1 and 4.2), by the end of last century it was then clear that radio sources of AGN origin preferentially inhabited overdense structures. This led to a further step in this kind of targeted studies around radio-AGN: use them as beacons to look for over-densities of galaxies at high (i.e.,  $z \sim 1 - 2$  and above) redshifts, beating some of the limitations which affected the-then-state-of-the-art methods for the search of high-redshift clusters of galaxies such as the partial absence of evolved galaxies and therefore of a red sequence (e.g., [McDonald et al. 2016](#)),

or the difficulty of detecting hot cluster gas by means of X-ray techniques in the more distant universe.

Pentericci et al. (2000) used VLT spectroscopic observations to provide one of the first pieces of evidence for the existence of an overdense region (marked by 14 Ly $\alpha$  emitters and one quasar) surrounding a clumpy radio galaxy set at redshift  $z = 2.16$ . Venemans et al. (2002) report the detection of a structure made of 20 Ly $\alpha$  emitters (out of 23 observed galaxies, with a success rate of 87%) around the luminous radio galaxy TN J1338-1942 set at  $z = 4.1$ . Such a structure extends for at least  $2.7 \text{ Mpc} \times 1.8 \text{ Mpc}$  in projection and constitutes an over-density of about 15 when compared with the field distribution of Ly $\alpha$  emitters at the same redshift. The inferred mass of the structure is about  $10^{15} M_{\odot}$  and, interestingly enough, the radio galaxy does not constitute the centre of the protocluster. These observations were subsequently complemented with the discovery within the same structure of a large population of Lyman-break galaxies, a factor  $\sim 2.5$  higher than the average number observed in random fields (Miley et al. 2004, see Miley and De Breuck 2008 for a review on high-redshift radio galaxies and their environments).

Stern et al. (2003) made use of Keck observations to report the discovery of a galaxy over-density associated with the  $z = 1.11$  radio galaxy MG1 J04426+0202. At variance with Pentericci et al. (2000) and Venemans et al. (2002), and likely due to the lower redshift of the source, in this case members of the over-density were identified as passive elliptical galaxies formed at high redshift. Venemans et al. (2007) extended the work of Pentericci et al. (2000) and Venemans et al. (2002) by searching for forming clusters of galaxies near 8 powerful ( $L_{2.7\text{GHz}} > 10^{33} \text{ erg s}^{-1} \text{ Hz}^{-1} \text{ sr}^{-1}$ ) radio galaxies at  $2.0 < z < 5.2$ . At least six of their eight fields were found to be overdense in Ly $\alpha$  emitters by a factor 3-5 when compared to the field density at similar redshifts. Furthermore, the emitters showed significant clustering in velocity space. From their results, Venemans et al. (2007) estimated that roughly 75% of powerful high redshift radio galaxies reside in a protocluster. Hatch et al. (2011) imaged the fields surrounding six,  $2.2 < z < 2.6$ , radio-AGN, finding over-densities of physically associated galaxies for three of them which extended to  $\sim 4 \text{ Mpc}$  and contained approximately  $\sim 2 - 7 \cdot 10^{14} M_{\odot}$  mass. Doherty et al. (2010) spectroscopically confirmed the existence of two protoclusters surrounding two high redshift radio galaxies set at  $z = 2.16$  and  $z = 2.93$ . These authors were also able to identify two massive red galaxies, one of which turned out to be the first red and mainly passively evolving galaxy confirmed to belong to a  $z > 2$  protocluster.

More recently, Mayo et al. (2012) used counts-in-cells analyses (which consist in counting sources within cells of different sizes) to detect over-densities of  $24\mu\text{m}$ , *Spitzer*-selected galaxies around 63 High Redshift ( $1 \leq z \leq 5.2$ ) Radio Galaxies (HzRGs). They concluded that over 95% of the targeted HzRGs lie in higher than average density fields. Galametz et al. (2012) also used a counts-in-cells analysis to identify over-densities of *Spitzer*/IRAC-selected galaxies in the fields of 48,  $1.2 < z < 3$ , radio sources from the Spitzer High-Redshift Radio Galaxy program (SHzRG – Seymour et al. 2007; De Breuck et al. 2010).

Using relatively shallow IRAC data, these authors showed that radio galaxies preferentially reside within medium-to-dense regions, with 73% of the targeted fields denser than average, in agreement with the results of [Venemans et al. \(2007\)](#). One of these structures was also spectroscopically confirmed ([Galametz et al. 2013b](#)).

The CARLA (Clusters Around Radio-Loud AGN) program ([Wylezalek et al. 2013](#)) expanded the work of [Galametz et al. \(2012\)](#) and investigated the environment of a larger sample of both obscured (e.g., type 2) and unobscured (e.g., type 1), luminous (rest-frame 500 MHz radio luminosities  $\geq 10^{27.5} \text{ W Hz}^{-1}$ ) radio-active AGN between redshift  $z = 1.2$  and  $z = 3.2$ , again by making use of *Spitzer*-IRAC observations. Data were obtained for 387 fields, 187 around radio-active quasars and 200 around radio galaxies, reaching a 95% completeness of 22.6 mag at  $3.6\mu\text{m}$  and of 22.9 mag at  $4.5\mu\text{m}$ . These authors found that 92% of the selected radio-active AGN resided in environments richer than average (cf. left-hand panel of Fig. 25), and concluded that these sources constitute ideal beacons for finding high-redshifts clusters and protoclusters. [Wylezalek et al. \(2013\)](#) also investigated how environment depends on different AGN physical properties (i.e., obscured vs unobscured sources) but found no correlation with either AGN type or radio luminosity. 16 out of 20 structures from the original CARLA selection were successively confirmed by using slitless grism spectroscopy on board of the *Hubble Space Telescope* ([Noirot et al. 2018](#)).

[Hatch et al. \(2014\)](#) compared the environments of powerful radio-AGN at  $1.3 < z < 3.2$  from the CARLA survey to those of a sample of inactive galaxies drawn from the UKIDSS Ultra Deep Survey (SpUDS – [Galametz et al. 2013a](#)) matched in mass and redshift, finding that – at all scales  $< 2 - 4 \text{ Mpc}$  – the structures that host radio-AGN were significantly denser than those hosting radio-quiet galaxies. Based on their results, [Hatch et al. \(2014\)](#) suggest that the dense Mpc-scale environment may foster the formation of a radio jet from an AGN and further speculate that virtually all the massive,  $M_* > 10^{14} M_\odot$ , clusters and protoclusters go through a radio-active AGN phase during  $1.3 < z < 3.2$ . This corresponds to a life-time for the radio-active AGN phase of at least 60 Myr, lower than the values from [Lin and Mohr \(2007\)](#) and [Magliocchetti et al. \(2017\)](#), which were however obtained in different redshift ranges, for different radio luminosity levels (CARLA sources are much brighter than those considered by [Lin and Mohr](#) and [Magliocchetti et al.](#)) and by using entirely different methods. [Hatch et al. \(2014\)](#) also expanded the work of [Wylezalek et al. \(2013\)](#) and reinvestigated the relationships between the large-scale environment of the CARLA AGN and their physical properties. Once again, no correlation was found, except for a low-significance ( $2.3\sigma$ ) positive dependence on black hole mass (cf. right-hand panel of Fig. 25).

[Rigby et al. \(2014\)](#) extended the search for over-densities around high-redshift radio-AGN to galaxies detected in the FIR by the SPIRE instrument onboard of the *Herschel* Space Observatory. By imaging regions around 19 extremely powerful radio-AGN ( $L_{500 \text{ MHz}} > 10^{28.5} \text{ W Hz}^{-1}$  at  $2.0 < z < 4.1$ ), they found that most of these fields were denser than average, with two of them clearly indicating the presence of (previously unknown) protoclusters made

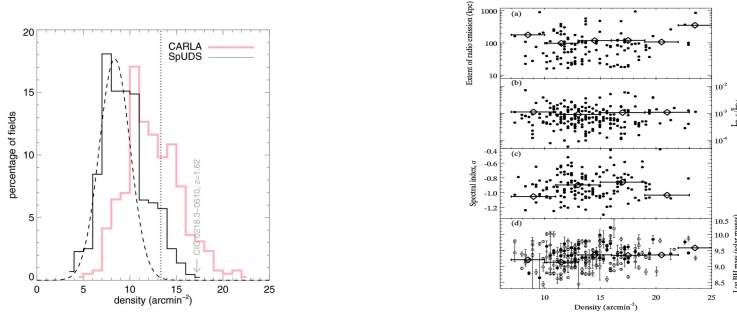


**Fig. 25** Left-hand panel: histogram of the densities of IRAC-selected sources in the CARLA fields and in the control UKIDSS Ultra Deep Survey (SpUDS – Galametz et al. 2013a) fields. The Gaussian fit to the low-density half of the SpUDS density distribution is shown by the dashed black curve and presents a peak at  $\Sigma_{\text{SpUDS}} = 8.3 \pm 1.6 \text{ arcmin}^{-2}$ . The vertical dotted line corresponds to  $\Sigma_{\text{SpUDS}} + 3\sigma$ , with  $\sigma$  standard deviation. 92.0% of the CARLA fields are denser than the SpUDS peak density. 18.7% of the SpUDS fields are denser than  $\Sigma_{\text{SpUDS}} + 2\sigma$  in contrast to 55.3% of the CARLA fields. Only 0.7% of the SpUDS fields are denser than  $\Sigma_{\text{SpUDS}} + 5\sigma$  as opposed to 9.6% of the CARLA fields. Figure from Wylezalek et al. (2013). Right-hand panel: relationships between the large-scale environment of the CARLA radio-AGN and properties of their radio emission and powering black hole (BH). From top to bottom: (a) the extent of the radio emission for resolved CARLA sources, (b) ratio of radio to bolometric AGN power (only for quasars), (c) radio spectral index  $\alpha$  (where  $S_\nu \propto \nu^\alpha$ ) and (d) black hole mass for the 211 CARLA AGN matched with the Shen et al. (2011) SDSS catalogue. Filled circles are black hole masses derived from fitting the MgII line in the optical spectra, whilst open circles are obtained from the CIV line. Open diamonds are the mean in each density bin. Figure from Hatch et al. (2014).

of galaxies undergoing intense star-formation activity ( $\text{SFR} \gtrsim 500\text{--}1000 M_\odot \text{ yr}^{-1}$ ), extending up to  $\sim 2\text{--}3 \text{ Mpc}$ . On the other hand, Cooke et al. (2016) report of a mature cluster, mostly formed by quiescent galaxies, surrounding a radio-AGN already at  $z = 1.58$ .

In a similar fashion to what done by the CARLA survey, the COBRA (Clusters Occupied by Bent Radio AGN) program (Paterno-Mahler et al. 2017) searches for overdense regions around radio-AGN with double-lobed structures which are not aligned with each other, but bent by forming angles  $< 180^\circ$ . The rationale behind this search is that the radio lobes of these AGNs are most likely bent because of the ram pressure that occurs due to the relative motion of the AGN host galaxy and the ICM (e.g., Feretti et al. 1992; Blanton et al. 2001; Giacintutti and Venturi 2009; Wing and Blanton 2011), which makes these sources good tracers for finding galaxy clusters. Indeed, out of 646 bent radio-AGN, 530 (corresponding to  $\sim 82\%$  of the original sample) are associated with over-densities – mostly at high,  $z = 1 - 3$ , redshifts – in the *Spitzer*/IRAC maps, and 190 are associated with galaxy cluster candidates. By following up on the previous work, Golden-Marx et al. (2021) also show for a subsample of 36 high- $z$  ( $0.35 < z < 2.2$ ) cluster candidates that radio-AGN with narrower ( $\lesssim 80^\circ$ ) opening angles reside in richer clusters (cf. Fig. 26), clearly indicating that the cluster environment impacts radio morphology.

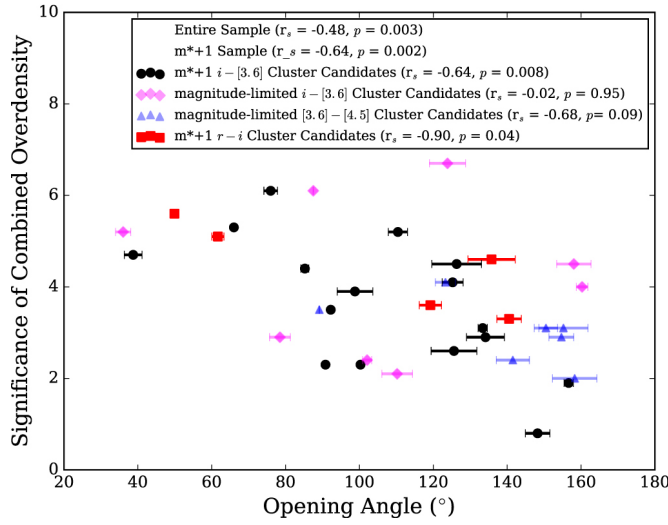


**Fig. 26** Significance of the combined over-density as a function of the opening angle of the bent radio source. All significances reported here are from [Golden-Marx et al. \(2019\)](#). Figure from [Golden-Marx et al. \(2021\)](#).

More insights on the inner structure of protoclusters surrounding bright radio galaxies and on the physical processes in action are provided in the recent work by [Gilli et al. \(2019\)](#) (see also [D’Amato et al. 2020](#)). These authors make use of deep *Chandra* observations centred on an over-density which develops along a compton-thick FR II galaxy set at redshift  $z = 1.7$ . The region presents significant diffuse X-ray emission. In particular, X-ray emission extending for  $\sim 240$  Kpc is found around the eastern lobe of the FR II and most of the star-forming galaxies in the over-density are distributed in an arc-like shape along the lobe edges. [Gilli et al. \(2019\)](#) propose that the diffuse X-rays originate from an expanding bubble of gas that is shock-heated by the FR II jet, and that star formation within galaxies in the proximity of the bubble is promoted by the compression of the cold interstellar medium. This result provides one of the first pieces of evidence for positive AGN feedback on cosmological (i.e., beyond the extension of the galaxy host of the radio-AGN) scales.

#### 4.3.2 Cross-matches of catalogues

With a somehow different approach from that presented in the first part of this Section, a number of studies have also investigated the environmental properties of mainly radio-AGN but also radio-emitting star-forming galaxies by matching catalogues of sources observed in the radio band (mostly at 1.4 GHz) with those obtained in the optical/NIR. The first pioneer works based on cross-correlation analyses appeared in the late 1970s (e.g., [Seldner and Peebles](#)

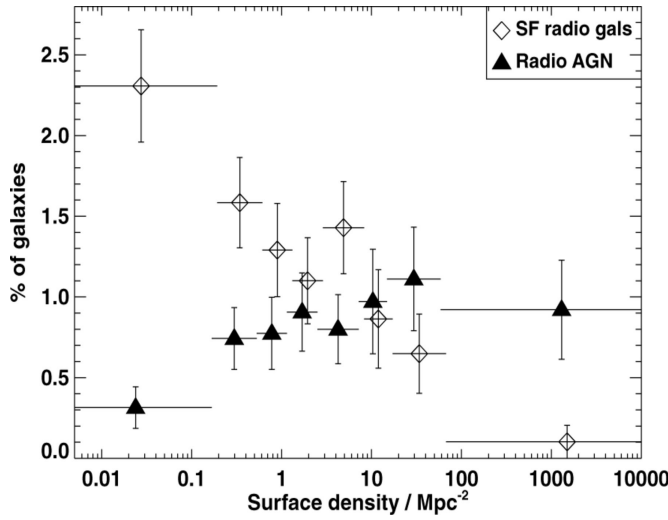


**Fig. 27** Fraction of galaxies within the 2dFGRS catalogue that are associated with radio sources securely classified as either star-forming or AGN, as a function of the local projected galaxy surface density. Error-bars correspond to Poissonian uncertainties. The frequency of star-forming radio sources is greatly suppressed in dense environments, while AGN activity is roughly independent of environment, except in the most underdense regions. Figure from Best (2004).

1978; Longair and Seldner 1979; Prestage and Peacock 1988 – cf. Sect. 4.1), but a great leap forward in this field was only possible starting from the beginning of the century when technology developments made large galaxy surveys possible.

Best (2004) combined the optical 2dFGRS with NVSS and used a Friends-of-Friends algorithm to investigate the environment of 91 local ( $z < 0.1$ ) radio-AGN mostly endowed with luminosities  $L_{1.4\text{GHz}} \geq 10^{22.8} \text{ W Hz}^{-1}$ . It was found that, while AGN activity of radio origin showed little dependence on local galaxy surface density except at the very lowest surface densities where such an activity is suppressed (cf. Fig. 27), the larger-scale environment was instead more important, since – in agreement with earlier works (e.g., Allington-Smith et al. 1993; Zirbel 1997) – radio-AGN were preferentially found in moderate-richness groups and poor clusters of galaxies. It was also found that the ratio of absorption-line to emission-line radio-AGN changed dramatically with environment, with essentially all radio-AGN in rich environments showing no emission lines in their optical spectra, result that led to conclude that such a difference could be due to the lack of cool gas in cluster galaxies. Best (2004) also repeated the investigation for a sample of 154 radio-emitting star-forming galaxies taken from the same NVSS parent catalogue. At variance with radio-AGN, these exhibited a strong correlation with environment, with star formation activity suppressed in high-density structures (cf. Fig. 27), a

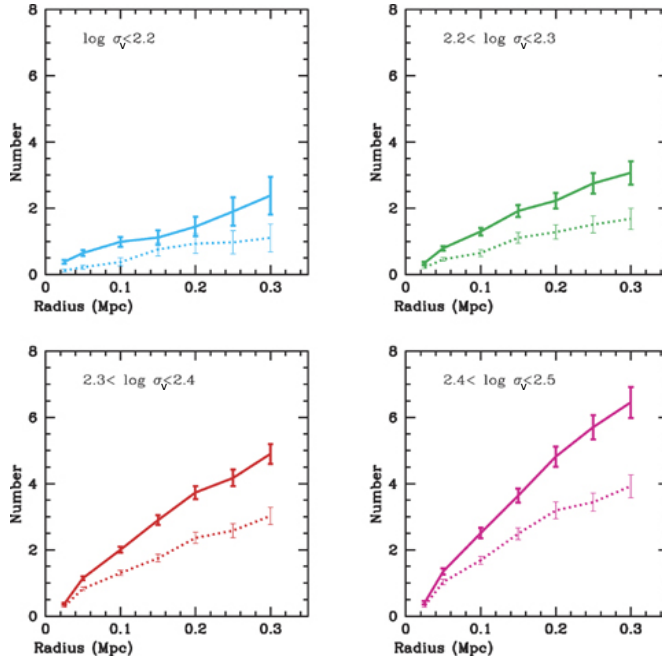


**Fig. 28** Galaxy counts within projected radius  $R$  for emission-line radio-active AGN (solid) and matched samples of radio-quiet AGN (dotted). Results are shown for four different ranges in the velocity dispersion  $\sigma_v$  of the hosts. Figure from [Kauffmann, Heckman, and Best \(2008\)](#).

result which was well-known at optical wavelengths (e.g., [Dressler et al. 1985](#)), but not yet seen in radio-selected objects.

[Kauffmann, Heckman, and Best \(2008\)](#) instead considered a particular sample of  $\sim 1600$ , local radio-active AGN with strong emission lines in their optical spectra, obtained by combining together NVSS and FIRST with spectroscopic information from the Sloan Digital Sky Survey DR4. AGN were selected from the population of radio emitters on the basis of a correlation between radio and  $H_\alpha$  (proxy for FIR) luminosity, corrected for extinction. These sources were then compared to a sample of radio-quiet AGN matched in redshift, stellar mass and velocity dispersion  $\sigma_v$  (proxy for the central black hole mass) of the host. While these authors found a remarkable agreement between the properties of radio-active and inactive AGN in terms of host galaxy structure, stellar populations and emission line properties in their optical spectra, they also observed a factor  $\sim 2 - 3$  enhancement in the local density surrounding radio-active AGN (cf. Fig. 28): in other words, radio-active AGN reside in denser environments with respect to radio-quiet ones, even though no dependence on radio luminosity was found.



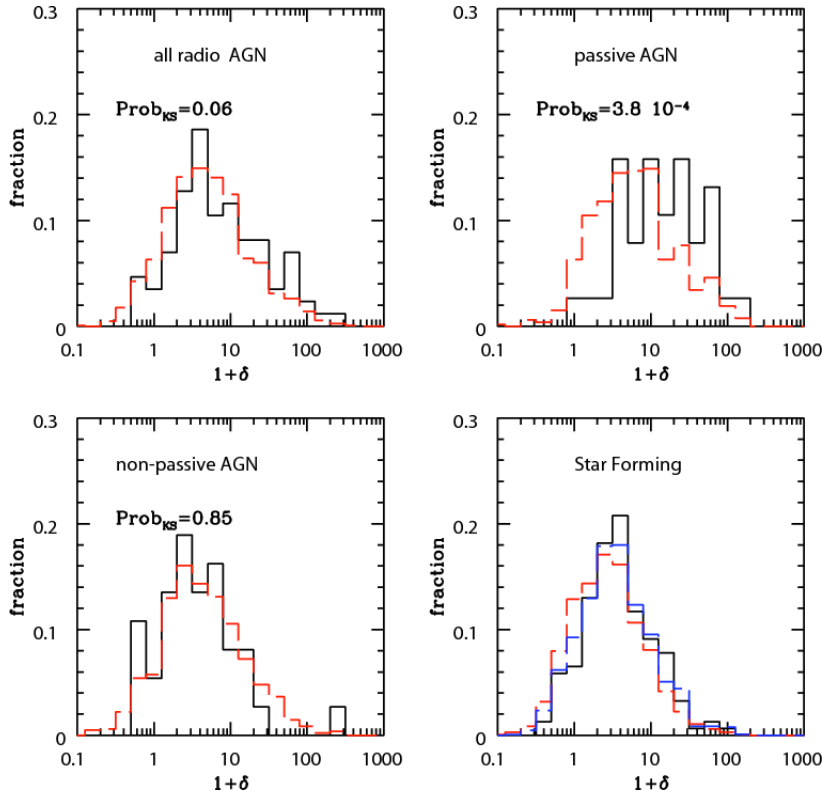


**Fig. 29** Black histograms: over-density distribution  $1+\delta$  of the radio sources in the [Bardelli et al. \(2010\)](#) sample. Red dashed histograms show the same quantity but for the control samples. Upper left panel: total AGN sample. Upper right panel: passive AGN. Lower left panel: non-passive AGN. Lower right panel: star-forming galaxies. The blue histogram corresponds to the control sample corrected for stellar mass distribution. Figure from [Bardelli et al. \(2010\)](#).

Few years later, [Bardelli et al. \(2010\)](#) moved the analysis to higher redshifts by investigating a sample of 315,  $0.1 < z < 0.9$ , radio sources obtained from the VLA-COSMOS survey ([Schinnerer et al. 2007](#); [Bondi et al. 2008](#)) via cross-correlation with galaxies endowed with a spectroscopic redshift from the z-COSMOS bright catalogue ([Lilly et al. 2009](#)). Radio galaxies were divided into passive AGN (i.e., very little star-forming activity), non-passive AGN (ongoing star-forming activity) and star-forming according to a combined method that first used the excess of their radio-derived SFRs with respect to those obtained from their optical SEDs to select AGN (cf. Sect. 2), and then a criterion based on  $[8.0-4.5] \mu\text{m}$  colours vs specific star-formation rates (as derived from the SEDs) to distinguish between passive and non-passive AGN. The authors conclude that the only class which is preferentially hosted within overdense structures is that of passive AGN (fraction increasing from  $\sim 2\%$  in underdense regions to  $\sim 15\%$  in overdense ones, cf. Fig. 29, where  $1+\delta$  is

the density contrast), while both non-passive AGN and radio-emitting star-forming galaxies are embedded in structures which do not differ from those hosting galaxies drawn from control samples. [Bardelli et al. \(2010\)](#) further observe a dependence of the radio luminosity on the stellar mass of the hosts for the sub-class of passive radio-AGN, dependency which however disappears for  $L_{1.4\text{GHz}} \gtrsim 10^{23.5} \text{ W Hz}^{-1}$ , luminosity beyond which also almost all passive radio-AGN are found to reside within overdense regions.

[Malavasi et al. \(2015\)](#) present an analysis similar to that of [Bardelli et al. \(2010\)](#) on the same COSMOS field, but based on photometric redshifts ([Ilbert et al. 2009](#)), which on one hand allow to expand the statistical significance and redshift range of the sample (1427 objects up to  $z \sim 2$ ) but at the price of larger uncertainties in the redshift determination. By using control samples with the same stellar mass and sSFR distributions of the original radio dataset, [Malavasi et al. \(2015\)](#) conclude that the environments surrounding radio-AGN are significantly denser than those occupied by inactive galaxies, especially for low-power –  $24 \leq \log(L_{1.4\text{GHz}}/[\text{W Hz}^{-1}]) < 24.5$  – radio-AGN, while the trend disappears for AGN of higher radio luminosities. Roughly at the same time, [Castignani et al. \(2014\)](#) focus on a sample of 32,  $1 < z < 2$ , FRI galaxies in the COSMOS field extracted from the catalogue of [Chiaberge et al. \(2009\)](#). These authors investigate the environments surrounding such sources subdivided into 21 low-luminosity radio galaxies (LLRGs) and 11 high-luminosity radio galaxies (HLRGs) – where LLRGs were selected to have 1.4 GHz rest frame luminosities lower than the fiducial FRI/FRII divide – and find overdensities extending up to  $\sim 2$  Mpc around  $\sim 70\%$  (22 out of 32) of the sources, independent of their radio luminosity. This is in agreement with e.g., the conclusions of [Wylezalek et al. \(2013\)](#) but – puzzling enough – at variance with those of [Malavasi et al. \(2015\)](#) obtained on the same COSMOS field and for a comparable redshift range and radio luminosity divide. A similar result on the independence of AGN radio luminosity from environment was also recently reported in [Kolwa et al. \(2019\)](#) for 2716,  $z \lesssim 0.8$  radio sources with luminosities  $10^{23} < L_{1.4\text{GHz}}/[\text{W Hz}^{-1}] < 10^{26}$  observed in the SDSS Stripe 82 field. By comparing their objects to a sample of control galaxies matched in redshift, colour and stellar mass of the hosts, [Kolwa et al. \(2019\)](#) also observe that the environments of their radio sources are similar to those of the control sample, except for the fact that radio-AGN are more prevalent within the most overdense regions such as galaxy clusters. These results lead the authors to conclude that environment is expected to play some (relatively minor) role on the production of radio activity from an AGN, but it is not the crucial ingredient. However, given the luminosity range probed by their sources, it is likely that the [Kolwa et al. \(2019\)](#) results are at least partially affected by the presence in their radio-AGN sample of a non-negligible fraction of radio-emitting star-forming galaxies (cf. Sect. 2) which generally inhabit structures indistinguishable from those occupied by their radio-quiet counterparts.

## 5 Discussion

Given the established evidence for a strong connection between extragalactic radio source activity and the formation and evolution of galaxies and larger structures such as groups and clusters, this review has concentrated on the Kpc-to-Mpc scale properties of radio-AGN and star-forming galaxies by providing an overview on their hosts and environments. The conclusions based on the most recent works are summarized below.

### 5.1 Hosts

AGN – It is widely agreed that radio-AGN are mainly hosted by the most massive galaxies both in the local (e.g., [Matthews et al. 1964](#); [Ekers and Ekers 1973](#); [Auriemma et al. 1977](#); [Jenkins 1982](#); [Best et al. 2005a](#); [Mauch and Sadler 2007](#); [Sabater et al. 2019](#); [Capetti et al. 2022](#)) and in the higher-redshift (e.g., [Lilly and Longair 1984](#); [Eales et al. 1997](#); [Jarvis et al. 2001](#); [De Breuck et al. 2002](#); [Willott et al. 2003](#); [Seymour et al. 2007](#); [Smolčić et al. 2009](#); [De Breuck et al. 2010](#); [Gürkan et al. 2014](#); [Drouart et al. 2016](#); [Magliocchetti et al. 2016](#)) universe. As a matter of fact, there are large variations in the level and relevance of radio activity of AGN origin within different extragalactic populations, with the probability for a source to host a radio-AGN observed to vary from as little as  $\sim 2 - 5\%$  in moderate-to-high ( $z \sim 0.5 - 2$ ) redshift AGN (e.g., [Hickox et al. 2009](#); [Magliocchetti et al. 2020](#)) up to virtually 100% in the most massive local ellipticals (e.g., [Brown et al. 2011](#); [Capetti et al. 2022](#); [Grossova et al. 2022](#)).

Many works had already investigated in the local universe the connection between the fraction of radio-AGN within a chosen population of galaxies and their optical/NIR luminosity (e.g., [Colla et al. 1975](#); [Auriemma et al. 1977](#); [Hummel et al. 1983](#)). These have been implemented in the more recent years with studies connecting such a fraction with the stellar mass of the hosts (e.g., [Best et al. 2005a](#); [Mauch and Sadler 2007](#); [Sabater et al. 2019](#); [Magliocchetti et al. 2020](#)). In all cases it has been found that the probability for a galaxy to host a radio-active AGN is a strong function of both their optical/NIR luminosity (proxy for the stellar mass in absence of this information) and mass, with a functional form of the kind  $\propto M_*^{2.5}$  (e.g., [Best et al. 2005a](#)). This dependence also appears to be stronger than that estimated for the mass of the black hole powering the radio-AGN ( $\propto M_*^{1.6}$  – e.g., [Best et al. 2005a](#); [Sabater et al. 2019](#)), evidence that would hint to a stronger link between radio-AGN activity and gas fuelling with respect to nuclear properties. However, in spite of this relation, no connection is observed between level of radio activity and host mass (e.g., [Mauch and Sadler 2007](#)). No connection has either been found between probability for radio-AGN emission and nuclear accretion properties, cosmological evolution or star-formation activity of the hosts (e.g., [Magliocchetti et al. 2020](#)). It therefore appears that the host mass is the main factor driving the formation and evolution of a radio-AGN.

These findings have also been confirmed up to  $z \sim 2$  (e.g., Smolčić et al. 2009; Williams and Röttgering 2015; Lin et al. 2017; Mo et al. 2020), together with the result of a global increase as a function of look-back time of the fraction of radio-active AGN within galaxies, observed to happen at all stellar masses. Such an increment is however differential, since relatively low-mass,  $M_* \lesssim 10^{10.75} M_\odot$ , galaxies are found to be up to 10 times more likely to host a radio-AGN at higher redshifts with respect to local results, while galaxies with a larger stellar mass content show little evolution. This shift of radio-AGN activity towards lower-mass, mainly star-forming galaxies has been interpreted as evidence for a change in the nuclear accretion properties of radio-emitting AGN from mostly hot/inefficient in the local universe, to cold/efficient as we approach cosmic noon at  $z \sim 2$ . Indeed, already in the local universe, radio-AGN are observed to show different accretion modes: cold/efficient in high-excitation radio galaxies or HERGs and hot/inefficient in low-excitation radio galaxies or LERGs (e.g., Hardcastle et al. 2007), although with a numerical prevalence of LERGs over HERGs. However, since at least up to  $z \sim 1$  HERGs display a stronger cosmological evolution than LERGs (e.g., Best et al. 2014; Pracy et al. 2016; Butler et al. 2019), this would explain the larger fraction of radio-AGN within HERG hosts (locally found to be less massive, bluer and more star-forming than LERGs – e.g., Best and Heckman 2012; Jannsen et al. 2012; Hardcastle et al. 2013; Sadler et al. 2014) observed at higher redshifts.

Things however do not seem to be too crystal clear beyond  $z \sim 1$ . The most recent studies indeed show a much less marked distinctions between HERG and LERG host properties with respect to what observed locally: their mass distributions tend to overlap (e.g., Fernandes et al. 2015; Delvecchio et al. 2017), except for a more pronounced tail observed below  $M_* \lesssim 10^{10.5} M_\odot$  in the case of HERGs (e.g., Williams et al. 2018; Butler et al. 2018b). Also the star-forming properties of HERG and LERG hosts are found to be more similar than what found in the local universe. These results likely stem from two main factors: 1) the cosmological evolution of the general galaxy population, which becomes more star-forming as cosmic noon is approached, with a global star-forming activity mainly shifting to larger-mass galaxies (cosmic downsizing), and 2) the different methods (spectroscopic vs photometric) applied to select HERGs and LERGs at low and high redshifts which produce more contaminated samples beyond  $z \sim 0.5 - 1$ .

Within this scenario, a special place is occupied by the morphological differences exhibited by radio-active AGN, also in connection with their accretion properties. Early works based on bright radio sources attributed different hosts to the two populations of FRI and FRII galaxies, with FRIs being almost ubiquitously observed within massive and passively evolving red galaxies (but see Ledlow et al. 1998, 2001 for few examples of FRIs within spirals), and FRIIs mainly associated to bluer, fainter and smaller galaxies (e.g., Lilly et al. 1984; Owen and Laing 1989; Baum et al. 1992; Zirbel 1996). Ledlow and Owen (1996) found in the optical properties of the host galaxy a crucial ingredient to account for the FRI-FRII dichotomy, which then had to be added to the already known ingredient of radio luminosity (Fanaroff and Riley 1974).

Indeed, it was shown that *all* the radio-AGN above the locus  $L_{\text{radio}} \propto L_{\text{optical}}^{1.8}$  were FRIIs, while those below it were FRIs. This meant that powerful FRI galaxies with radio luminosities comparable to those of FRIIs could exist, just as long as their host galaxies were also about two magnitudes brighter. However, despite its enormous success and the fact that it was further converted into a relationship between AGN power and black hole mass (Ghisellini and Celotti 2001), it was subsequently found that the Ledlow and Owen (1996) result suffered from a number of biases, most importantly luminosity issues since FRI and FRII galaxies had been sampled in different redshift ranges.

With the advent of deeper and wider surveys which started to provide more homogeneous large samples of fainter radio galaxies, it has become clear that, although there are indeed very few (although not zero) FRIs above the Ledlow and Owen (1996) divide, there is a large overlap between FRI and FRII galaxies below it (e.g., Best 2009; Lin et al. 2010; Wing and Blanton 2011; Mingo et al. 2019). To make things more complicated, the almost one-to-one correspondence between FRIs and LERGs and FRIIs and HERGs which was thought to hold at least to a zero-th order approximation, has in the recent years proven not to be true. Indeed, despite the fact that few FRIs are observed in association with a HERG, LERGs can instead assume both FRI and FRII morphologies (e.g., Laing et al. 1994; Tadhunter et al. 1998; Chiaberge et al. 1999, 2000; Hardcastle et al. 2006; Buttiglione et al. 2010; Capetti et al. 2017a,b; Miraghaei and Best 2017; Mingo et al. 2022). However, while there is nowadays a general consensus on this result, disagreement still remains on the possible mechanisms causing the FRI-FRII dichotomy, also in connection with their HERG and LERG distinction.

In particular, two main scenarios have emerged: the first one attributes differences in radio morphology to the large-scale (i.e., host galaxy and environment, see also below in this Section) properties of radio-AGN which influence the interaction between the radio jet and the external medium (e.g., Kaiser and Best 2007; Wing and Blanton 2011; Miraghaei and Best 2017; Mingo et al. 2019, 2022), with those between HERGs and LERGs being instead dictated by different fuelling mechanisms as discussed earlier. According to this framework, HERGs are powered by accretion of cold gas, provided by e.g., a recent merger with a gas-rich galaxy, while LERGs accrete hot intergalactic gas from dense environments at a low rate (e.g., Best and Heckman 2012), with fuelling from major mergers strongly disfavoured by recent observations (e.g., Ellison et al. 2015). On the other hand, other works do not observe any difference in the host and/or environmental properties of FRI and FRII galaxies, except in the rare cases of FRII HERGs (e.g., Lin et al. 2010; Capetti et al. 2017b; Jimenez-Gallardo et al. 2019; Massaro et al. 2019, 2020; Vardoulaki et al. 2021) or even between those of HERGs and LERGs (e.g., Fernandes et al. 2015), so that an alternative mechanism for their large-scale radio behaviour has to be invoked. In this case, ageing processes can be thought as the main driver for the observed morphological differences, with an evolutionary pattern that proceeds from FRII HERGs that switch from efficient to inefficient accretion due to gas starvation and transform themselves into FRII LERGs, sources that

still maintain their large radio structures thanks to the past nuclear activity at high efficiency (e.g., Ghisellini and Celotti 2001; Tadhunter 2016; Macconi et al. 2020; Grandi et al. 2021). The switch off/change in accretion mode will eventually show in the radio morphology with the delay needed to reach Kpc-to-Mpc distances, and the source will ultimately turn into an FRI galaxy.

A further important point to stress is that, while as already discussed, local  $-z \lesssim 1$  – observations indicate that radio-active AGN mostly reside within passive ellipticals, hosts of very little ongoing star-forming activity (e.g., Siebenmorgen et al. 2004; Dicken et al. 2012; Gürkan et al. 2015), the situation becomes dramatically different at higher redshifts (e.g., Dey et al. 1997; Pentericci et al. 1998, 1999; Williams and Röttgering 2015; Lin et al. 2017). Indeed, the advent of facilities such as SCUBA, *Spitzer* and *Herschel* probing the IR and sub-millimeter regimes to high sensitivity levels, has opened a new window on our knowledge of the physical status of radio-AGN during cosmic noon at  $z \sim 1.5$ –2 and beyond. All the works based on these observations (e.g., Archibald et al. 2001; Reuland et al. 2004; Seymour et al. 2007, 2011; Rawlings et al. 2013; Drouart et al. 2014; Podigachoski et al. 2015; Magliocchetti et al. 2014b, 2016, 2018a) have clearly shown that in the  $z \sim 1$ –3 range and beyond, radio-AGN hosts produce stars at very high rates, up to  $\sim 10^3 M_\odot \text{ yr}^{-1}$ . Such an activity is observed to increase with look-back time, up to the highest redshifts probed by the observations, and in most cases also to be in excess with respect to those exhibited at the same epochs by inactive galaxies or by the hosts of radio-quiet AGN (e.g., Drouart et al. 2014; Kalfountzou et al. 2014, 2017). It is then clear that the *negative* radio-mode feedback (e.g., Croton et al. 2006; Fanidakis et al. 2012; Weinberger et al. 2018), which invokes the presence of a radio jet to warm up or even expel the cold gas contained within massive galaxies (therefore halting their star-formation processes so to reproduce the locally observed physical properties and number density) can only be valid in the nearby universe. In the high-redshift universe instead, radio-AGN activity and build-up of the stellar mass at vigorous rates co-exist within the same galaxy. This would imply the presence of *positive* feedback (Silk and Nusser 2010), whereby radio jets increase the star-formation activity by compressing the intergalactic medium. Alternatively, as some observational results seem to indicate (e.g., Seymour et al. 2011; Rawlings et al. 2013; Drouart et al. 2014; Magliocchetti et al. 2014b, 2016, 2018a; Podigachoski et al. 2015) it is possible that radio-AGN and star-formation activities proceed parallel to each other and only result coeval thanks to the availability of large reservoirs of gas within massive galaxies at  $z \sim 2$ . More work in this direction is needed to assess the validity of one of the two scenarios and also to understand the drastic change in feedback behaviour when moving from  $z \sim 1.5$  down to the local universe.

*Star-Forming Galaxies* – At all the (relatively low,  $z \lesssim 1$ ) redshifts probed by present facilities, radio-emitting star-forming galaxies appear in all respect identical to star-forming galaxies selected at any other wavelength, with spectral types ranging from spirals to irregulars and dwarfs. Although only  $\lesssim 10^{-4}$  of the bolometric luminosity produced by a non-AGN powered galaxy is radi-

ated at radio wavelengths (Condon 1992), the importance of radio selection for star-forming galaxies relies on the fact that it can provide estimates of the star-formation activity of such sources in a way which is unaffected by the presence of dust up to the earliest epochs. In order to do that, a solid calibration of the relation between radio luminosity and infrared luminosity (or alternatively SFR) is mandatory. This is why a lot of effort has been put in the recent years to provide calibrations as precise as possible at all redshifts and for all galaxy types. From an observational point of view, it has been found at least in the local universe that radio and infrared luminosities show an incredibly tight, approximately linear, correlation over more than 5 orders of magnitude in infrared luminosity (e.g., Helou et al. 1985; De Jong et al. 1985; Condon 1992; Yun et al. 2001), irrespective of galaxy type and level of star-forming activity, as long as the galaxy hosts episodes of star-formation. This relation, originally found at 1.4 GHz, has also been observed to hold at different frequencies (e.g., Delhaize et al. 2017; Gürkan et al. 2018). The theoretical reasons behind it are still not fully understood, as many factors involved in the process of shaping a galaxy should intervene to produce at least some modifications which are not (yet) clearly visible in the available data.

One of the most important open questions associated to the IR-radio correlation is its eventual evolution with redshift, as erroneous estimates of the  $q_{\text{IR}} \propto L_{\text{IR}}/L_{\text{radio}}$  value at high  $z$ 's would hamper the huge potential of present and future radio surveys such as SKA to investigate the history of formation and evolution of galaxies since the cosmic dawn. Early studies which exploited IR data from the *Spitzer* and *Herschel* satellites found a general independence of the IR-radio correlation from redshift (e.g., Appleton et al. 2004; Vlahakis et al. 2007; Ibar et al. 2008; Garn et al. 2009; Jarvis et al. 2010; Chapman et al. 2010; Sargent et al. 2010; Mao et al. 2011). Then, more recent works based on different source selection and stacking analyses, have started to infer a slight but statistically solid evidence for the ratio between IR and radio luminosity to decrease with look-back time (Ivison et al. 2010a,b; Bourne et al. 2011; Magnelli et al. 2015; Calistro Rivera et al. 2017; Delhaize et al. 2017). The reason for such discrepant results is to be found in the different selection criteria, as in principle while e.g., the radio selection favours higher  $L_{\text{radio}}/\text{SFR}$  ratios, the opposite is true for the FIR and sub-millimetre selections which favour high SFRs.

More insights on the cosmological evolution of the IR-radio correlation have been recently provided by the results of Molnar et al. (2018) and Delvecchio et al. (2021). Indeed, while the first work shows that a different evolution is observed for star-forming galaxies of different morphological types, hinting to an increasing presence and contribution of radio-emitting AGN within bulk-dominated star-forming galaxies at higher redshifts, the second study finds in the stellar mass the main driver of such a redshift dependence, with galaxies of higher stellar masses displaying lower values of the  $q_{\text{IR}}$  parameter. However, despite all the progress made in the very recent years, a convergence on the IR-radio relation for what concerns both its deviation from linearity and eventual



redshift evolution is still far from being reached (e.g., [Bonato et al. 2021](#); [Molnar et al. 2021](#); [Smith et al. 2021](#); [Tisanic et al. 2022](#)).

## 5.2 Environment

*AGN* – While – starting from the very early works (e.g., [Seldner and Peebles 1978](#); [Longair and Seldner 1979](#); [Hill and Lilly 1991](#); [Peacock and Nicholson 1991](#); [Allington-Smith et al. 1993](#); [Zirbel 1997](#)) – virtually all the studies presented in the literature converge at indicating that radio-AGN preferentially reside within overdense structures, the three (or rather five if one also includes cross-correlation studies) methods presented in Sect. 4 provide different information on the large-scale structure behaviour of these objects. To summarize them in a few words, we might say that the method based on clustering returns more information on the very large/cosmological (i.e., at Mpc level and beyond) scales traced by radio sources and also on the dark matter content of the regions that host them. On the other hand, very different results are obtained if one searches for structures around known radio-AGN or if one pinpoints radio-AGN within known structures. Indeed, in the first case one finds that virtually all radio-AGN are surrounded by over-densities (e.g., [Venemans et al. 2007](#); [Mayo et al. 2012](#); [Galametz et al. 2012](#); [Castignani et al. 2014](#); [Wylezalek et al. 2013](#); [Rigby et al. 2014](#)), while the second method shows that only about 20–30% of them inhabit rich (group- and cluster-like) structures (e.g., [Best et al. 2007](#); [Magliocchetti and Brüggen 2007](#); [Lin and Mohr 2007](#); [Croft et al. 2007](#); [Magliocchetti et al. 2018b](#); [Croston et al. 2019](#)). The reason for this discrepancy is not known, but it is likely related to the different redshift ranges probed by the two methods (much more local sources are considered in the second one), and/or – under the assumption of a strong correlation between radio luminosity and environmental density (e.g., [Bardelli et al. 2010](#); [Magliocchetti et al. 2018b](#); [Croston et al. 2019](#); [Mo et al. 2020](#), but see further in this Section for different points of view) – to the fact that generally the first method images much brighter radio sources than the second one. In any case, we note that these findings also have implications for the life-time of the radio-AGN phenomenon, and it is therefore of no surprise if works based on the different methods illustrated above find different values, ranging from  $\sim 60$  Myr up to a few Gyr (e.g., [Lin and Mohr 2007](#); [Smolčić et al. 2011](#); [Hatch et al. 2014](#); [Magliocchetti et al. 2017](#)). We also note that recent studies based on direct LOFAR observations which – we remind – sample lower frequencies and therefore older emission, would tend to better agree with the high-end values provided above for the radio-active phase of an AGN ( $\tau > 200$  Myr – [Heesen et al. 2018](#)).

The fact that – at variance with what observed for e.g., optical AGN (e.g., [Ellingson et al. 1991](#); [Porciani et al. 2004](#); [Kauffmann et al. 2008](#); [Mandelbaum et al. 2009](#); [Donoso et al. 2010](#); [Sabater et al. 2013](#); [Retana-Montenegro and Röttgering 2017](#)) – most of the radio-AGN reside in overdense/cluster-like structures, has important implications not only for the investigation of

the radio-AGN phenomenon *per se*, but also for the study of the interaction between radio-AGN activity and their surrounding structures, both in terms of companion galaxies and ICM. First of all, regardless of the adopted method, all studies report estimates for the masses of the dark matter hosts of radio-AGN to be of the order of  $10^{13.5}-10^{14} M_{\odot}$  (e.g., Magliocchetti et al. 2004; Hickox et al. 2009; Mandelbaum et al. 2009; Lindsay et al. 2014a; Hatch et al. 2014; Magliocchetti et al. 2017; Retana-Montenegro and Röttgering 2017; Hale et al. 2018; D’Amato et al. 2020; Uchiyama et al. 2022), with a value which remains unchanged at all probed epochs, from as early as  $z \sim 4$  (Uchiyama et al. 2022) down to the local universe (cf. Magliocchetti et al. 2017 and references therein). This leads us to draw the fundamental conclusion that *the environmental properties of radio-AGN remain unchanged throughout all cosmic ages*.

Furthermore, it has been found that the BCG of a cluster or group of galaxies is much more likely to host a radio-AGN than any other galaxy belonging to the over-density, and that this likelihood is a strongly increasing function of its stellar mass and of the AGN radio luminosity (e.g., Best et al. 2007; Lin and Mohr 2007; Croft et al. 2007; Smolčić et al. 2011; Mo et al. 2018; Magliocchetti et al. 2018b; Croston et al. 2019). The above findings clearly push towards a strong connection between radio activity and over-density/ICM properties. Although a whole review would be needed to tackle this fundamental aspect of galaxy evolution known under the name of ‘feedback’, here we suffice saying that indeed plenty of evidence has been reported for the above interaction, both in the case of extended radio sources presenting clear jetted structures (e.g., Magliocchetti and Brüggén 2007; Paterno-Mahler et al. 2017; Gilli et al. 2019; D’Amato et al. 2020; Golden-Marx et al. 2021) and for the whole population of radio-AGN regardless of their morphological division (e.g., Croston et al. 2005; Lin and Mohr 2007; Ineson et al. 2013, 2015), although no dependence is inferred between environmental richness and extension of the radio-AGN, at least in the case of Giant Radio Galaxies (e.g., Lan and Prochaska 2021). A strong connection has been also reported between radio-AGN activity, environmental properties and star-forming processes within the host galaxy (e.g., Bardelli et al. 2010; Miraghaei 2020), whereby mostly radio-AGN associated to passive galaxies are found to reside within over-densities.

However, despite all the progress made in the field, the details of the interaction between radio-AGN and ICM are far from being fully understood. For instance, there is still no consensus on which (large) scales are affected by the presence of a radio-AGN, or how radio feedback precisely works. This lack of knowledge is somehow related to the uncertainties we still have on the environmental properties of radio-AGN of different types, differences that likely reflect – amongst others – different accreting modes. So, while for instance there seems to be a general consensus on the fact that locally FRI and/or radiatively inefficient galaxies tend to reside in denser environments than FR II and/or radiatively efficient ones (e.g., Prestage and Peacock 1988; Zirbel 1997; Best 2004; Wing and Blanton 2011; Ineson et al. 2013, 2015; Miraghaei and Best 2017; Croston et al. 2019, but see Massaro et al. 2019, 2020

for a discarding view), just as radio-AGN hosted by early-type/red galaxies do (e.g., [Bardelli et al. 2010](#); [Miraghaei 2020](#)), it is still not clear whether FR II galaxies are embedded in lower density environments only at low redshifts (e.g., [Allington-Smith et al. 1993](#); [Zirbel 1997](#); [Ineson et al. 2015](#)) or at all cosmological epochs. To our knowledge, except for very few cases that present somehow discarding conclusions (e.g., [Hale et al. 2018](#); [Vardoulaki et al. 2021](#)), this kind of systematic investigation has only been performed up to  $z \sim 0.5$ . An extension of the analysis to higher redshifts is therefore mandatory in order to provide a definite answer. Just as an example, the mere existence of a protocluster serendipitously found surrounding a FR II galaxy at  $z = 1.7$  ([Gilli et al. 2019](#)), and the fact that most high-redshift radio galaxies are indeed FR IIs ([Miley and De Breuck 2008](#)), show that at high redshifts these sources can indeed reside in overdense structures. And if this is the case, does it imply a different cosmological evolution for FR II and FR I galaxies also in terms of their environmental properties? Also, do the above results unequivocally point towards different fuelling mechanisms for the different sub-populations of radio-AGN mentioned above as studies of their host galaxies seem to indicate (cf. Sect. 3)?

Even more intricate is the case of AGN of different radio luminosities. Indeed, no consensus has been reached for what concerns their environmental properties despite all the effort put in by the scientific community. The number of works that claim no dependence (e.g., [Hill and Lilly 1991](#); [Magliocchetti et al. 2004](#); [Best et al. 2007](#); [Kauffmann et al. 2008](#); [Fine et al. 2011](#); [Wylezalek et al. 2013](#); [Castignani et al. 2014](#); [Magliocchetti et al. 2017](#); [Kolwa et al. 2019](#)) almost equals that of those that do find a difference, with brighter radio-AGN belonging to denser structures (e.g., [Longair and Seldner 1979](#); [Yates et al. 1989](#); [Overzier et al. 2003](#); [Bardelli et al. 2010](#); [Hale et al. 2018](#); [Magliocchetti et al. 2018b](#); [Croston et al. 2019](#); [Mo et al. 2020](#)). The reason for such a striking disagreement is unknown, although some works advocate the different luminosities and/or redshift intervals considered in the various analyses. It is also not clear whether the claimed dependency holds for the whole radio-AGN population or only for some sub-class of objects (e.g., [Ineson et al. 2013, 2015](#)). Furthermore, a few studies mainly sampling the higher-redshift universe (e.g., [Donoso et al. 2010](#); [Malavasi et al. 2015](#); [Uchiyama et al. 2022](#)) refer of the opposite effect, i.e., fainter radio-AGN being surrounded by denser environments.

There are other open issues connected with the physics of the radio-AGN phenomenon and of its accreting black hole. Amongst a few, whether it is true that AGN that emit both in the radio and in the MIR have a preference to reside within underdense structures (at variance with radio-AGN which are also X-ray emitters), as observed by [Tasse et al. \(2008\)](#) and [Magliocchetti et al. \(2018b\)](#) but with a somehow low significance level, finding that if confirmed would imply an intimate connection between nuclear activity and environmental properties even for AGN that are already radio emitters. Also, if there is indeed a dependency of the radio-AGN environmental properties on their black-hole mass, or at least on some threshold value of  $\sim 10^9 M_\odot$ ,

as the works by Hatch et al. (2014) but mostly by Retana-Montenegro and Röttgering (2017) seem to suggest. And lastly, it is still has to be further confirmed whether indeed radio-active galaxies and radio-active quasars cluster differently (i.e., are hosted by different structures), as suggested by the work of Donoso et al. (2010).

All these answers require wider radio surveys which would be able to return large samples of sources divided per morphological type, redshift interval, radio luminosity, accretion mode, etc, deep enough to probe the whole population of radio-active AGN up to the early phases of our Universe. Luckily, all this is within reach with the advent of SKA in the next decade.

*Star-Forming Galaxies* – Radio-active star-forming galaxies are a much more straightforward case than AGN: they exhibit no environmental differences when compared to their radio-quiet counterparts (e.g., Bardelli et al. 2010; Magliocchetti et al. 2017, 2018b; Hale et al. 2018; Chakraborty et al. 2020), and are mainly found in average-to-under-dense structures. Dense environments are shown to inhibit the presence of radio-active star-forming galaxies (Best 2004; Sabater et al. 2013), precisely in the same way it is observed for their radio-quiet counterparts. This holds at least up to  $z \sim 1.5$ . At earlier epochs, evidence collected at all wavelengths but radio (due to lack of sensitivity of present facilities) indicates that intense,  $SFR > 20 - 30 M_{\odot} \text{ yr}^{-1}$ , star-forming activity shifts to galaxies embedded within denser/protocluster-like structures (e.g., Magliocchetti et al. 2014a). Once again, the advent of SKA will unequivocally confirm or refuse whether this conclusion is also valid at radio wavelengths.

**Acknowledgements** I wish to thank my friends and colleagues from IAPS, A. Traficante, S. Molinari, S. Pezzuto, A. Di Giorgio, M. Benedettini, E. Schisano and also my kids Tommaso D. Metcalf and Eva G. Metcalf for putting up with me during these long months of writing further affected by the pandemic, F. De Angelis for being the safest safe for the various versions of the manuscript and J. Noceti for unconditional support (both in presence and in absence) towards the completion of the task. I would also like to thank S.J. Maddox, G. de Zotti, L. Danese, A. Celotti and J.V. Wall for everything they taught me on extragalactic radio astronomy and surveys in general. Last but not least, a warm thank you is due to the editor L. Feretti who offered me the opportunity to write this review and also gave me the freedom to lay it out the way it was closest to my chords.

## References

- Abazajian KN, Adelman-McCarthy JK, Agüeros M, Allam S, et al (2009) The Seventh Data Release of the Sloan Digital Sky Survey. *ApJS* 182:543
- Aghanim N, Akrami Y, Ashdown M, Aumont J, et al (2018) Planck 2018 results. VI. Cosmological parameters. *A&A* 641:6
- Aihara H, Armstrong R, Bickerton S, Bosch J, et al (2018) First data release of the Hyper Suprime-Cam Subaru Strategic Program. *PASP* 70:8. <https://doi.org/10.1093/pasj/psab122>
- Alberts S, Rujopakarn W, Rieke G, Jagannathan P, Nyland K (2020) Completing the Census of AGN in GOODS-S/HUDF: New Ultra-deep Radio Imaging and Predictions for JWST. *ApJ* 901:168. <https://doi.org/10.1051/0004-6361/201629367>

- Allington-Smith JA, Ellis RS, Zirbel EL, Oemler A (1993) The Evolution of Galaxies in Radio-selected Groups. *ApJ* 404:521. <https://doi.org/10.1086/172305>
- Allison R, Lindsay SN, Sherwin BD, de Bernardis F, et al (2015) The Atacama Cosmology Telescope: measuring radio galaxy bias through cross-correlation with lensing. *MNRAS* 451:849. <https://doi.org/10.1093/mnras/stv991>
- Alonso D, Bellini E, Hale C, Jarvis MJ, Schwarz DJ (2021) Cross-correlating radio continuum surveys and CMB lensing: constraining redshift distributions, galaxy bias, and cosmology. *MNRAS* 502:876. <https://doi.org/10.1093/mnras/stab046>
- Amblard A, Cooray A, Serra P, Temi P, et al (2010) Herschel-ATLAS: Dust temperature and redshift distribution of SPIRE and PACS detected sources using submillimetre colours. *A&A* 518:L9. <https://doi.org/10.1051/0004-6361/201014586>
- Antonucci R (1993) Unified models for active galactic nuclei and quasars. *ARA&A* 31:473. <https://doi.org/10.1146/annurev.aa.31.090193.002353>
- Appleton PN, Fadda DT, Marleau FR, Frayer DT, et al (2004) The Far- and Mid-Infrared/Radio Correlations in the Spitzer Extragalactic First Look Survey. *ApJS* 154:147
- Archibald EN, Dunlop JS, Huges DH, Rawlings S, Eales SA, Ivison RJ (2001) A sub-millimetre survey of the star formation history of radio galaxies. *MNRAS* 323:417. <https://doi.org/10.1046/j.1365-8711.2001.04188.x>
- Auriemma C, Perola GC, Ekers RD, Fanti R, Lari C, Jaffe WJ, Ulrich MH (1977) A Determination of the Local Radio Luminosity Function of Elliptical Galaxies. *A&A* 57:41
- Baldi RD, Capetti A (2008) Recent star formation in nearby 3CR radio-galaxies from UV HST observations. *A&A* 489:989. <https://doi.org/10.1051/0004-6361:20078745>
- Baldi RD, Capetti A (2010) Spectro-photometric properties of the bulk of the radio-loud AGN population. *A&A* 519:48. <https://doi.org/10.1051/0004-6361/201014446>
- Baldi RD, Chiaberge M, Capetti A, Sparks W, et al (2010) The 1.6  $\mu$ m Near-infrared Nuclei of 3C Radio Galaxies: Jets, Thermal Emission, or Scattered Light? *ApJ* 725:2426. <https://doi.org/10.1088/0004-637x/725/2/2426>
- Baldwin J, Phillips M, Terlevich R (1981) Classification parameters for the emission-line spectra of extragalactic objects. *PASP* 93:5. <https://doi.org/10.1086/130766>
- Bardelli S, Schinnerer E, Smolčić V, Zamorani G, et al (2010) Properties and environment of radio-emitting galaxies in the VLA-zCOSMOS survey. *A&A* 511:1. <https://doi.org/10.1051/0004-6361/200912809>
- Baugh CM (1996) The real-space correlation function measured from the APM Galaxy Survey. *MNRAS* 280:267. <https://doi.org/10.1093/mnras/280.1.267>
- Baum SA, Heckman TM, van Breugel W (1992) Spectroscopy of Emission-Line Nebulae in Powerful Radio Galaxies: Interpretation. *ApJ* 389:208. <https://doi.org/10.1086/171198>
- Becker RH, White RL, Helfand DJ (1995) The FIRST Survey: Faint Images of the Radio Sky at Twenty Centimeters. *ApJ* 450:559. <https://doi.org/10.1086/176166>
- Bell EF (2003) Estimating Star Formation Rates from Infrared and Radio Luminosities: The Origin of the Radio-Infrared Correlation. *ApJ* 586:794. <https://doi.org/10.1086/367829>
- Bennett AS (1962) The preparation of the revised 3C catalogue of radio sources. *MNRAS* 125:75. <https://doi.org/10.1093/mnras/125.1.75>
- Best PN (2000) The cluster environments of the  $z \sim 1$  3CR radio galaxies. *MNRAS* 317:720. <https://doi.org/10.1046/j.1365-8711.2000.03712.x>
- Best PN (2004) The environmental dependence of radio-loud AGN activity and star formation in the 2dFGRS. *MNRAS* 351:70. <https://doi.org/10.1111/j.1365-2966.2004.07752.x>
- Best PN (2009) Radio source populations: Results from SDSS. *Astron Nachr* 330:184. <https://doi.org/10.1002/asna.200811152>
- Best PN, Heckman TM (2012) On the fundamental dichotomy in the local radio-AGN population: accretion, evolution and host galaxy properties. *MNRAS* 421:1569. <https://doi.org/10.1111/j.1365-2966.2012.20414.x>
- Best PN, Longair MS, Röttgering HJA (1998) HST, radio and infrared observations of 28 3CR radio galaxies at redshift  $z \sim 1$  – II. Old stellar populations in central cluster galaxies. *MNRAS* 295:549. <https://doi.org/10.1046/j.1365-8711.1998.01245.x>
- Best PN, Kauffmann G, Heckman TM, Brinchmann J, Charlot S, Ivezić Ž, White SDM (2005a) The host galaxies of radio-loud active galactic nuclei: mass dependences, gas cooling and active galactic nuclei feedback. *MNRAS* 362:25. <https://doi.org/10.1111/j.>

- 1365-2966.2005.09192.x
- Best PN, Kauffmann G, Heckman TM, Ivesic Z (2005b) A sample of radio-loud active galactic nuclei in the Sloan Digital Sky Survey. *MNRAS* 362:9. <https://doi.org/10.1111/j.1365-2966.2005.09283.x>
- Best PN, Kaiser C, Heckman T, Kauffmann G (2006) AGN-controlled cooling in elliptical galaxies. *MNRAS* 368:L67. <https://doi.org/10.1111/j.1745-3933.2006.00159.x>
- Best PN, von der Linden A, Kauffmann G, Heckman TM, Kaiser CR (2007) On the prevalence of radio-loud active galactic nuclei in brightest cluster galaxies: implications for AGN heating of cooling flows. *MNRAS* 379:894. <https://doi.org/10.1111/j.1365-2966.2007.11937.x>
- Best PN, Ker LM, Simpson C, Rigby EE, Sabater J (2014) The cosmic evolution of radio-AGN feedback to  $z = 1$ . *MNRAS* 445:955. <https://doi.org/10.1093/mnras/stu1776>
- Birzan L, Rafferty DA, Brüggén M, Intema HT (2017) A study of high-redshift AGN feedback in SZ cluster samples. *MNRAS* 471:1766. <https://doi.org/10.1093/mnras/stx1505>
- Blake C, Wall JV (2002a) Measurement of the angular correlation function of radio galaxies from the NRAO VLA Sky Survey. *MNRAS* 329:37. <https://doi.org/10.1046/j.1365-8711.2002.05163.x>
- Blake C, Wall JV (2002b) Quantifying angular clustering in wide-area radio surveys. *MNRAS* 337:993. <https://doi.org/10.1046/j.1365-8711.2002.05979.x>
- Blanton EL, Gregg MD, Helfand DJ, Becker RH, Leighly KM (2001) The Environments of a Complete Moderate-Redshift Sample of FIRST Bent-Double Radio Sources. *AJ* 121:2915. <https://doi.org/10.1086/321074>
- Bohringer H, Voges W, Huchra JP, McLean B, et al (2000) The Northern ROSAT All-Sky (NORAS) Galaxy Cluster Survey. I. X-Ray Properties of Clusters Detected as Extended X-Ray Sources. *ApJS* 129:435
- Bohringer H, Collins CA, Guzzo L, Schuecker P, et al (2004) The ROSAT-ESO Flux Limited X-ray (REFLEX) Galaxy cluster survey. V. The cluster catalogue. *A&A* 425:367. <https://doi.org/10.1051/0004-6361:20034484>
- Bolton JG, Savage A, Wright AE (1979) The Parkes 2700 MHz survey (14th part): catalogue and new optical identifications. *Aust J Phys Suppl* 46:1
- Bonato M, Prandoni I, De Zotti G, Best PN, et al (2021) The LOFAR Two-metre Sky Survey Deep Fields. A new analysis of low-frequency radio luminosity as a star-formation tracer in the Lockman Hole region. *A&A* 656:48. <https://doi.org/10.1051/0004-6361/202141286>
- Bondi M, Ciliegi P, Schinnerer E, Smolčić V, Jahnke K, Carilli C, Zamorani G (2008) The VLA-COSMOS Survey. III. Further Catalog Analysis and the Radio Source Counts. *ApJ* 681:1129. <https://doi.org/10.1086/589324>
- Bonzini M, Mainieri V, Padovani P, Andreani P, et al (2015) Star formation properties of sub-mJy radio sources. *MNRAS* 453:1079. <https://doi.org/10.1093/mnras/stv1675>
- Bourne N, Dunne L, Ivison RJ, Maddox SJ, Dickinson M, Frayer DT (2011) Evolution of the far-infrared-radio correlation and infrared spectral energy distributions of massive galaxies over  $z = 0 - 2$ . *MNRAS* 410:1155
- Bower RG, Benson AJ, Malbon R, Helly JC, Frenk CS, Baugh CM, Cole S, Lacey CG (2006) Breaking the hierarchy of galaxy formation. *MNRAS* 370:645. <https://doi.org/10.1111/j.1365-2966.2006.10519.x>
- Brand K, Rawlings S, Hill GJ, Tufts JR (2005) The three-dimensional clustering of radio galaxies in the Texas-Oxford NVSS structure survey. *MNRAS* 357:1231. <https://doi.org/10.1111/j.1365-2966.2005.08719.x>
- Brodwin M, Dey A, Brown MJI, Pope A, Armus L, Busmann S, Desai V, Jannuzi BT, Le Floc'h E (2008) Clustering of Dust-Obscured Galaxies at  $z \sim 2$ . *ApJ* 687:L65
- Brodwin M, Greer CH, Leitch EM, Stanford SA, et al (2015) The Massive and Distant Clusters of WISE Survey. III. Sunyaev-Zel'dovich Masses of Galaxy Clusters at  $z \sim 1$ . *ApJ* 806:26
- Brown MJI, Jannuzi BT, Floyd DJE, Mould JR (2011) The Ubiquitous Radio Continuum Emission from the Most Massive Early-type Galaxies. *ApJ* 731:L41. <https://doi.org/10.1088/2041-8205/731/2/L41>
- Brunetti G, Jones TW (2014) Cosmic Rays in Galaxy Clusters and Their Nonthermal Emission. *IJMPD* 23:430007–98. <https://doi.org/10.1142/s0218271814300079>



- Bruzual G, Charlot S (2003) Stellar population synthesis at the resolution of 2003. *MNRAS* 344:1000. <https://doi.org/10.1046/j.1365-8711.2003.06897.x>
- Butler A, Huynh M, Delhaize J, Smolčić V, et al (2018a) The XXL Survey. XVIII. ATCA 2.1 GHz radio source catalogue and source counts for the XXL-South field. *A&A* 620:3. <https://doi.org/10.1051/0004-6361/201630129>
- Butler A, Huynh M, Delvecchio I, Kapińska A, et al (2018b) The XXL Survey. XXXI. Classification and host galaxy properties of 2.1 GHz ATCA XXL-S radio sources. *A&A* 620:16. <https://doi.org/10.1051/0004-6361/201732379>
- Butler A, Huynh M, Kapińska A, Delvecchio I, Smolčić V, Chiappetti L, Koulouridis E, Pierre M (2019) The XXL Survey. XXXVI. Evolution and black hole feedback of high-excitation and low-excitation radio galaxies in XXL-S. *A&A* 625:111. <https://doi.org/10.1051/0004-6361/201834581>
- Buttiglione S, Capetti A, Celotti A, Axon DJ, Chiaberge M, Macchetto FD, Sparks WB (2010) An optical spectroscopic survey of the 3CR sample of radio galaxies with  $z < 0.3$ . II. Spectroscopic classes and accretion modes in radio-loud AGN. *A&A* 509:6
- Calistro Rivera G, Williams WL, Hardcastle MJ, Duncan K, et al (2017) The LOFAR window on star-forming galaxies and AGNs - curved radio SEDs and IR-radio correlation at  $0 < z < 2.5$ . *MNRAS* 469:3468. <https://doi.org/10.1093/mnras/stx1040>
- Cannon R, Drinkwater M, Edge A, Eisenstein D, et al (2006) The 2dF-SDSS LRG and QSO (2SLAQ) Luminous Red Galaxy Survey. *MNRAS* 372:425. <https://doi.org/10.1111/j.1365-2966.2006.10875.x>
- Capetti A, Massaro F, Baldi RD (2017a) FRICAT: A FIRST catalog of FR I radio galaxies. *A&A* 598:49. <https://doi.org/10.1051/0004-6361/201629287>
- Capetti A, Massaro F, Baldi RD (2017b) FRIICAT: A FIRST catalog of FR II radio galaxies. *A&A* 601:81. <https://doi.org/10.1051/0004-6361/201630247>
- Capetti A, Brienza M, Balmaverde B, Best PN, et al (2022) The LOFAR view of giant, early-type galaxies: radio emission from active nuclei and star formation. *A&A* arXiv:2202.08593. <https://doi.org/10.1051/0004-6361/202142911>
- Carilli C, Yun MS (1999) The Radio-to-Submillimeter Spectral Index as a Redshift Indicator. *ApJ* 513:L13. <https://doi.org/10.1086/311909>
- Castignani G, Chiaberge M, Celotti A, Norman C, De Zotti G (2014) Cluster Candidates around Low-power Radio Galaxies at  $z \sim 1 - 2$  in COSMOS. *ApJ* 792:114. <https://doi.org/10.1088/0004-637x/792/2/114>
- Ceraj L, Smolčić V, Delvecchio I, A B, et al (2020) The XXL Survey. XLIII. The quasar radio loudness dichotomy exposed via radio luminosity functions obtained by combining results from COSMOS and XXL-S X-ray selected quasars. *A&A* 642:125. <https://doi.org/10.1051/0004-6361/201936776>
- Chakraborty A, Dutta P, Datta A, Roy N (2020) The study of the angular and spatial distribution of radio-selected AGNs and star-forming galaxies in the ELAIS N1 field. *MNRAS* 494:3392. <https://doi.org/10.1093/mnras/staa945>
- Chapman SC, Blain AW, Smail I, Ivison RJ (2005) A Redshift Survey of the sub-millimetre Galaxy Population. *ApJ* 662:772. <https://doi.org/10.1086/428082>
- Chapman SC, Ivison RJ, Roseboom IG, Auld R, et al (2010) Herschel-SPIRE, far-infrared properties of millimetre-bright and -faint radio galaxies. *MNRAS* 409:L13. <https://doi.org/10.1111/j.1745-3933.2010.00956.x>
- Chen YM, Kauffmann G, Heckman TM, Tremonti CA, et al (2013) Evolution of the most massive galaxies to  $z \sim 0.6$  II. The link between radio AGN activity and star formation. *MNRAS* 429:2643. <https://doi.org/10.1093/mnras/sts544>
- Chi X, Wolfendale AW (1990) Implications of the correlation between radio and far-infrared emission for spiral galaxies. *MNRAS* 245:101. <https://doi.org/10.1093/mnras/245.1.101>
- Chiaberge M, Capetti A, Celotti A (1999) The HST view of FR I radio galaxies: evidence for non-thermal nuclear sources. *A&A* 349:77
- Chiaberge M, Capetti A, Celotti A (2000) The HST view of the FR I / FR II dichotomy. *A&A* 355:873
- Chiaberge M, Tremblay G, Capetti A, Macchetto FD, Tozzi P, Sparks WB (2009) Low-Power Radio Galaxies in the Distant Universe: A Search for FR I at  $1 < z < 2$  in the Cosmos Field. *ApJ* 696:1103. <https://doi.org/10.1088/0004-637x/696/2/1103>



- Colla G, Fanti C, Fanti R, Gioia I, Lari C, Lequeux J, Lucas R, Ulrich MH (1975) A complete sample of radio sources identified with elliptical galaxies: radio luminosity function and other properties. *A&A* 38:209
- Colless M, Dalton G, Maddox SJ, Sutherland WJ, et al (2001) The 2dF Galaxy Redshift Survey: spectra and redshifts. *MNRAS* 328:1039. <https://doi.org/10.1046/j.1365-8711.2001.04902.x>
- Condon JJ (1992) Radio emission from normal galaxies. *ARA&A* 30:575. <https://doi.org/10.1146/annurev.aa.30.090192.003043>
- Condon JJ, Cotton WD, Greisen EW, Yin QF, Perley RA, Taylor GB, Broderick JJ (1998) The NRAO VLA Sky Survey. *AJ* 115:1693. <https://doi.org/10.1086/300337>
- Condon JJ, Kellermann KI, Kimball AE, Ivezić Z, Perley RA (2013) Active Galactic Nucleus and Starburst Radio Emission from Optically Selected Quasi-stellar Objects. *ApJ* 768:37. <https://doi.org/10.1088/0004-637x/768/1/37>
- Cooke EA, Hatch NA, Stern D, Rettura A, et al (2016) A Mature Galaxy Cluster at  $z = 1.58$  around the Radio Galaxy 7C1753+6311. *ApJ* 816:83. <https://doi.org/10.3847/0004-637x/816/2/83>
- Cowie LL, Songalia A, Hu EM, Cohen JG (1996) New Insight on Galaxy Formation and Evolution From Keck Spectroscopy of the Hawaii Deep Fields. *AJ* 112:839. <https://doi.org/10.1086/118058>
- Cress CM, Helfand DJ, Becker RH, Gregg MD, White RL (1996) The Angular Two-Point Correlation Function for the FIRST Radio Survey. *ApJ* 473:7
- Croft S, de Vries W, Becker RH (2007) Radio AGNs in 13,240 Galaxy Clusters from the Sloan Digital Sky Survey. *ApJ* 667:L13. <https://doi.org/10.1086/522086>
- Croston JH, Hardcastle MJ, Birkinshaw M, Worrall DM (2003) XMM-Newton observations of the hot-gas atmospheres of 3C 66B and 3C 449. *MNRAS* 346:1041. <https://doi.org/10.1111/j.1365-2966.2003.07165.x>
- Croston JH, Hardcastle MJ, Birkinshaw M (2005) Evidence for radio-source heating of groups. *MNRAS* 357:279. <https://doi.org/10.1111/j.1365-2966.2005.08665.x>
- Croston JH, Hardcastle MJ, Mingo B, Best PN, et al (2019) The environments of radio-loud AGN from the LOFAR Two-Metre Sky Survey (LoTSS). *A&A* 622:10. <https://doi.org/10.1051/0004-6361/201834019>
- Croton DJ, Springel V, White SDM, De Lucia G, et al (2006) The many lives of active galactic nuclei: cooling flows, black holes and the luminosities and colours of galaxies. *MNRAS* 365:11. <https://doi.org/10.1111/j.1365-2966.2005.09675.x>
- Dabhade HJA, Pand Röttgering, Bagchi J, Shimwell TW, et al (2020) Giant radio galaxies in the LOFAR Two-metre Sky Survey. I. Radio and environmental properties. *A&A* 635:5. <https://doi.org/10.1051/0004-6361/201935589>
- Dalton GB, Efsthathiou G, Maddox SJ, Sutherland WJ (1992) Spatial correlations in a redshift survey of APM galaxy clusters. *ApJ* 390:L1. <https://doi.org/10.1086/186357>
- D'Amato Q, Gilli R, Prandoni I, Vignali C, et al (2020) Discovery of molecular gas fueling galaxy growth in a protocluster at  $z = 1.7$ . *A&A* 641:L6. <https://doi.org/10.1051/0004-6361/202038711>
- Darvish B, Mobasher B, Martin DC, Sobral D, Scoville N, Stroe A, Hemmati S, Kartaltepe J (2017) Cosmic Web of Galaxies in the COSMOS Field: Public Catalog and Different Quenching for Centrals and Satellites. *ApJ* 837:16. <https://doi.org/10.3847/1538-4357/837/1/16>
- Davies LJM, Huynh MT, Hopkins AM, Seymour N, et al (2017) Galaxy And Mass Assembly: the 1.4 GHz SFR indicator,  $SFR - M_*$  relation and predictions for ASKAP-GAMA. *MNRAS* 466:2312
- De Breuck C, van Breugel W, Stanford SA, Röttgering H, Miley G, Stern D (2002) Optical and Near-Infrared Imaging of Ultra-Steep-Spectrum Radio Sources: The  $K - z$  Diagram of Radio-selected and Optically Selected Galaxies. *ApJ* 123:637
- De Breuck C, Seymour N, Stern D, Willner SP, et al (2010) The Spitzer High-redshift Radio Galaxy Survey. *ApJ* 725:36. <https://doi.org/10.1088/0004-637x/725/1/36>
- De Jong T, Klein U R, Wielebinski, Wunderlich E (1985) Radio continuum and far-infrared emission from spiral galaxies: a close correlation. *A&A* 147:L6
- De Zotti G, Massardi M, Negrello M, Wall JV (2010) Radio and millimeter continuum surveys and their astrophysical implications. *A&ARev* 18:1–65. <https://doi.org/10.1007/>

- s00159-009-0026-0
- Dekel A, Lahav O (1999) Stochastic Nonlinear Galaxy Bias. *ApJ* 520:24. <https://doi.org/10.1086/307428>
- Del Moro A, Alexander DM, Mullaney JR, Daddi E, et al (2013) GOODS-Herschel: radio-excess signature of hidden AGN activity in distant star-forming galaxies. *A&A* 549:59
- Delhaize J, Smolčić V, Delvecchio I, Novak M, et al (2017) The VLA-COSMOS 3 GHz Large Project: The infrared-radio correlation of star-forming galaxies and AGN to  $z \simeq 6$ . *A&A* 602:4
- Delvecchio I, Smolčić V, Zamorani G, Lagos CDP, et al (2017) The VLA-COSMOS 3 GHz Large Project: AGN and host-galaxy properties out to  $z \sim 6$ . *A&A* 602:3. <https://doi.org/10.1051/0004-6361/201629367>
- Delvecchio I, Daddi E, Sargent MT, Jarvis MJ, et al (2021) The infrared-radio correlation of star-forming galaxies is strongly  $M_*$ -dependent but nearly redshift-invariant since  $z \sim 4$ . *A&A* 647:123. <https://doi.org/10.1051/0004-6361/202039647>
- Dey A, van Breugel W, Vacca WD, Antonucci R (1997) Triggered Star Formation in a Massive Galaxy at  $z = 3.8$ : 4C 41.17. *ApJ* 490:698. <https://doi.org/10.1086/304911>
- Dicken D, Tadhunter C, Axon D, Robinson A, Morganti R, Kharb P (2010) The Origin of the Infrared Emission in Radio Galaxies. III. Analysis of 3CRR Objects. *ApJ* 722:1333. <https://doi.org/10.1088/0004-637x/722/2/1333>
- Dicken D, Tadhunter C, Axon D, Morganti R, et al (2012) Spitzer Mid-IR Spectroscopy of Powerful 2 Jy and 3CRR Radio Galaxies. I. Evidence against a Strong Starburst-AGN Connection in Radio-loud AGN. *ApJ* 172:21. <https://doi.org/10.1088/0004-637x/745/2/172>
- Doherty M, Tanaka M, De Breuck C, Ly C, et al (2010) Optical and near-IR spectroscopy of candidate red galaxies in two  $z \sim 2.5$  protoclusters. *A&A* 509:83
- Dolfi A, Branchini E, Bilicki M, Balaguera-Antolínez A, Prandoni I, Pandit R (2019) Clustering properties of TGSS radio sources. *A&A* 623:48. <https://doi.org/10.1051/0004-6361/201834317>
- Donley JL, Rieke GH, Rigby JR, Perez-Gonzalez PG (2005) Unveiling a Population of AGNs Not Detected in X-Rays. *ApJ* 634:169. <https://doi.org/10.1086/491668>
- Donley JL, Koekemoer AM, Brusa M, Capak P, et al (2012) Identifying Luminous Active Galactic Nuclei in Deep Surveys: Revised IRAC Selection Criteria. *ApJ* 748:142. <https://doi.org/10.1088/0004-637x/748/2/142>
- Donoso E, Kauffmann G, Best PN (2009) Evolution of the radio-loud galaxy population. *MNRAS* 392:617. <https://doi.org/10.1111/j.1365-2966.2008.14068.x>
- Donoso E, Cheng L, Kauffmann G, Best PN, Heckman TM (2010) Clustering of radio galaxies and quasars. *MNRAS* 407:1078. <https://doi.org/10.1111/j.1365-2966.2010.16907.x>
- Dressler A (1980) Galaxy morphology in rich clusters: implications for the formation and evolution of galaxies. *ApJ* 236:351. <https://doi.org/10.1086/157753>
- Dressler A, Thompson IB, Shectman SA (1985) Statistics of emission-line galaxies in rich clusters. *ApJ* 288:481. <https://doi.org/10.1086/162813>
- Driver SP, Hill DT, Kelvin LS, Robotham ASG, et al (2011) Galaxy and Mass Assembly (GAMA): survey diagnostics and core data release. *MNRAS* 413:971
- Drouart G, De Breuck C, Vernet J, Seymour N, et al (2014) Rapidly growing black holes and host galaxies in the distant Universe from the Herschel Radio Galaxy Evolution Project. *A&A* 566:53. <https://doi.org/10.1051/0004-6361/201323310>
- Drouart G, Rocca-Volmerange B, De Breuck C, Fioc M, Lehnert M, Seymour N, Stern D, J V (2016) Disentangling star formation and AGN activity in powerful infrared luminous radio galaxies at  $1 < z < 4$ . *A&A* 593:109. <https://doi.org/10.1051/0004-6361/201526880>
- Duncan KJ, Kondapally R, Brown MJI, Bonato M, et al (2021) The LOFAR Two-meter Sky Survey: Deep Fields Data Release 1. IV. Photometric redshifts and stellar masses. *A&A* 648:4. <https://doi.org/10.1051/0004-6361/202038809>
- Dunlop J, Peacock JA (1990) The redshift cut-off in the luminosity function of radio galaxies and quasars. *MNRAS* 247:19
- Dunn RJ, Allen SW, Taylor GB, Shurkin KF, Gentile G, Fabian AC, Reynolds CS (2010) The radio properties of a complete, X-ray selected sample of nearby, massive elliptical galaxies. *MNRAS* 404:180. <https://doi.org/10.1111/j.1365-2966.2010.16314.x>

- Eales S, Rawlings S, Law-Green D, Cotter G, Lacy M (1997) A first sample of faint radio sources with virtually complete redshifts – I. Infrared images, the Hubble diagram and the alignment effect. *MNRAS* 291:593. <https://doi.org/10.1093/mnras/291.4.593>
- Eales S, Dunne L, Clements D, Cooray A, et al (2010) The Herschel ATLAS. *PASP* 891:499
- Edge DO, Shakeshaft JR, McAdam WB, Baldwin JE, Archer S (1959) A survey of radio sources at a frequency of 159 Mc/s. *Mem R Astron Soc* 68:37
- Ekers RD, Ekers JA (1973) A Survey of Elliptical Galaxies at 6 cm. *A&A* 24:247
- Ellingson E, Yee HK, Green RF (1991) Quasars and Active Galactic Nuclei in Rich Environments. II. The Evolution of Radio-loud Quasars. *ApJ* 371:49. <https://doi.org/10.1086/169869>
- Ellison SL, Patton DR, Hickox RC (2015) Galaxy pairs in the Sloan Digital Sky Survey XII. The fuelling mechanism of low-excitation radio-loud AGN. *MNRAS* 451:L35. <https://doi.org/10.1093/mnras/451.1/slv061>
- Fabbiano G, Gioia I, Trinchieri G (1989) Radio Emission and the Hot Interstellar Medium of Early-Type Galaxies. *ApJ* 347:127. <https://doi.org/10.1086/168103>
- Fadda D, Jannuzi BT, Ford A, Storrie-Lombardi LJ (2004) The Spitzer Space Telescope First-Look Survey: KPNO Mosaic-1 R-Band Images and Source Catalogs. *AJ* 128:1. <https://doi.org/10.1086/421366>
- Falkendal T, De Breuck C, Lehnert MD, Drouart G, et al (2019) Massive galaxies on the road to quenching: ALMA observations of powerful high redshift radio galaxies. *A&A* 621:27. <https://doi.org/10.1051/0004-6361/201732485>
- Fanaroff BL, Riley JM (1974) The morphology of extragalactic radio sources of high and low luminosity. *MNRAS* 167:31. <https://doi.org/10.1093/mnras/167.1.31p>
- Fanidakis N, Baugh CM, Benson AJ, Bower RG, et al (2012) The evolution of active galactic nuclei across cosmic time: what is downsizing? *MNRAS* 419:2797
- Fanti C, Fanti R, Feretti L, Ficarra A, et al (1982) Radio and optical observations of 9 nearby Abell Clusters: A 262, A 347, A 569, A 779, A 1213, A 1228, A 2162, A 2666. *A&A* 105:200
- Feretti L, Perola GC, Fanti R (1992) Tailed radio sources as probes of the intergalactic medium pressure. *A&A* 265:9
- Fernandes CA, Jarvis MJ, Martínez-Sansigre A, Rawlings S, et al (2015) Black hole masses, accretion rates and hot- and cold-mode accretion in radio galaxies at  $z \sim 1$ . *MNRAS* 447:1184
- Fine S, Shanks T, Nikoloudakis N, Sawangwit U (2011) Evolution in the clustering strength of radio galaxies. *MNRAS* 418:2251. <https://doi.org/10.1111/j.1365-2966.2011.19527.x>
- Fragos T, Lehmer B, Tremmel M, Tzanavaris P, et al (2013) X-Ray Binary Evolution Across Cosmic Time. *ApJ* 764:41. <https://doi.org/10.1088/0004-637x/764/1/41>
- Galametz A, Stern D, De Breuck C, Hatch N, et al (2012) The Mid-infrared Environments of High-redshift Radio Galaxies. *ApJ* 749:169. <https://doi.org/10.1088/0004-637x/749/2/169>
- Galametz A, Grazian A, Fontana A, Ferguson HC, et al (2013a) CANDELS Multiwavelength Catalogs: Source Identification and Photometry in the CANDELS UKIDSS Ultra-deep Survey Field. *ApJS* 206:10
- Galametz A, Stern D, Pentericci L, De Breuck C, et al (2013b) A large-scale galaxy structure at  $z \simeq 2.02$  associated with the radio galaxy MRC 0156-252. *A&A* 559:2. <https://doi.org/10.1051/0004-6361/201322345>
- Garn T, Green DA, Riley JM, Alexander P (2009) The relationship between star formation rate and radio synchrotron luminosity at  $0 < z < 2$ . *MNRAS* 397:1101. <https://doi.org/10.1111/j.1365-2966.2009.15073.x>
- Gendre MA, Best PN, Wall JV, Ker LM (2013) The relation between morphology, accretion modes and environmental factors in local radio AGN. *MNRAS* 430:3086. <https://doi.org/10.1093/mnras/stt116>
- Ghisellini G, Celotti A (2001) The dividing line between FR I and FR II radio-galaxies. *A&A* 379:L1. <https://doi.org/10.1051/0004-6361:20011338>
- Giacintutti S, Venturi T (2009) Tailed radio galaxies as tracers of galaxy clusters. Serendipitous discoveries with the GMRT. *A&A* 505:55. <https://doi.org/10.1051/0004-6361/200912609>

- Gilli R, Mignoli M, Peca A, Nanni R, et al (2019) Discovery of a galaxy overdensity around a powerful, heavily obscured FR II radio galaxy at  $z = 1.7$ : star formation promoted by large-scale AGN feedback? *A&A* 632:26. <https://doi.org/10.1051/0004-6361/201936121>
- Golden-Marx E, Blanton EL, Paterno-Mahler R, Brodwin M, et al (2019) The High-redshift Clusters Occupied by Bent Radio AGN (COBRA) Survey: Follow-up Optical Imaging. *ApJ* 887:50. <https://doi.org/10.3847/1538-4357/ab5106>
- Golden-Marx E, Blanton EL, Paterno-Mahler R, Brodwin M, et al (2021) The High-redshift Clusters Occupied by Bent Radio AGN (COBRA) Survey: Radio Source Properties. *ApJ* 907:65. <https://doi.org/10.3847/1538-4357/abcd96>
- Gonzalez A, Gettings DP, Brodwin M, Eisenhardt PRM, et al (2019) The Massive and Distant Clusters of WISE Survey. I. Survey Overview and a Catalog of  $> 2000$  Galaxy Clusters at  $z \sim 1$ . *ApJS* 240:33
- Gozaliasl G, Finoguenov A, Tanaka M, Dolag K, et al (2019) Chandra centres for COSMOS X-ray galaxy groups: differences in stellar properties between central dominant and offset brightest group galaxies. *MNRAS* 483:3545
- Grandi P, Torresi E, Macconi D, Boccardi B, Capetti A (2021) Jet Accretion System in the Nearby mJy Radio Galaxies. *ApJ* 911:17. <https://doi.org/10.3847/1538-4357/abe776>
- Griffin MJ, Abergel A, Abreu A, Ade PAR, et al (2010) The Herschel-SPIRE instrument and its in-flight performance. *A&A* 518:L3
- Grossova R, Werner N, Massaro F, Lakhchaura K, et al (2022) Very Large Array Radio Study of a Sample of Nearby X-Ray and Optically Bright Early-type Galaxies. *ApJS* 258:30. <https://doi.org/10.3847/1538-4365/ac366c>
- Gürkan G, Hardcastle MJ, Jarvis MJ (2014) The Wide-field Infrared Survey Explorer properties of complete samples of radio-loud active galactic nucleus. *MNRAS* 438:1149. <https://doi.org/10.1093/mnras/stt2264>
- Gürkan G, Hardcastle MJ, Jarvis MJ, Smith DJB, et al (2015) Herschel-ATLAS: the connection between star formation and AGN activity in radio-loud and radio-quiet active galaxies. *MNRAS* 452:3776. <https://doi.org/10.1093/mnras/stv1502>
- Gürkan G, Hardcastle MJ, Smith DJB, Best PN, et al (2018) LOFAR/H-ATLAS: the low-frequency radio luminosity-star formation rate relation. *MNRAS* 474:3010. <https://doi.org/10.1093/mnras/sty016>
- van Haarlem MP, Wise MW, Gunst AW, Heald G, et al (2013) LOFAR: The Low-Frequency ARray. *A&A* 556:2
- Hale CL, Jarvis MJ, Delvecchio I, Hatfield PW, Novak M, Smolčić V, Zamorani G (2018) The clustering and bias of radio-selected AGN and star-forming galaxies in the COSMOS field. *MNRAS* 474:4133
- Hardcastle MJ, Croston JH (2020) Radio galaxies and feedback from AGN jets. *NewAR* 88:101539. <https://doi.org/10.1016/j.newar.2020.101539>
- Hardcastle MJ, Evans DA, Croston JH (2006) The X-ray nuclei of intermediate-redshift radio sources. *MNRAS* 370:1893. <https://doi.org/10.1111/j.1365-2966.2006.10615.x>
- Hardcastle MJ, Evans DA, Croston JH (2007) Hot and cold gas accretion and feedback in radio-loud active galaxies. *MNRAS* 376:1849. <https://doi.org/10.1111/j.1365-2966.2007.11572.x>
- Hardcastle MJ, Virdee JS, Jarvis MJ, Bonfield DG, et al (2010) Herschel-ATLAS: far-infrared properties of radio-selected galaxies. *MNRAS* 409:122. <https://doi.org/10.1111/j.1365-2966.2010.17791.x>
- Hardcastle MJ, Ching JHY, Virdee JS, Jarvis MJ, et al (2013) Herschel-ATLAS/GAMA: a difference between star formation rates in strong-line and weak-line radio galaxies. *MNRAS* 429:2407. <https://doi.org/10.1093/mnras/sts510>
- Hardcastle MJ, Williams WL, Best PN, Croston JH, et al (2019) Radio-loud AGN in the first LoTSS data release. The lifetimes and environmental impact of jet-driven sources. *A&A* 622:12. <https://doi.org/10.1051/0004-6361/201833893>
- Harwit M, Pacini F (1975) Infrared galaxies: evolutionary stages of massive star formation. *ApJ* 200:L127. <https://doi.org/10.1086/181913>
- Harwood JJ, Vernstrom T, Stroe A (2020) Unveiling the cause of hybrid morphology radio sources (HyMoRS). *MNRAS* 491:803
- Hatch NA, De Breuck C, Galametz A, Miley GK, et al (2011) Galaxy protocluster candidates around  $z \sim 2.4$  radio galaxies. *MNRAS* 410:1537

- Hatch NA, Wylezalek D, Kurk JD, Stern D, et al (2014) Why  $z > 1$  radio-loud galaxies are commonly located in protoclusters. *MNRAS* 445:280. <https://doi.org/10.1093/mnras/stu1725>
- Hawkins E, Maddox SJ, Cole S, Lahav O, et al (2003) The 2dF Galaxy Redshift Survey: correlation functions, peculiar velocities and the matter density of the Universe. *MNRAS* 346:78. <https://doi.org/10.1046/j.1365-2966.2003.07063.x>
- Heckman T, Smith EP, Baum SA, van Breugel WJM, Miley GK, Illingworth GD, Bothun GD, Balick B (1986) Galaxy Collisions and Mergers: The Genesis of Very Powerful Radio Sources? *ApJ* 311:526. <https://doi.org/10.1086/164793>
- Heckman TM, Best PN (2014) The Coevolution of Galaxies and Supermassive Black Holes: Insights from Surveys of the Contemporary Universe. *ARA&A* 52:589. <https://doi.org/10.1146/annurev-astro-081913-035722>
- Heeschen DS (1970) Radio Observations of E and S0 Galaxies. *AJ* 75:523. <https://doi.org/10.1086/110987>
- Heesen V, Croston JH, Morganti R, Hardcastle MJ, et al (2018) LOFAR reveals the giant: a low-frequency radio continuum study of the outflow in the nearby FR I radio galaxy 3C 31. *MNRAS* 474:5049
- Heinis S, Milliard B, Arnouts S, Blaizot J, et al (2007) Clustering Properties of Rest-Frame UV-Selected Galaxies. II. Migration of Star Formation Sites with Cosmic Time from GALEX and CFHTLS. *ApJS* 173:503. <https://doi.org/10.1086/520580>
- Helou G, Soifer BT, Rowan-Robinson M (1985) Thermal infrared and nonthermal radio: remarkable correlation in disks of galaxies. *ApJ* 298:L7. <https://doi.org/10.1086/184556>
- Helsdon SF, Ponman TJ (2000) Are X-ray properties of loose groups different from those of compact groups? *MNRAS* 319:933. <https://doi.org/10.1046/j.1365-8711.2000.03916.x>
- Heywood I, Blundell KM, Rawlings S (2007) The prevalence of Fanaroff-Riley type I radio quasars. *MNRAS* 381:1093. <https://doi.org/10.1111/j.1365-2966.2007.12278.x>
- Hickox RC, Jones C, Forman WR, Murray SS, et al (2009) Host Galaxies, Clustering, Eddington Ratios, and Evolution of Radio, X-Ray, and Infrared-Selected AGNs. *ApJ* 696:891. <https://doi.org/10.1088/0004-637x/696/1/891>
- Hickox RC, Wardlow JL, Smail I, Myers AD, et al (2012) The LABOCA survey of the Extended Chandra Deep Field-South: clustering of submillimetre galaxies. *MNRAS* 421:284. <https://doi.org/10.1111/j.1365-2966.2011.20303.x>
- Hill GJ, Lilly SJ (1991) A Change in the Cluster Environments of Radio Galaxies with Cosmic Epoch. *ApJ* 367:1. <https://doi.org/10.1086/169597>
- Hine RG, Longair MS (1979) Optical spectra of 3CR radio galaxies. *MNRAS* 188:111. <https://doi.org/10.1093/mnras/188.1.111>
- Ho LC (2008) Nuclear activity in nearby galaxies. *ARA&A* 46:475. <https://doi.org/10.1146/annurev.astro.45.051806.110546>
- Holland WS, Robson EI, Gear WK, Cunningham CR, et al (1999) SCUBA: a common-user submillimetre camera operating on the James Clerk Maxwell Telescope. *MNRAS* 303:659. <https://doi.org/10.1046/j.1365-8711.1999.02111.x>
- Huchra JP, Macri LM, Masters KL, Jarrett TH, et al (2012) The 2MASS Redshift Survey-Description and Data Release. *ApJS* 199:26. <https://doi.org/10.1088/0067-0049/199/2/26>
- Hummel E, Kotanyi CG, Ekers RD (1983) Radio continuum emission of nearby elliptical galaxies: statistical properties. *A&A* 127:205
- Ibar E, Cirasuolo M, Ivison R, Best P, et al (2008) Exploring the infrared/radio correlation at high redshift. *MNRAS* 386:953. <https://doi.org/10.1111/j.1365-2966.2008.13077.x>
- Ilbert O, Capak P, Salvato M, Aussel H, et al (2009) Cosmos Photometric Redshifts with 30-Bands for 2-deg<sup>2</sup>. *ApJ* 690:1236
- Ineson J, Croston JH, Hardcastle MJ, Kraft RP, Evans DA, Jarvis MJ (2013) Radio-loud Active Galactic Nucleus: is There a Link between Luminosity and Cluster Environment? *ApJ* 770:136. <https://doi.org/10.1088/0004-637x/770/2/136>
- Ineson J, Croston JH, Hardcastle MJ, Kraft RP, Evans DA, Jarvis MJ (2015) The link between accretion mode and environment in radio-loud active galaxies. *MNRAS* 453:2682. <https://doi.org/10.1093/mnras/stv1807>
- Ivison RJ, Alexander DM, Biggs AD, Brandt WN, et al (2010a) BLAST: the far-infrared/radio correlation in distant galaxies. *MNRAS* 402:245



- Ivison RJ, Magnelli B, Ibar E, Andreani P, et al (2010b) The far-infrared/radio correlation as probed by Herschel. *A&A* 518:L31
- Jaffe WG, Perola GC (1976) A Westerbork survey of rich clusters of galaxies. II. The luminosity function of bright cluster galaxies at 1415 MHz. *A&A* 46:275
- Jannsen RM, Röttgering HJ, Best PN, Brinchmann J (2012) The triggering probability of radio-loud AGN. A comparison of high and low excitation radio galaxies in hosts of different colors. *A&A* 541:62. <https://doi.org/10.1051/0004-6361/201219052>
- Jarrett TH, Chester T, Cutri R, Schneider S, Skrutskie M, Huchra JP (2000) 2MASS Extended Source Catalog: Overview and Algorithms. *AJ* 119:2498. <https://doi.org/10.1086/301330>
- Jarvis ME, Harrison CM, Mainieri V, Alexander DM, et al (2021) The quasar feedback survey: discovering hidden Radio-AGN and their connection to the host galaxy ionized gas. *MNRAS* 503:1780. <https://doi.org/10.1093/mnras/stab549>
- Jarvis MJ, Rawlings S, Eales S, Blundell KM, Bunker AJ, Croft S, McLure RJ, Willott CJ (2001) A sample of 6C radio sources designed to find objects at redshift  $z > 4$  - III. Imaging and the radio galaxy  $K - z$  relation. *MNRAS* 326:585. <https://doi.org/10.1111/j.1365-2966.2001.04730.x>
- Jarvis MJ, Smith DJB, Bonfield DG, Hardcastle MJ, et al (2010) Herschel-ATLAS: the far-infrared-radio correlation at  $z < 0.5$ . *MNRAS* 409:92. <https://doi.org/10.1111/j.1365-2966.2010.17772.x>
- Jarvis MJ, Bonfield DG, Bruce VA, Geach JE, et al (2013) The VISTA Extragalactic Observations (VIDEO) survey. *MNRAS* 428:1281
- Jenkins CR (1982) Radio observations of early-type galaxies. *MNRAS* 200:705. <https://doi.org/10.1093/mnras/200.3.705>
- Jimenez-Gallardo A, Massaro F, Capetti A, Prieto MA, et al (2019) COMP2CAT: hunting compact double radio sources in the local Universe. *A&A* 627:108. <https://doi.org/10.1051/0004-6361/201935104>
- Jones DH, Saunders W, Colless M, Read MA, et al (2004) The 6dF Galaxy Survey: samples, observational techniques and the first data release. *MNRAS* 355:747. <https://doi.org/10.1111/j.1365-2966.2004.08353.x>
- Kaiser CK, Best PN (2007) Luminosity function, sizes and FR dichotomy of radio-loud AGN. *MNRAS* 381:1548. <https://doi.org/10.1111/j.1365-2966.2007.12350.x>
- Kaiser N (1984) On the spatial correlations of Abell clusters. *ApJ* 284:L9. <https://doi.org/10.1086/184341>
- Kalfountzou E, Stevens JA, Jarvis MJ, Hardcastle MJ, et al (2014) Herschel-ATLAS: far-infrared properties of radio-loud and radio-quiet quasars. *MNRAS* 442:1181. <https://doi.org/10.1093/mnras/stu782>
- Kalfountzou E, Stevens JA, Jarvis MJ, Hardcastle MJ, et al (2017) Observational evidence that positive and negative AGN feedback depends on galaxy mass and jet power. *MNRAS* 471:28. <https://doi.org/10.1093/mnras/stx1333>
- Kauffmann G, Heckman TN, Best PN (2008) Radio jets in galaxies with actively accreting black holes: new insights from the SDSS. *MNRAS* 384:953. <https://doi.org/10.1111/j.1365-2966.2007.12752.x>
- Kellermann KI, Sramek R, Schmidt M, Shaffer DB, Green R (1989) VLA Observations of Objects in the Palomar Bright Quasar Survey. *AJ* 98:1195. <https://doi.org/10.1086/115207>
- Kimball AE, Kellermann KI, Condon JJ, Ivezić Z, Perley RA (2011) The Two-component Radio Luminosity Function of Quasi-stellar Objects: Star Formation and Active Galactic Nucleus. *ApJ* 739:L29. <https://doi.org/10.1088/2041-8205/739/1/L29>
- Knapp GR, Patten BM (1991) Millimeter and Submillimeter Observations of Nearby Radio Galaxies. *AJ* 101:1609. <https://doi.org/10.1086/115791>
- Kolwa S, Jarvis MJ, McAlpine K, Heywood I (2019) The relation between galaxy density and radio jet power for 1.4 GHz VLA selected AGN in Stripe 82. *MNRAS* 482:5156
- Kondapally R, Best PN, Hardcastle MJ, Nisbet D, et al (2021) The LOFAR Two-meter Sky Survey: Deep Fields Data Release 1. III. Host-galaxy identifications and value added catalogues. *A&A* 648:3. <https://doi.org/10.1051/0004-6361/202038813>
- Kovacs A, Chapman SC, Dowell CD, Blain AW, Ivison RJ, Smail I, Phillips TG (2006) SHARC-2 350  $\mu$ m Observations of Distant Submillimeter-selected Galaxies. *ApJ*

- 650:592. <https://doi.org/10.1086/506341>
- Kraft RP, Forman WR, Jones C, Murray SS, Hardcastle MJ, Worrall DM (2002) Chandra Observations of the X-Ray Jet in Centaurus A. *ApJ* 569:54. <https://doi.org/10.1086/339062>
- Laigle C, McCracken HJ, Ilbert O, Hsieh BC, et al (2016) The COSMOS2015 Catalog: Exploring the  $1 < z < 6$  Universe with Half a Million Galaxies. *ApJS* 224:24
- Laing RA, Riley JM, Longair MS (1983) Bright radio sources at 178 MHz: flux densities, optical identifications and the cosmological evolution of powerful radio galaxies. *MNRAS* 204:151. <https://doi.org/10.1093/mnras/204.1.151>
- Laing RA, Jenkins CR, Wall JV, Unger SW (1994) Spectrophotometry of a Complete Sample of 3CR Radio Sources: Implications for Unified Models. In: Bicknell GV, Dopita MA, Quinn PJ (eds) *The First Stromlo Symposium: The Physics of Active Galaxies*. ASP Conference Series, vol 54. p 201
- Lan TW, Prochaska JX (2021) On the environments of Giant Radio Galaxies. *MNRAS* 502:5104. <https://doi.org/10.1093/mnras/stab297>
- Laor A (2000) On Black Hole Masses and Radio Loudness in Active Galactic Nuclei. *ApJ* 543:L111. <https://doi.org/10.1086/317280>
- Lari C, Perola GC (1978) Radio properties of Abell Clusters. *IAUS* 79:137. <https://doi.org/10.1017/s0074180900144456>
- Ledlow MJ, Owen FN (1996) 20 CM VLA Survey of Abell Clusters of Galaxies. VI. Radio/Optical Luminosity Functions. *AJ* 112:9. <https://doi.org/10.1086/117985>
- Ledlow MJ, Owen FN, Keel WC (1998) Unusual FRI radio galaxy in A428. *ApJ* 495:227
- Ledlow MJ, Owen FN, Yun MS, Hill JM (2001) A Large-Scale Jet and FR I Radio Source in a Spiral Galaxy: The Host Properties and External Environment. *ApJ* 552:120. <https://doi.org/10.1086/320458>
- Lilly SJ, Longair MS (1984) Stellar populations in distant radio galaxies. *MNRAS* 211:833. <https://doi.org/10.1093/mnras/211.4.833>
- Lilly SJ, Prestage RM (1987) Surface photometry of powerful radio galaxies -II. Relations with the radio, optical, and clustering properties. *MNRAS* 225:531. <https://doi.org/10.1093/mnras/225.3.531>
- Lilly SJ, McLean IS, Longair MS (1984) Surface photometry of powerful radio galaxies: their relation to Abell cluster cD galaxies. *MNRAS* 209:401. <https://doi.org/10.1093/mnras/209.3.401>
- Lilly SJ, Le Brun V, Maier C, Mainieri V, et al (2009) The zCOSMOS 10k-Bright Spectroscopic Sample. *ApJS* 184:218. <https://doi.org/10.1088/0067-0049/184/2/218>
- Limber DN (1953) The analysis of counts of the extragalactic nebulae in terms of a fluctuating density field. *ApJ* 117:134. <https://doi.org/10.1086/145672>
- Lin L, Dickinson M, Jian HY, Merson AL, et al (2012) Clustering Properties of BzK-selected Galaxies in GOODS-N: Environmental Quenching and Triggering of Star Formation at  $z \sim 2$ . *ApJ* 756:71. <https://doi.org/10.1088/0004-637x/756/1/71>
- Lin YT, Mohr JJ (2007) Radio sources in galaxy clusters: radial distribution, and 1.4 GHz and K-band bivariate luminosity functions. *ApJS* 170:71
- Lin YT, Shen Y, Strauss MA, Richards GT, Lunnan R (2010) On the Populations of Radio Galaxies with Extended Morphology at  $z < 0.3$ . *ApJ* 723:1119. <https://doi.org/10.1088/0004-637x/723/2/1119>
- Lin YT, Hsieh BC, Lin SC, Oguri M, al (2017) First Results on the Cluster Galaxy Population from the Subaru Hyper Suprime-Cam Survey. III. Brightest Cluster Galaxies, Stellar Mass Distribution, and Active Galaxies. *ApJ* 851:139. <https://doi.org/10.3847/1538-4357/aa9bf5>
- von der Linden A, Best PN, Kauffmann G, White SD (2007) How special are brightest group and cluster galaxies? *MNRAS* 379:867. <https://doi.org/10.1111/j.1365-2966.2007.11940.x>
- Lindsay SN, Jarvis MJ, McAlpine K (2014a) Evolution in the bias of faint radio sources to  $z \sim 2.2$ . *MNRAS* 440:2322. <https://doi.org/10.1093/mnras/stu453>
- Lindsay SN, Jarvis MJ, Santos MG, Brown MJI, et al (2014b) Galaxy and Mass Assembly: the evolution of bias in the radio source population to  $z \sim 1.5$ . *MNRAS* 440:1527. <https://doi.org/10.1093/mnras/stu354>



- Longair MS, Seldner M (1979) The clustering of galaxies about extragalactic radio sources. *MNRAS* 189:433. <https://doi.org/10.1093/mnras/189.3.433>
- Lutz D, Mainieri V, Rafferty D, Shao L, et al (2010) The LABOCA Survey of the Extended Chandra Deep Field South: Two Modes of Star Formation in Active Galactic Nucleus Hosts? *ApJ* 712:1287. <https://doi.org/10.1088/0004-637x/712/2/1287>
- Lutz D, Poglitsch A, Altieri B, Andreani P, et al (2011) PACS Evolutionary Probe (PEP) - A Herschel key program. *A&A* 532:90. <https://doi.org/10.1051/0004-6361/201117107>
- Macconi D, Torresi E, Grandi P, Boccardi B, Vignali C (2020) Radio morphology-accretion mode link in Fanaroff-Riley type II low-excitation radio galaxies. *MNRAS* 493:4355. <https://doi.org/10.1093/mnras/staa560>
- Madau P, Dickinson M (2014) Cosmic Star-Formation History. *ARA&A* 52:415. <https://doi.org/10.1146/annurev-astro-081811-125615>
- Madgwick DS, Hawkins E, Lahav O, Maddox SJ, et al (2003) The 2dF Galaxy Redshift Survey: galaxy clustering per spectral type. *MNRAS* 344:847. <https://doi.org/10.1046/j.1365-8711.2003.06861.x>
- Magliocchetti M, Maddox SJ, Jackson CA, Bland-Hawthorn J, et al (2002) The 2dF Galaxy Redshift Survey: the population of nearby radio galaxies at the 1-mJy level. *MNRAS* 333:100. <https://doi.org/10.1046/j.1365-8711.2002.05386.x>
- Magliocchetti M, Brügger M (2007) The interplay between radio galaxies and cluster environment. *MNRAS* 379:260. <https://doi.org/10.1111/j.1365-2966.2007.11939.x>
- Magliocchetti M, Maddox SJ (1999) The redshift evolution of clustering in the Hubble Deep Field. *MNRAS* 306:988. <https://doi.org/10.1046/j.1365-8711.1999.02612.x>
- Magliocchetti M, Porciani C (2003) The halo distribution of 2dF galaxies. *MNRAS* 346:186. <https://doi.org/10.1046/j.1365-2966.2003.07094.x>
- Magliocchetti M, Maddox SJ, Wall JV, Benn CR, Cotter G (2000) The redshift distribution of FIRST radio sources at 1mJy. *MNRAS* 318:1047. <https://doi.org/10.1046/j.1365-8711.2000.03813.x>
- Magliocchetti M, Maddox SJ, Hawkins E, Peacock JA, et al (2004) The 2dF galaxy redshift survey: clustering properties of radio galaxies. *MNRAS* 350:1485. <https://doi.org/10.1111/j.1365-2966.2004.07751.x>
- Magliocchetti M, Andreani P, Zwaan MA (2008a) The radio properties of optically obscured Spitzer sources. *MNRAS* 383:479
- Magliocchetti M, Cirasuolo M, McLure RJ, Dunlop JS, et al (2008b) On the evolution of clustering of 24- $\mu$ m-selected galaxies. *MNRAS* 383:1131
- Magliocchetti M, Santini P, Rodighiero G, Grazian A, et al (2011) The PEP survey: clustering of infrared-selected galaxies and structure formation at  $z \sim 2$  in GOODS-South. *MNRAS* 416:1105. <https://doi.org/10.1111/j.1365-2966.2011.19109.x>
- Magliocchetti M, Popesso P, Rosario D, Lutz D, et al (2013) The Herschel-PEP survey: evidence for downsizing in the hosts of dusty star-forming systems. *MNRAS* 433:127. <https://doi.org/10.1093/mnras/stt708>
- Magliocchetti M, Lapi A, Negrello M, De Zotti G, Danese L (2014a) Cosmic dichotomy in the hosts of rapidly star-forming systems at low and high redshifts. *MNRAS* 437:2263
- Magliocchetti M, Lutz D, Rosario D, Berta S, et al (2014b) The PEP survey: infrared properties of radio-selected AGN. *MNRAS* 442:682. <https://doi.org/10.1093/mnras/stu863>
- Magliocchetti M, Lutz D, Santini P, Salvato M, Popesso P, Berta S, Pozzi F (2016) The PEP survey: evidence for intense star-forming activity in the majority of radio-selected AGN at  $z \geq 1$ . *MNRAS* 456:431
- Magliocchetti M, Popesso P, Brusa M, Salvato M, Laigle C, McCracken HJ, Ilbert O (2017) The clustering properties of radio-selected AGN and star-forming galaxies up to redshifts  $z \sim 3$ . *MNRAS* 464:3271. <https://doi.org/10.1093/mnras/stw2541>
- Magliocchetti M, Popesso P, Brusa M, Salvato M (2018a) A census of radio-selected AGNs on the COSMOS field and of their FIR properties. *MNRAS* 473:2493
- Magliocchetti M, Popesso P, Brusa M, Salvato M (2018b) The environmental properties of radio-emitting AGN. *MNRAS* 478:3848. <https://doi.org/10.1093/mnras/sty1309>
- Magliocchetti M, Pentericci L, Cirasuolo M, Zamorani G, et al (2020) The role of galaxy mass on AGN emission: a view from the VANDELS survey. *MNRAS* 493:3838. <https://doi.org/10.1093/mnras/staa410>

- Magliocchetti M, Maddox SJ, Lahav O, Wall JV (1998) Variance and skewness in the FIRST survey. *MNRAS* 300:257. [https://doi.org/10.1007/978-3-540-49460-7\\_21](https://doi.org/10.1007/978-3-540-49460-7_21)
- Magliocchetti M, Maddox SJ, Lahav O, Wall JV (1999) Constraints on the clustering, biasing and redshift distribution of radio sources. *MNRAS* 306:943. <https://doi.org/10.1046/j.1365-8711.1999.02596.x>
- Magnelli B, Ivison RJ, Lutz D, Valtchanov I, et al (2015) The far-infrared/radio correlation and radio spectral index of galaxies in the SFR- $M_*$  plane up to  $z \sim 2$ . *A&A* 573:45
- Malavasi N, Bardelli S, Ciliegi P, Ilbert O, Pozzetti L, Zucca E (2015) The environment of radio sources in the VLA-COSMOS survey field. *A&A* 576:101. <https://doi.org/10.1051/0004-6361/201425155>
- Mandelbaum R, Li C, Kauffmann G, White SD (2009) Halo masses for optically selected and for radio-loud AGN from clustering and galaxy-galaxy lensing. *MNRAS* 393:377. <https://doi.org/10.1111/j.1365-2966.2008.14235.x>
- Mao MY, Huynh MT, Norris RP, Dickinson M, Frayer D, Helou G, Monikiewicz JA (2011) No Evidence for Evolution in the Far-infrared-Radio Correlation out to  $z \sim 2$  in the Extended Chandra Deep Field South. *ApJ* 731:79. <https://doi.org/10.1088/0004-637x/731/2/79>
- Martin AM, Giovanelli R, Haynes MP, Guzzo L (2012) The Clustering Characteristics of HI-selected Galaxies from the 40% ALFALFA Survey. *ApJ* 750:38. <https://doi.org/10.1088/0004-637x/750/1/38>
- Massardi M, Ekers RD, Murphy T, Mahony E, et al (2011) The Australia Telescope 20 GHz (AT20G) Survey: analysis of the extragalactic source sample. *MNRAS* 412:318. <https://doi.org/10.1111/j.1365-2966.2010.17917.x>
- Massaro F, Álvarez-Crespo N, Capetti A, Baldi RD, Pillitteri I, Campana R, Paggi A (2019) Deciphering the Large-scale Environment of Radio Galaxies in the Local Universe: Where Are They Born? Where Do They Grow? Where Do They Die? *ApJS* 240:20. <https://doi.org/10.3847/1538-4365/aaf1c7>
- Massaro F, Capetti A, Paggi A, Baldi RD, et al (2020) Deciphering the Large-Scale Environment of Radio Galaxies in the Local Universe II: a Statistical Analysis of Environmental Properties. *ApJS* 247:71. <https://doi.org/10.3847/1538-4365/ab799e>
- Masson C (1978) Phd thesis. PhD thesis, University of Cambridge
- Masson C (1979) A test of clustering among radio sources in 0.16 SR of the 6C survey. *MNRAS* 188:261. <https://doi.org/10.1093/mnras/188.2.261>
- Matthews TA, Morgan WW, Schmidt M (1964) A Discussion on Galaxies Identified with Radio Sources. *ApJ* 140:35. <https://doi.org/10.1086/147890>
- Mauch T, Sadler EM (2007) Radio sources in the 6dFGS: local luminosity functions at 1.4 GHz for star-forming galaxies and radio-loud AGN. *MNRAS* 375:931. <https://doi.org/10.1111/j.1365-2966.2006.11353.x>
- Mayo JH, Vernet J, De Breuck C, Galametz A, Seymour N, Stern D (2012) Overdensities of 24 $\mu$ m sources in the vicinities of high-redshift radio galaxies. *A&A* 539:33. <https://doi.org/10.1051/0004-6361/201118254>
- McAlpine K, Jarvis MJ, Bonfield DG (2013) Evolution of faint radio sources in the VIDEO-XMM3 field. *MNRAS* 436:1084. <https://doi.org/10.1093/mnras/stt1638>
- McDonald M, Stalder B, Bayliss M, Allen SW, et al (2016) Star-forming brightest cluster galaxies at  $0.25 < z < 1.25$ : a transitioning fuel supply. *ApJ* 817:86. <https://doi.org/10.3847/0004-637x/817/2/86>
- McLure RJ, Dunlop JS (2000) The evolution of 3CR radio galaxies from  $z \sim 1$ . *MNRAS* 317:249. <https://doi.org/10.1046/j.1365-8711.2000.03509.x>
- McLure RJ, Dunlop JS (2001) The cluster environments of powerful radio-loud and radio-quiet active galactic nuclei. *MNRAS* 321:515. <https://doi.org/10.1046/j.1365-8711.2001.04087.x>
- McLure RJ, Jarvis MJ (2004) The relationship between radio luminosity and black hole mass in optically selected quasars. *MNRAS* 353:L45. <https://doi.org/10.1111/j.1365-2966.2004.08305.x>
- McLure RJ, Kukula MJ, Dunlop JS, Baum SA, O'Dea CP, Huges DH (1999) A comparative HST imaging study of the host galaxies of radio-quiet quasars, radio-loud quasars and radio galaxies - I. *MNRAS* 308:377. <https://doi.org/10.1046/j.1365-8711.1999.02676.x>

- McLure RJ, Willott CJ, Jarvis MJ, Rawlings S, Hill GJ, Mitchell E, Dunlop JS, Wold M (2004) A sample of radio galaxies spanning three decades in radio luminosity – I. The host galaxy properties and black hole masses. *MNRAS* 351:347. <https://doi.org/10.1111/j.1365-2966.2004.07793.x>
- McLure RJ, Pentericci L, Cimatti A, Dunlop JS, et al (2018) The VANDELS ESO public spectroscopic survey. *MNRAS* 479:25
- McNamara BR, Nulsen PEJ (2012) Mechanical feedback from active galactic nuclei in galaxies, groups and clusters. *New J Phys* 14:055023. <https://doi.org/10.1088/1367-2630/14/5/055023>
- Merloni A, Heinz S (2007) Measuring the kinetic power of active galactic nuclei in the radio mode. *MNRAS* 381:589. <https://doi.org/10.1111/j.1365-2966.2007.12253.x>
- Merloni A, Rudnick G, Di Matteo T (2004) Tracing the cosmological assembly of stars and supermassive black holes in galaxies. *MNRAS* 354:L37. <https://doi.org/10.1111/j.1365-2966.2004.08382.x>
- Metcalf RB, Magliocchetti M (2006) The role of black hole mass in quasar radio activity. *MNRAS* 365:101. <https://doi.org/10.1111/j.1365-2966.2005.09649.x>
- Miley GK, De Breuck C (2008) Distant radio galaxies and their environments. *A&A Rev* 15:67. <https://doi.org/10.1007/s00159-007-0008-z>
- Miley GK, Overzier RA, Tsvetanov ZI, Bouwens RJ, et al (2004) A large population of ‘Lyman-break’ galaxies in a protocluster at redshift  $z \sim 4.1$ . *Nature* 427:47. <https://doi.org/10.1038/nature02125>
- Miller CJ, Nichol RC, Reichart D, Wechsler RH, et al (2005) The C4 Clustering Algorithm: Clusters of Galaxies in the Sloan Digital Sky Survey. *AJ* 130:968. <https://doi.org/10.1086/431357>
- Miller NA, Bonzini M, Fomalont EB, Kellermann KI, et al (2013) The Very Large Array 1.4 GHz Survey of the Extended Chandra Deep Field South: Second Data Release. *ApJS* 205:13. <https://doi.org/10.1088/0067-0049/205/2/13>
- Mingo B, Watson MG, Rosen SR, Hardcastle MJ, et al (2016) The MIXR sample: AGN activity versus star formation across the cross-correlation of WISE, 3XMM, and FIRST/NVSS. *MNRAS* 462:2631. <https://doi.org/10.1093/mnras/stw1826>
- Mingo B, Croston JH, Hardcastle MJ, Best PN, et al (2019) Revisiting the Fanaroff-Riley dichotomy and radio-galaxy morphology with the LOFAR Two-Metre Sky Survey (LoTSS). *MNRAS* 488:2701. <https://doi.org/10.1093/mnras/stz1901>
- Mingo B, Croston JH, Best PN, Duncan KJ, et al (2022) Accretion mode versus radio morphology in the LOFAR Deep Fields. *MNRAS* 511:3250. <https://doi.org/10.1093/mnras/stac140>
- Miraghaei H (2020) The Effect of Environment on AGN Activity: The Properties of Radio and Optical AGN in Void, Isolated, and Group Galaxies. *AJ* 160:227. <https://doi.org/10.3847/1538-3881/abafbl>
- Miraghaei H, Best PN (2017) The nuclear properties and extended morphologies of powerful radio galaxies: the roles of host galaxy and environment. *MNRAS* 466:4346. <https://doi.org/10.1093/mnras/stx007>
- Mo HJ, White SDM (1996) An analytic model for the spatial clustering of dark matter haloes. *MNRAS* 282:347. <https://doi.org/10.1093/mnras/282.2.347>
- Mo W, Gonzalez A, Stern D, Brodwin M, et al (2018) The Massive and Distant Clusters of WISE Survey. IV. The Distribution of Active Galactic Nuclei in Galaxy Clusters at  $z \sim 1$ . *ApJ* 869:131. <https://doi.org/10.3847/1538-4357/aaef83>
- Mo W, Gonzalez A, Brodwin M, Decker B, et al (2020) The Massive and Distant Clusters of WISE Survey. VIII. Radio Activity in Massive Galaxy Clusters. *ApJ* 901:131. <https://doi.org/10.3847/1538-4357/abb08d>
- Molnar DC, Sargent MT, Delhaize J, Delvecchio I, et al (2018) The infrared-radio correlation of spheroid- and disc-dominated star-forming galaxies to  $z \sim 1.5$  in the COSMOS field. *MNRAS* 475:827
- Molnar DC, Sargent MT, Leslie S, Magnelli B, et al (2021) The non-linear infrared-radio correlation of low- $z$  galaxies: implications for redshift evolution, a new radio SFR recipe, and how to minimize selection bias. *MNRAS* 504:118. <https://doi.org/10.1093/mnras/stab746>

- Murphy EJ (2009) The Far-Infrared-Radio Correlation at High Redshifts: Physical Considerations and Prospects for the Square Kilometer Array. *ApJ* 706:482. <https://doi.org/10.1088/0004-637x/706/1/482>
- Murphy EJ, Condon JJ, Schinnerer E, Kennicutt RC, et al (2011) Calibrating Extinction-free Star Formation Rate Diagnostics with 33 GHz Free-free Emission in NGC 6946. *ApJ* 737:67. <https://doi.org/10.1088/0004-637x/737/2/67>
- Murphy EJ, Bremseth J, Mason BS, Condon JJ, et al (2012) The Star Formation in Radio Survey: GBT 33 GHz Observations of Nearby Galaxy Nuclei and Extranuclear Star-forming Regions. *ApJ* 761:97. <https://doi.org/10.1088/0004-637x/761/2/97>
- Muzzin A, Marchesini D, Stefanon M, Franx M, et al (2013) A Public  $K_s$ -selected Catalog in the COSMOS/ULTRAVISTA Field: Photometry, Photometric Redshifts, and Stellar Population Parameters. *ApJS* 206:8
- Narayan R, Yi I (1995) Advection-dominated Accretion: Underfed Black Holes and Neutron Stars. *ApJ* 452:710. <https://doi.org/10.1086/176343>
- Narayanan VK, Berlind AA, Weinberg DH (2000) Locally biased Galaxy Formation and Large Scale Structure. *ApJS* 136:1. <https://doi.org/10.1086/308140>
- Neugebauer G, Habing HJ, van Duinen R, Aumann HH, Baud B, et al (1984) The Infrared Astronomical Satellite (IRAS) mission. *ApJ* 278:L1. <https://doi.org/10.1086/184209>
- Noiro D G Stern, Mei S, Wylezalek D, et al (2018) HST Grism Confirmation of 16 Structures at  $1.4 < z < 2.8$  from the Clusters Around Radio-Loud AGN (CARLA) Survey. *ApJ* 859:38. <https://doi.org/10.3847/1538-4357/aabadb>
- Nolan LA, Dunlop JS, Kukula MJ, Hughes DH, Boroson T, Jimenez R (2001) The ages of quasar host galaxies. *MNRAS* 323:308. <https://doi.org/10.1046/j.1365-8711.2001.04174.x>
- O'Dea CP, Saikia D (2021) Compact steep-spectrum and peaked-spectrum radio sources. *A&Rv* 29:3
- Osmond JP, Ponman TJ (2004) The GEMS project: X-ray analysis and statistical properties of the group sample. *MNRAS* 350:1511. <https://doi.org/10.1111/j.1365-2966.2004.07742.x>
- Overzier R, Röttgering HJA, Rengelink RB, Wilman R (2003) The spatial clustering of radio sources in NVSS and FIRST: implications for galaxy clustering evolution. *A&A* 405:53. <https://doi.org/10.1051/0004-6361:20030527>
- Owen FN, Laing R (1989) CCD surface photometry of radio galaxies – 1. FR class I and II sources. *MNRAS* 238:357. <https://doi.org/10.1093/mnras/238.2.357>
- Owen FN, Rudnick L (1976) Radio sources with wide-angle tails in Abell clusters of galaxies. *ApJ* 205:L1. <https://doi.org/10.1086/182077>
- Owen FN, White RA (1991) Surface photometry of radio galaxies – II Cluster sources. *MNRAS* 249:164. <https://doi.org/10.1093/mnras/249.1.164>
- Pace C, Salim S (2016) Suppression of Star Formation in the Hosts of Low-excitation Radio Galaxies. *ApJ* 818:65. <https://doi.org/10.3847/0004-637x/818/1/65>
- Padovani P (2016) The faint radio sky: radio astronomy becomes mainstream. *A&A Rev* 24:13. <https://doi.org/10.1007/s00159-016-0098-6>
- Padovani P, Alexander DM, Assef RJ, De Marco B, et al (2017) Active galactic nuclei: what's in a name? *A&A Rev* 25:2. <https://doi.org/10.1007/s00159-017-0102-9>
- Panessa F, Baldi RD, Laor P Aand Padovani, Behar E, McHardy I (2019) The origin of radio emission from radio-quiet active galactic nuclei. *NatAs* 3:387. <https://doi.org/10.1038/s41550-019-0765-4>
- Park SQ, Barmby P, Fazio GG, Nandra K, et al (2008) AEGIS: Radio and Mid-infrared Selection of Obscured AGN Candidates. *ApJ* 678:744. <https://doi.org/10.1086/587136>
- Paterno-Mahler R, Blanton EL, Brodwin M, Ashby ML, Golden-Marx E, Decker B, Wing JD, Anand G (2017) The High-redshift Clusters Occupied by Bent Radio AGN (CO-BRA) Survey: The Spitzer Catalog. *ApJ* 844:78. <https://doi.org/10.3847/1538-4357/aa7b89>
- Peacock JA (1999) *Cosmological Physics*. Cambridge University Press
- Peacock JA, Nicholson D (1991) The large-scale clustering of radio galaxies. *MNRAS* 253:307. <https://doi.org/10.1093/mnras/253.2.307>
- Peebles PJE (1980) *The Large-Scale Structure of the Universe*. Princeton Series in Physics, Princeton University Press. <https://doi.org/10.23943/princeton/9780691209838.001>

0001

- Pentericci L, Röttgering HJ, Miley GK, Spinrad H, McCarthy PJ, van Breugel WJ, Macchetto F (1998) HST Images of the Extremely Clumpy Radio Galaxy 1138-262 at  $z = 2.2$ . *ApJ* 504:139. <https://doi.org/10.1086/306087>
- Pentericci L, Röttgering HJ, Miley GK, McCarthy PJ, Spinrad H, van Breugel WJ, Macchetto F (1999) HST images and properties of the most distant radio galaxies. *ApJ* 341:329
- Pentericci L, Kurk JD, Röttgering HJA, Miley GK, et al (2000) A search for clusters at high redshift. II. A proto cluster around a radio galaxy at  $z = 2.16$ . *A&A* 361:L25
- Pentericci L, McLure RJ, Garilli B, Cucciati O, et al (2018) The VANDELS ESO public spectroscopic survey: Observations and first data release. *A&A* 616:74
- Pierre M, Pacaud F, Adami C, Alis S, et al (2016) The XXL Survey. I. Scientific motivations – XMM-Newton observing plan – Follow-up observations and simulation programme. *A&A* 592:1. <https://doi.org/10.1051/0004-6361/201526766>
- Pilbratt GL, Riedinger JR, Passvogel T, Crone G, et al (2010) Herschel Space Observatory. An ESA facility for far-infrared and submillimetre astronomy. *A&A* 518:L1. <https://doi.org/10.1051/0004-6361/201014759>
- Pilkington JD, Scott PF (1965) A survey of radio sources between declinations  $20^\circ$  and  $40^\circ$ . *Mem R Astron Soc* 169:183
- Podigachoski P, Barthel PD, Haas M, Leipski C, et al (2015) Star formation in  $z > 1$  3CR host galaxies as seen by Herschel. *A&A* 575:80. <https://doi.org/10.1051/0004-6361/201425137>
- Porciani C, Magliocchetti M, Norberg P (2004) Cosmic evolution of quasar clustering: implications for the host haloes. *MNRAS* 355:1010. <https://doi.org/10.1111/j.1365-2966.2004.08408.x>
- Pracy MB, Ching JHY, Sadler EM, Croom SM, et al (2016) GAMA/WiggleZ: the 1.4 GHz radio luminosity functions of high- and low-excitation radio galaxies and their redshift evolution to  $z = 0.75$ . *MNRAS* 460:2. <https://doi.org/10.1093/mnras/stw910>
- Prandoni I, Gregorini L, Parma P, de Ruiter HR, Vettolani G, Wieringa MH, Ekers RD (2001) The ATESP radio survey. III. Source counts. *A&A* 365:392. <https://doi.org/10.1051/0004-6361:20000142>
- Prandoni I, Guglielmino G, Morganti R, Vaccari M, Maini A, Röttgering HJ, Jarvis MJ, Garrett MA (2018) The Lockman Hole Project: new constraints on the sub-mJy source counts from a wide-area 1.4 GHz mosaic. *MNRAS* 481:4548. <https://doi.org/10.1093/mnras/sty2521>
- Press WH, Schechter P (1974) Formation of Galaxies and Clusters of Galaxies by Self-Similar Gravitational Condensation. *ApJ* 187:425. <https://doi.org/10.1086/152650>
- Prestage RM, Peacock JA (1988) The cluster environments of powerful radio galaxies. *MNRAS* 230:131. <https://doi.org/10.1093/mnras/230.1.131>
- Ramos Almeida C, Bessiere PS, Tadhunter CN, Inskip KJ, Morganti R, Dicken D, González-Serrano JJ, Holt J (2013) The environments of luminous radio galaxies and type-2 quasars. *MNRAS* 436:997. <https://doi.org/10.1093/mnras/stt1595>
- Rana S, Bagla JS (2019) Angular clustering of point sources at 150 MHz in the TGSS survey. *MNRAS* 485:5891. <https://doi.org/10.1093/mnras/stz831>
- Rawlings JI, Seymour N, Page MJ, De Breuck C, et al (2013) Polycyclic aromatic hydrocarbon emission in powerful high-redshift radio galaxies. *MNRAS* 429:744
- Retana-Montenegro E, Röttgering HJ (2017) Probing the radio loud/quiet AGN dichotomy with quasar clustering. *A&A* 600:97. <https://doi.org/10.1051/0004-6361/201526433>
- Reuland M, Röttgering H, van Breugel W, De Breuck C (2004) Dust and star formation in distant radio galaxies. *MNRAS* 353:377. <https://doi.org/10.1111/j.1365-2966.2004.08063.x>
- Rigby EE, Hatch NA, Röttgering HJA, Sibthorpe B (2014) Searching for large-scale structures around high-redshift radio galaxies with Herschel. *MNRAS* 437:1882
- Rykoff ES, Rozo E, Busha MT, Cunha CE, et al (2014) redMaPPer. I. Algorithm and SDSS DR8 Catalog. *ApJ* 785:104. <https://doi.org/10.1088/0004-637x/785/2/104>
- Sabater J, Best PN, Argudo-Fernández M (2013) Effect of the interactions and environment on nuclear activity. *MNRAS* 430:638. <https://doi.org/10.1093/mnras/sts675>



- Sabater J, Best PN, Hardcastle MJ, Shimwell TW, et al (2019) The LoTSS view of radio AGN in the local Universe. The most massive galaxies are always switched on. *A&A* 622:17. <https://doi.org/10.1051/0004-6361/201833883>
- Sabater J, Best PN, Tasse C, Hardcastle MJ, et al (2021) The LOFAR Two-metre Sky Survey: Deep Fields Data Release 1. II. The ELAIS-N1 LOFAR deep field. *A&A* 648:2. <https://doi.org/10.1051/0004-6361/202038828>
- Sadler EM (1999) Activity in elliptical galaxies. *AdSpR* 23:823. [https://doi.org/10.1016/s0273-1177\(99\)00212-4](https://doi.org/10.1016/s0273-1177(99)00212-4)
- Sadler EM, Ekers RD, Mahony EK, Mauch T, Murphy T (2014) The local radio-galaxy population at 20 GHz. *MNRAS* 438:796
- Salomé Q, Salomé P, Combes F, Hamer S, Heywood I (2016) Star formation efficiency along the radio jet in Centaurus A. *A&A* 586:45
- Sargent M, Schinnerer E, Murphy E, Carilli CL, et al (2010) No Evolution in the IR-Radio Relation for IR-luminous Galaxies at  $z < 2$  in the COSMOS Field. *ApJ* 714:L190
- Saunders W, Rowan-Robinson M, Lawrence A (1992) The spatial correlation function of IRAS galaxies on small and intermediate scales. *MNRAS* 258:134. <https://doi.org/10.1093/mnras/258.1.134>
- Schinnerer E, Smolčić V, Carilli CL, Bondi M, et al (2007) The VLA-COSMOS Survey. II. Source Catalog of the Large Project. *ApJS* 172:46. <https://doi.org/10.1086/516587>
- Scoccimarro R, Sheth RK, Hui L, Jain B (2001) How Many Galaxies Fit in a Halo? Constraints on Galaxy Formation Efficiency from Spatial Clustering. *ApJ* 546:20. <https://doi.org/10.1086/318261>
- Seldner M, Peebles PJE (1978) Statistical analysis of catalogs of extragalactic objects. X. Clustering of 4C radio sources. *ApJ* 225:7. <https://doi.org/10.1086/156464>
- Seldner M, Peebles PJE (1981) Clustering of 4C radio sources. *MNRAS* 194:251. <https://doi.org/10.1093/mnras/194.2.251>
- Seldner M, Siebers B, Groth EJ, Peebles PJ (1977) New reduction of the Lick catalog of galaxies. *AJ* 82:249. <https://doi.org/10.1086/112039>
- Seymour N, Stern D, De Breuck C, Vernet J, et al (2007) The Massive Hosts of Radio Galaxies across Cosmic Time. *ApJS* 171:353. <https://doi.org/10.1086/517887>
- Seymour N, Symeonidis M, Page MJ, Amblard A, et al (2011) HerMES: SPIRE emission from radio-selected active galactic nuclei. *MNRAS* 413:1777. <https://doi.org/10.1111/j.1365-2966.2011.18253.x>
- Shao L, Lutz D, Nordon R, Maiolino R, et al (2010) Star formation in AGN hosts in GOODS-N. *A&A* 518:L26. <https://doi.org/10.1051/0004-6361/201014606>
- Shen Y, Richards GT, Strauss MA, Hall PB, et al (2011) A Catalog of Quasar Properties from Sloan Digital Sky Survey Data Release 7. *ApJS* 194:45. <https://doi.org/10.1088/0067-0049/194/2/45>
- Shimwell TW, Tasse C, Hardcastle MJ, Mechev AP, et al (2019) The LOFAR Two-metre Sky Survey. II. First data release. *A&A* 622:1
- Shimwell TW, Hardcastle MJ, Tasse C, Best PN, et al (2022) The LOFAR Two-metre Sky Survey. V. Second data release. *A&A* 659:1
- Siebenmorgen R, Freudling W, Krügel E, Haas M (2004) ISOCAM survey and dust models of 3CR radio galaxies and quasars. *A&A* 421:129. <https://doi.org/10.1051/0004-6361:20035908>
- Siewert TM, Hale C, Bhardwaj N, Biermann M, et al (2020) One- and two-point source statistics from the LOFAR Two-metre Sky Survey first data release. *A&A* 643:100. <https://doi.org/10.1051/0004-6361/201936592>
- Silk J, Nusser A (2010) The Massive-black-hole-Velocity-dispersion Relation and the Halo Baryon Fraction: A Case for Positive Active Galactic Nucleus Feedback. *ApJ* 725:556. <https://doi.org/10.1088/0004-637x/725/1/556>
- Simpson C, Martínez-Sansigre A, Rawlings S, Ivison R, et al (2006) Radio imaging of the Subaru/XMM-Newton Deep Field - I. The 100- $\mu$ Jy catalogue, optical identifications, and the nature of the faint radio source population. *MNRAS* 372:741. <https://doi.org/10.1111/j.1365-2966.2006.10907.x>
- Singal AK, Rajpurohit K (2014) Fanaroff-Riley dichotomy of radio galaxies and the Malmquist bias. *MNRAS* 442:1656. <https://doi.org/10.1093/mnras/stu986>

- Smith DA, Wilson AS, Arnaud KA, Terashima Y, Young AJ (2002) A Chandra X-Ray Study of Cygnus, A. III. The Cluster of Galaxies. *ApJ* 565:195. <https://doi.org/10.1086/324539>
- Smith DJ, Haskell P, Gürkan G, Best PN, et al (2021) The LOFAR Two-metre Sky Survey Deep Fields. The star-formation rate-radio luminosity relation at low frequencies. *A&A* 648:6. <https://doi.org/10.1051/0004-6361/202039343>
- Smolčić V (2009) The Radio AGN Population Dichotomy: Green Valley Seyferts Versus Red Sequence Low-Excitation Active Galactic Nuclei. *ApJ* 699:L43. <https://doi.org/10.1088/0004-637x/699/1/143>
- Smolčić V, Riechers DA (2011) The Molecular Gas Content of  $z < 0.1$  Radio Galaxies: Linking the Active Galactic Nucleus Accretion Mode to Host Galaxy Properties. *ApJ* 730:64. <https://doi.org/10.1088/0004-637X/730/2/64>
- Smolčić V, Schinnerer E, Scodreggio M, Franzetti P, et al (2008) A New Method to Separate Star-forming from AGN Galaxies at Intermediate Redshift: The Submillijansky Radio Population in the VLA-COSMOS Survey. *ApJS* 177:14. <https://doi.org/10.1086/588028>
- Smolčić V, Zamorani G, Schinnerer E, Bardelli S, et al (2009) Cosmic Evolution of Radio Selected Active Galactic Nuclei in the Cosmos Field. *ApJ* 696:24. <https://doi.org/10.1088/0004-637x/696/1/24>
- Smolčić V, Finoguenov A, Zamorani G, Schinnerer E, Tanaka M, Giodini S, Scoville N (2011) On the occupation of X-ray-selected galaxy groups by radio active galactic nuclei since  $z = 1.3$ . *MNRAS* 416:L31. <https://doi.org/10.1111/j.1745-3933.2011.01092.x>
- Smolčić V, Novak M, Bondi M, Ciliegi P, et al (2017a) The VLA-COSMOS 3 GHz Large Project: Cosmic evolution of radio AGN and implications for radio-mode feedback since  $z \sim 5$ . *A&A* 602:6. <https://doi.org/10.1051/0004-6361/201730685>
- Smolčić V, Novak M, Delvecchio I, Bondi M, et al (2017b) The VLA-COSMOS 3 GHz Large Project: Continuum data and source catalog release. *A&A* 602:6. <https://doi.org/10.1051/0004-6361/201628704>
- Starikova S, Berta S, Franceschini A, Marchetti L, Rodighiero G, Vaccari M, Vikhlinin A (2012) Clustering of Star-forming Galaxies Detected in Mid-infrared with the Spitzer Wide-area Survey. *ApJ* 751:126. <https://doi.org/10.1088/0004-637x/751/2/126>
- Stern D, Spinrad H (1999) Search Techniques for Distant Galaxies. *PASP* 111:1475. <https://doi.org/10.1086/316471>
- Stern D, Holden B, Stanford SA, Spinrad H (2003) Confirmation of a Radio-selected Galaxy Overdensity at  $z = 1.11$ . *AJ* 125:2759. <https://doi.org/10.1086/374229>
- Stern D, Assef RJ, Benford DJ, Blain A, et al (2012) Mid-infrared Selection of Active Galactic Nuclei with the Wide-Field Infrared Survey Explorer. I. Characterizing WISE-selected Active Galactic Nuclei in COSMOS. *ApJ* 753:30. <https://doi.org/10.1088/0004-637x/753/1/30>
- Tadhunter CN (2016) Radio AGN in the local universe: unification, triggering and evolution. *A&ARev* 24:10. <https://doi.org/10.1007/s00159-016-0094-x>
- Tadhunter CN, Morganti R, Robinson A, Dickson R, Villar-Martin M, Fosbury RAE (1998) The nature of the optical-radio correlations for powerful radio galaxies. *MNRAS* 298:1035. <https://doi.org/10.1046/j.1365-8711.1998.01706.x>
- Tasse C, Best PN, Röttgering H, Le Borgne D (2008) Radio-loud AGN in the XMM-LSS field. II. A dichotomy in environment and accretion mode? *A&A* 490:893. <https://doi.org/10.1051/0004-6361:20079299>
- Tasse C, Shimwell T, Hardcastle MJ, O'Sullivan SP, et al (2021) The LOFAR Two-meter Sky Survey: Deep Fields Data Release 1. I. Direction-dependent calibration and imaging. *A&A* 648:1. <https://doi.org/10.1051/0004-6361/202038804>
- Tisanic K, De Zotti G, Amiri A, Khoram A, Tavasoli S, Vidovic-Tisanic Z (2022) Infrared-radio relation in the local Universe. *A&A* 658:21. <https://doi.org/10.1051/0004-6361/202140402>
- Tiwari P, Zhao R, Zheng J, Zhao G, Bacon D, Schwarz DJ (2021) Galaxy power spectrum and biasing results from the LOFAR Two-metre Sky Survey (first data release). *ApJ arXiv:2104.03320*
- Truch MDP, Ade PAR, Bock JJ, Chapin EL, et al (2009) The Balloon-borne Large Aperture Submillimeter Telescope (BLAST) 2006: Calibration and Flight Performance. *ApJ* 707:1723. <https://doi.org/10.1088/0004-637x/707/2/1723>



- Uchiyama H, Yamashita T, Toshikawa J, Kashikawa N, et al (2022) A Wide and Deep Exploration of Radio Galaxies with Subaru HSC (WERGS). VI. Distant Filamentary Structures Pointed by High- $z$  Radio Galaxies at  $z \sim 4$ . *ApJ* 926:76
- Urry M, Padovani P (1995) Unified Schemes for Radio-Loud Active Galactic Nuclei. *PASP* 107:803. <https://doi.org/10.1086/133630>
- Van Kampen E, Smith DJB, Maddox S, Hopkins AM, et al (2012) Herschel-ATLAS/GAMA: spatial clustering of low-redshift submm galaxies. *MNRAS* 426:3455. <https://doi.org/10.1111/j.1365-2966.2012.21949.x>
- Vardoulaki E, Jiménez Andrade EF, Delvecchio I, Smolčić V, et al (2021) FR-type radio sources at 3 GHz VLA-COSMOS: Relation to physical properties and large-scale environment. *A&A* 648:102. <https://doi.org/10.1051/0004-6361/202039488>
- Veilleux S, Osterbrock D (1987) Spectral Classification of Emission-Line Galaxies. *APJS* 63:295. <https://doi.org/10.1086/191166>
- Venemans BP, Kurk JD, Miley GK, Röttgering HJA, et al (2002) The most distant structure of galaxies known: A protocluster at  $z = 4.1$ . *ApJ* 569:L11
- Venemans BP, Röttgering HJA, Miley GK, van Breugel WJM, et al (2007) Protoclusters associated with  $z > 2$  radio galaxies. I. Characteristics of high redshift protoclusters. *A&A* 461:823
- Virdee JS, Hardcastle MJ, Rawlings S, Rigopoulou D, et al (2013) Herschel-ATLAS/GAMA: What determines the far-infrared properties of radio galaxies? *MNRAS* 432:609. <https://doi.org/10.1093/mnras/stt488>
- Vlahakis C, Eales S, Dunne L (2007) The far-infrared radio relationship at high and low redshift. *MNRAS* 379:1042. <https://doi.org/10.1111/j.1365-2966.2007.12007.x>
- Voelk HJ (1989) The correlation between radio and far-infrared emission for disk galaxies: a calorimeter theory. *A&A* 218:67
- Wake DA, Croom SM, Sadler EM, Johnston HM (2008) The clustering of radio galaxies at  $z \sim 0.55$  from the 2SLAQ LRG survey. *MNRAS* 391:1674. <https://doi.org/10.1111/j.1365-2966.2008.14039.x>
- Wall JV, Peacock JA (1985) Bright extragalactic radio sources at 2.7 GHz – III. The all-sky catalogue. *MNRAS* 216:173. <https://doi.org/10.1093/mnras/216.2.173>
- Webster A (1976a) The clustering of radio sources – I. The theory of power-spectrum analysis. *MNRAS* 175:61. <https://doi.org/10.1093/mnras/175.1.61>
- Webster A (1976b) The clustering of radio sources – II. The 4C, G13 and MCI surveys. *MNRAS* 175:71
- Weinberger R, Springel V, Pakmor R, Nelson D, et al (2018) Supermassive black holes and their feedback effects in the Illustris-TNG simulation. *MNRAS* 479:4056. <https://doi.org/10.1093/mnras/sty1733>
- Weinmann SM, Neisten E, Dekel A (2011) On the puzzling plateau in the specific star formation rate at  $z = 2 - 7$ . *MNRAS* 417:2737. <https://doi.org/10.1111/j.1365-2966.2011.19440.x>
- Wen ZL, Han JL, Liu FS (2012) A Catalog of 132,684 Clusters of Galaxies Identified from Sloan Digital Sky Survey III. *ApJS* 199:34. <https://doi.org/10.1088/0067-0049/199/2/34>
- Werner MW, Roellig TL, Low FJ, Rieke GH, et al (2004) The Spitzer Space Telescope Mission. *ApJS* 154:1. <https://doi.org/10.1016/j.asr.2005.04.012>
- White SDM, Davis M, Efstathiou G, Frenk CS (1987) Galaxy distribution in a cold dark matter universe. *Nature* 330:451. <https://doi.org/10.1038/330451a0>
- Williams WL, Röttgering HJA (2015) Radio-AGN feedback: when the little ones were monsters. *MNRAS* 450:1538. <https://doi.org/10.1093/mnras/stv692>
- Williams WL, van Weeren RJ, Röttgering HJA, Best P, et al (2016) LOFAR 150-MHz observations of the Boötes field: catalogue and source counts. *MNRAS* 460:385. <https://doi.org/10.1093/mnras/stw1056>
- Williams WL, Calistro Rivera G, Best PN, Hardcastle MJ, et al (2018) LOFAR-Boötes: properties of high- and low-excitation radio galaxies at  $0.5 < z < 2$ . *MNRAS* 475:429
- Willis AG, Strom RG, Wilson AS (1975) 3C236, DA240; the largest radio sources known. *Nature* 250:625
- Willott CJ, Rawlings S, Jarvis MJ, Blundell KM (2003) Near-infrared imaging and the  $K - z$  relation for radio galaxies in the 7C Redshift Survey. *MNRAS* 339:173. <https://doi.org/10.1046/j.1365-8711.2003.00711.x>

- [//doi.org/10.1046/j.1365-8711.2003.06172.x](https://doi.org/10.1046/j.1365-8711.2003.06172.x)
- Windhorst RA, Miley GK, Owen FN, Kron RG, Koo DC (1985) Sub-millijansky 1.4 GHz source counts and multicolor studies of weak radio galaxy populations. *ApJ* 289:494. <https://doi.org/10.1086/162911>
- Wing JD, Blanton EL (2011) Galaxy Cluster Environments of Radio Sources. *ApJ* 141:88. <https://doi.org/10.1088/0004-6256/141/3/88>
- Wright EL, Eisenhardt PRM, Mainzer AK, Ressler ME, et al (2010) The Wide-field Infrared Survey Explorer (WISE): Mission Description and Initial On-orbit Performance. *AJ* 140:1868. <https://doi.org/10.1088/0004-6256/140/6/1868>
- Wylezalek D, Galametz A, Stern D, Vernet J, et al (2013) Galaxy Clusters around Radio-loud Active Galactic Nuclei at  $1.3 < z < 3.2$  as seen by Spitzer. *ApJ* 769:79. <https://doi.org/10.1088/0004-637x/769/1/79>
- Yates MG, Miller L, Peacock JA (1989) Cluster environment of powerful radio galaxies. *MNRAS* 240:129
- York DG, Adelman J, Anderson J John E, Anderson SF, et al (2000) The Sloan Digital Sky Survey: Technical Summary. *AJ* 120:1579
- Yun MS, Reddy-Naveen A, Condon JJ (2001) Radio Properties of Infrared-selected Galaxies in the IRAS 2 Jy Sample. *ApJ* 554:803. <https://doi.org/10.1086/323145>
- Zheng XC, Röttgering HJA, Best PN, van der Wel A, et al (2020) Link between radio-loud AGNs and host-galaxy shape. *A&A* 644:12. <https://doi.org/10.1051/0004-6361/202038646>
- Zirbel EL (1996) Properties of host galaxies of powerful radio sources. *ApJ* 473:713. <https://doi.org/10.1086/178184>
- Zirbel EL (1997) The Megaparsec Environments of Radio Galaxies. *ApJ* 476:489. <https://doi.org/10.1086/303626>
- Zirbel EL, Baum SA (1995) On the FR I/FR II Dichotomy in Powerful Radio Sources: Analysis of Their Emission-Line and Radio Luminosities. *ApJ* 448:521. <https://doi.org/10.1086/175984>